THE UNIVERSITY OF CHICAGO

ENVIRONMENTALLY TUNED CONSERVATION OF ADAPTIVE BIOMOLECULAR CONDENSATION

A DISSERTATION SUBMITTED TO

THE FACULTY OF THE DIVISION OF THE BIOLOGICAL SCIENCES

AND THE PRITZKER SCHOOL OF MEDICINE

IN CANDIDACY FOR THE DEGREE OF

DOCTOR OF PHILOSOPHY

COMMITTEE ON GENETICS, GENOMICS, AND SYSTEMS BIOLOGY

BY

SAMANTHA MAKALA KEYPORT KIK

CHICAGO, ILLINOIS

AUGUST 2023

To Brandon

TABLE OF CONTENTS

LIST OF FIGURES vii
LIST OF TABLES viii
ACKNOWLEDGEMENTS ix
ABSTRACT xi
CHAPTER 1 1
INTRODUCTION 1
CHAPTER 2 7
AN ADAPTIVE BIOMOLECULAR CONDENSATION RESPONSE IS CONSERVED ACROSS ENVIRONMENTALLY DIVERGENT SPECIES 7
2.1 ABSTRACT 7
2.2 INTRODUCTION 8
2.3 RESULTS 12
2.3.1 Evolutionary divergence results in distinct growth ranges 12
2.3.2 Heat shock responses track temperature tolerance 14
2.3.3 Condensation is conserved across species 18
2.3.4 Condensation of Pab1 is conserved, encoded in sequence, and environmentally tuned 22
2.3.5 Phenotypic consequences of altering condensation is conserved 24
2.3.6 Pab1 condensate structural dynamics 25
2.4 DISCUSSION 30
2.4.1 Transcriptomic remodeling 31
2.4.2 Biomolecular condensation 33
2.4.3 Sequence-encoded behavior 34
2.4.4 Phenotypic consequences of condensation 36
2.4.5 Evolutionary and molecular insights 36
2.5 METHODS 37
2.5.1 Experimental model and subject details 37
Phylogenetic relationships 37
Identification of orthologs 37
Maximum specific growth assays 38
Strain construction 38
Spot assay 38
Flow cytometry 39
qPCR 39
RNA-sequencing 40
Sample preparation 40
Library Generation 40

Data Processing 41
Data Analysis 42
Annotation of genes 42
In vivo biochemical fractionation and mass spectrometry sample preparation 42
Mass spectrometry 44
Sample Preparation 44
Mass Spectrometry - DIA Chromatogram Library Generation 44
Mass Spectrometry - Sample Analysis 45
Data Processing 46
Calculation of pSup 46
Pab1 wild-type and mutant protein purification 48
Dynamic light scattering of purified protein 48
Hydrogen-Deuterium Exchange 49
Condensate preparation for HDX-MS 49
HDX labeling 49
LC-MS and HDX-MS data analysis 49
2.5.2 Data Code and Availability 52
Code and data analysis 52
Statistical Tests 52
Data Availability 52
2.6 SUPPORTING INFORMATION 53
2.7 COMPETING INTERESTS 57
2.8 AUTHOR CONTRIBUTIONS 57
2.9 ACKNOWLEDGEMENTS 58
CHAPTER 3 59
CHARACTERIZATION OF HEAT SENSITIVE PROTEIN NUG1 59
3.1 INTRODUCTION 59
3.2 RESULTS 64
3.2.1 Identification of sensor candidates 64
3.2.2 Description of Nug1 behavior in vitro 66
3.2.3 Evolutionary structural analysis of Nug1 70
3.2.4 Cryophilic replacement of Nug1 73
3.3 CONCLUSIONS AND FUTURE DIRECTIONS 78
3.4 METHODS 83
3.4.1 Data and Code Availability 83
Experimental data and code for analysis 83
3.4.2 Experimental model and subject details 83
Identification of Hsf1 binding sites in the yeast proteome 83
Protein purification 84
In vitro TSP 85
Experimental buffers for *in vitro* TSP 86

Dynamic light scattering 86
Evolutionary analysis 86
Strain construction 87
Screening CRISPR genetic manipulations 87
In vivo TSP and western blot analysis 88
Flow cytometry 90
Plasmids used in this study 91
3.5 AUTHOR CONTRIBUTIONS 91
CHAPTER 4 91
CONCLUSIONS AND FUTURE DIRECTIONS 92
4.1 Biomolecular condensation as a sensing mechanism 92
4.2 The function(s) of biomolecular condensation 94
4.3 Hot topic 95
REFERENCES 96

LIST OF FIGURES

2.1 Three fungal species are adapted to divergent environments, and transcriptional heat shock responses track their temperature tolerance 14

2.2 Transcriptome changes upon heat shock reflect largely conserved responses to stress, except environmental stress response regulators Msn2/4 16

2.3 Condensation is conserved across species, and tuned to their respective thermal niches 21

2.4 Conserved, environmentally tuned condensation response is adaptive across divergent species 23

2.5 HDX-MS investigation of Pab1 ortholog monomers and condensates reveals conservation of condensate structure and mechanism 29

2.6 Growth, recovery, and death phenotypes of each three species 53

2.7 Expression dynamics across temperatures 54

2.8 Strong correlations in biological replicates and within treatment condition comparisons 55

3.1 The transcriptional heat shock response and biomolecular condensation are induced by temperature 60

3.2 Identifying potential Hsp70 binding sites using a sliding window analysis of the condensing proteome 65

3.3 Purified Nug1's condensation is sensitive to salt, detergent, pH, and temperature 67

3.4 Predicted structural properties of Nug1 are largely conserved among fungi 71

3.5 Using a cryophilic replacement allele to search for transcriptional and condensation phenotype 75

LIST OF TABLES

2.1 Yeast strains used in this study 50

2.2 Plasmids used in this study 51

2.3 Pab1 baseline size estimations 56

2.4 Pab1 $T_{condense}$ and estimations and size measurements 57

ACKNOWLEDGEMENTS

Thank you to the many people who helped me make this project possible: my committee members Dr. Tobin Sosnick, Dr. Ben Glick, and Dr. David Pincus; my administrators Susan Levison, Shani Charles, Amy Murphy, and Lisa Anderson; my department chairs over the years Dr. Douglas Bishop, Dr. Yoav Gilad, Dr. Marcelo Nobrega, and Dr. Luis Barriero; lab assistants Dorian Smith and Gayle; the Biophysics Core Facility Director, Dr. Elena Solomaha; UCCCC Sequencing Core staff Willian J. Buikema, Kay Grennan, and Paul Gardner; the Chicago Center for Teaching; my career mentor Dr. Eileen Dolan; my undergraduate research mentors Dr. John Kelly and Father Steven Mitten; my cohort members Dr. Anthony Hung, Kathryn Farris, Dr. Selene Clay, Katherine Aracena, and Dr. Grace Hansen; my collaborator Dr. Asif Ali; my brilliant colleagues Dr. Edward J. Wallace, Dr. Chris D. Katanski, Dr. Catherine Triandafillou, Dr. Haneul Yoo, Dr. Jared A. M. Bard, Hendrik Glauninger, Caitlin Wong Hickernell, Kyle Lin, Rosalind Pan, Aparna Sirnivasen, Joshua Melamed, and Dana Christopher; and all of my amazing friends and family.

To my advisor, D. Allan Drummond, who will serve as a lifelong mentor and *friend*, thank you for always being available, thank you for forgiving my short-term memory, thank you for encouraging my never-ending confusion, and thank you for allowing me to ask all the questions. I will be forever indebted to you for making me a better scientist and critical thinker.

To the Kiks, my family by marriage, thank you for your unconditional support and serious attempts to understand what I study. I could not have a more caring, fun, and kind-hearted second family.

To Ben, my almost-Irish twin and partner in crime, thank you for being proud of me. Thank you for always being a relief and useful distraction throughout life, and especially during graduate school. You will be my best friend forever.

To Ted, my eldest brother and sometimes biggest critic (in a brotherly way), thank you for making me a stronger person. I don't think I would be who I am without you as my role model. Thank you for the immensely useful career advice and for always being available for a phone call. I know I can count on you and Anna for life.

To Dad, my voice of reason, thank you for your unquestioning support. You are a rock in my life. Thank you for never asking me when I will graduate. Thank you for never being angry or impatient with me. I love you.

To Mom, my inspiration, thank you for everything. You are the reason I'm here. You have inspired curiosity in ways you probably never meant. I know you think I was curious from birth but curiosity must be fostered, and you allowed me to indulge. Thank you for the knowledge, the connections, the encouragement, and the nagging. Today and every day forward are the days I am thankful for all of it.

To Mary and Ana, my best friends and maids of honor, thank you for battling through graduate school with me from the sidelines. I know I can count on you two for life.

To Brandon, my husband, I can hardly begin to describe how grateful I am for you. You have always supported me without an iota of hesitation. You are half of my brain and most of my moral compass. Thank you for telling me when I'm wrong and confirming when I'm right. Thank you for listening throughout my successes and failures, for encouraging a day off, for encouraging the grind, and for everything in between. I owe you the absolute world.

ABSTRACT

Cells must be able to survive a wide array of physiological stresses posed by their environment. Primordial stresses such as heat induce conserved, robust transcriptional changes across the tree of life to help cells adapt to the new environment. However, mechanisms for transcriptional activation remain incompletely characterized. Additionally, recent work has identified that reversible, specific, and adaptive stress-induced biomolecular condensates form during heat shock, but their function remains unknown. Because each response occurs near-instantaneously with the onset of increased temperature, we hypothesized that the condensation response may serve to activate the transcriptional response. In this work I characterize the growth, transcription, and condensation responses spanning three thermal niches and nearly 100 million years of evolutionary time to quantify the conserved relationship between temperature, condensation, and transcription. Through *in vitro* characterization of two individual condensing proteins, we show that condensation is genetically encoded and calibrated to the environment at which the source organism is adapted. We show that stress-induced biomolecular condensation is adaptive, conserved, integrated with the growth and transcriptional responses, and tuned to features of the cellular and organismal environment to initiate at niche-specific levels.

CHAPTER 1

INTRODUCTION

Increased temperature is an ancient signal to which all organisms must be able to sense and respond. Despite the discovery of heat shock response decades ago (Ritossa 1962; Tissières, Mitchell, and Tracy 1974), how cells mechanistically sense temperature remains unresolved. Temperature is unlike other external environmental signals like salt or ethanol because it is not a molecule, but rather a form of energy. Without a canonical ligand-receptor signal transduction mechanism, how does the cell sense the energetic change in its surroundings?

The heat shock response itself may provide clues to its cognate temperature sensing mechanism. Heat shock factor 1 (Hsf1) induces a subset of heat shock genes (Gasch et al. 2000; Solís et al. 2016; Pincus et al. 2018) upon temperature increase, but is held inactive under non-stress conditions by molecular chaperone Hsp70 (Zheng et al. 2016; Krakowiak et al. 2018). Hsf1 and Hsp70 are at the center of a proposed feedback mechanism for the response: Hsp70 repressively binds Hsf1 until the cell experiences stress, when newly-produced Hsp70 clients titrate Hsp70 away from Hsf1, leading to the activation of the heat shock genes (Mosser, Theodorakis, and Morimoto 1988; Shi, Mosser, and Morimoto 1998; Krakowiak et al. 2018; Masser et al. 2019). One of the induced genes is Hsp70, which can rebind and repress Hsf1 after the stress has been mitigated. But what are the heat-induced clients of Hsp70?

It has been proposed that increased temperature leads to protein misfolding, and it is these proteins which serve as Hsp70 clients (Kmiecik, Le Breton, and Mayer, n.d.; Vabulas et al. 2010; Morano, Grant, and Moye-Rowley 2012; Sottile and Nadin 2018). Consistent with this hypothesis, inducing protein misfolding by expressing non-native amino acid analogs or unstable reporter proteins indeed leads to Hsf1 activation (Trotter et al. 2001; Geiler-Samerotte et al. 2011). However, no endogenous protein which misfolds or even exposes an Hsp70 binding site in response to heat shock has ever been identified. Instead, upon an increase in temperature, protein and RNA clusters form, termed biomolecular condensates, which contain largely folded and sometimes even active protein (Riback et al. 2017; Wallace et al. 2015). It is possible that these stress-induced condensates may be the primary sensors of heat stress. There are several observations and lines of evidence which support this hypothesis:

1. Upon stress, Hsp70 is recruited to endogenous and exogenous condensates (Cherkasov et al. 2013). However, Hsp70 itself is not part of the condensate, as it remains soluble after biochemical fractionation (Wallace et al. 2015). Even though Hsp70 will re-localize to exogenous aggregates (e.g., firefly luciferase), the endogenous condensates within the same cells are disaggregated first, and this clearance is correlated with reentry of the cells to the cell cycle (Cherkasov et al. 2013; Kroschwald et al. 2015). *In vitro* work has further established that endogenous condensates are better substrates for Hsp70 than model exogenous aggregates, as they are cleared with significantly more efficiency (Yoo et al. 2022).
2. There is overwhelming evidence that ongoing translation is required for Hsf1 activation. When cells are treated with translation inhibitor cycloheximide, the

Hsf1 transcriptional response is largely attenuated (Amici et al. 1992; Baler, Welch, and Voellmy 1992; Liu, Lightfoot, and Stevens 1996; Tanabe et al. 1997; Tye et al. 2019; Albert et al. 2019; Tye and Churchman 2021). This result leads to the hypothesis that newly-synthesized polypeptides, which have not yet found their native structure at the onset of stress, become clients of Hsp70, thus activating Hsf1. In this sense, newly-synthesized polypeptides are the sensor of heat stress. However, old and new evidence challenges the requirement for active translation. At high heat shock temperatures in mammalian cells, the Hsf1 response is robustly activated even in the presence of cycloheximide (Baler, Welch, and Voellmy 1992). Further, we observe Hsf1 transcriptional activation in the absence of translation (due to treatment with cycloheximide or glucose starvation) but only with intracellular acidification (Triandafillou et al. 2020), which occurs when cells are heat shocked. These results suggest that there are heat sensors for Hsf1 that are translation-independent and pH-dependent.

3. Unlike exogenous reporters, no endogenous protein has been shown to misfold after heat shock. Instead, proteins which are sequestered in heat-induced condensates are returned to solubility during recovery (Wallace et al. 2015). This result is inconsistent with large-scale protein misfolding, where many proteins would be degraded. Further, condensed aminoacyl-tRNA synthetase complex retains its enzymatic activity and specificity, suggesting condensed protein complexes possess structural integrity and functional stability (Wallace et al. 2015). *In vitro* work demonstrates that purified Pab1 retains its shape at condensation-inducing heat shock temperatures (Riback et al. 2017). Taken

together, condensates contain functional, largely folded proteins which are distinct from misfolded protein aggregates.

4. Consistent with the previous evidence that condensates do not contain misfolded, toxic aggregates, prevention of their formation during stress decreases cell fitness (Wallace et al. 2015; Iserman et al. 2020). These results lead to the generally accepted model that condensation is adaptive and functional for dealing with heat stress (Kroschwald et al. 2015; Wallace et al. 2015; Protter and Parker 2016).
5. The transcriptional heat shock response is activated within minutes after stress (Pincus et al. 2018). As such, temperature sensors must be even quicker in order for the signal to be interpreted by Hsp70. Consistent with this logic, a small subset of proteins in yeast, termed superaggregators, are substantially enriched in condensates after only 2 minutes of heat stress (Wallace et al. 2015). Further, the intracellular pH drops in the cytoplasm of cells, and condensates have been shown both *in vivo* and *in vitro* to form at low pH (Munder et al. 2016; Riback et al. 2017; Franzmann et al. 2018; Kroschwald et al. 2018; Iserman et al. 2020). The temperature and pH-induced process of biomolecular condensation is fast, autonomous, encoded in the sequence of proteins (Yoo, Triandafillou, and Drummond 2019), making it a strong candidate for sensing environmental changes.
6. Stress-induced condensates have been observed across multiple organisms – from cyanobacteria, to fungi, to plants, to mammalian cells (Pattanayak et al. 2020; Wallace et al. 2015; Jung et al. 2020; Sui et al. 2020). They are observed

across numerous stresses, with some common components and some stress- or organism-specific. The ubiquitous appearance and conservation of condensates across the tree of life during stress suggests that they are functional. However, the exact functions of biomolecular condensates remains mysterious.

In combination, these observations support a parsimonious model for heat sensing: heat and pH sensitive endogenous condensates form in cells at the onset of stress and serve as the evolved and tuned substrates of Hsp70, whether or not the cell is actively translating proteins. Yet isolating strong evidence supporting this model has proved difficult (Glauninger et al. 2022).

One major challenge is quantifying evolutionary conservation of condensates on an organismal level. Are condensates conserved in terms of the biophysical forces that drive their formation, individual molecular identity, or sequence-encoded properties? To answer this question, I describe the condensation behavior across three fungi which are evolutionarily adapted to different thermal niches. We observe that the individual molecules and sequence-dependence are largely conserved and yet tuned to the thermal environment to which each organism is adapted. The results of this work are discussed in Chapter 2.

I also undertook a rigorous yet unsuccessful approach to search for sensors of the transcriptional heat shock response. The hypothesis remains open, and I present my approach and offer my recommendations for future iterations of this project in Chapter 3.

Aside from summarizing my work to quantify condensation conservation as well as characterizing temperature-sensitive proteins, I hope this thesis emphasizes the complex role of temperature in biology. Often viewed (and used!) experimentally as a stress, I propose that

this ancient, primordial cellular experience is a signal to the organism about its environment. Clearly cells have evolved mechanisms to respond to and survive increased temperature conditions. Unlike a reaction to an unexpected event, cells across the tree of life have a consistent and organized response to increased thermal energy. Yet, a given temperature holds an entirely different meaning to Antarctic fish than it does to extremophilic bacteria living in a thermal vent. Temperature is a signal that represents something unique to each organism depending on its adapted environment.

CHAPTER 2

AN ADAPTIVE BIOMOLECULAR CONDENSATION RESPONSE IS CONSERVED ACROSS ENVIRONMENTALLY DIVERGENT SPECIES

This chapter will be submitted for publication in summer 2023 with the following co-authors: Samantha Keyport Kik, Dana Christopher, Caitlin Wong Hickernell, Hendrik Glauninger, Jared A. M. Bard, Tobin R. Sosnick, Michael Ford, and D. Allan Drummond. Author contributions are listed in section 2.7.

2.1 ABSTRACT

Cellular responses to maladaptive environmental changes—stresses—allow for organismal adaptation to diverse and dynamic conditions. Across the tree of life, cells upregulate a highly conserved transcriptional program in response to so-called proteotoxic stresses such as heat shock. Correspondingly, in eukaryotes, these stresses induce the formation of biomolecular condensates, clusters of mRNA and protein which are referred to as stress granules under severe stress. However, major questions remain about this stress-induced response. How conserved is the condensation response relative to the transcriptional response? How does it vary across environmental niches, and to what extent does it correspond with the conserved

transcriptional response? To answer these fundamental questions, we studied the growth, transcriptional, and condensation heat-induced stress responses in three fungal species adapted to thrive in different thermal environments: cryophilic *S. kudriavzevii*, mesophilic *S. cerevisiae*, and thermotolerant *K. marxianus*. Here we show that transcriptional heat shock responses track each species' evolved temperature range of growth. Further, orthologous proteins—including poly(A)-binding protein, Pab1, a core marker of stress granules—form condensates *in vivo* at temperatures systematically tuned to the temperature at which the organisms activate the transcriptional heat shock response and slow their growth. *In vitro*, purified Pab1 from each species condenses autonomously at niche-specific temperatures. Homologous mutations in Pab1 cause similar shifts in relative condensation temperature across species, and crucially, mutations which suppress condensation *in vitro* also reduce fitness during heat stress. Our findings indicate that stress-induced protein condensation is adaptive, conserved, integrated with the growth and transcriptional responses, and tuned to features of the cellular and organismal environment to initiate at niche-specific levels.

2.2 INTRODUCTION

In response to a rapid increase in temperature—heat shock—eukaryotic cells respond by transcriptionally inducing a conserved set of genes encoding molecular chaperones (Susan Lindquist 1986; Solís et al. 2016; Pincus et al. 2018), repressing translation of most transcripts (Cherkasov et al. 2013) and growth, and accumulating protein and mRNA molecules in biomolecular condensates (Wallace et al. 2015; Cherkasov et al. 2013). Until recently, these actions have been conceived of as a response to protein damage, denaturation, and aggregation caused by heat, with chaperones (Le Breton and Mayer 2016; Vabulas et al. 2010;

Sottile and Nadin 2018).

However, substantial evidence now supports an alternative model describing the events following heat shock: physiological changes in temperature are directly sensed by specific proteins, triggering their biomolecular condensation without damage or denaturation (Wallace et al. 2015); condensation is adaptive rather than deleterious, even affecting several of the translational changes observed (Riback et al. 2017; Iserman et al. 2020); chaperones act as regulators of the condensation response (Zheng et al. 2016; Krakowiak et al. 2018; Yoo et al. 2022); and temperature itself often acts as a physiological signal carrying adaptive information (Triandafillou et al. 2020). Remarkably, although adaptive biomolecular condensation was recognized last among these phenomena, it plays a central role in each of aspect of the response, leading to the prediction that condensation should be both conserved and intimately coordinated with other aspects of the response across species—a prediction which motivates the present study.

To more clearly see the proposed interrelationships between condensation and more well-established aspects of the cellular response to heat shock, consider transcriptional upregulation of specific genes, a defining feature of the response since its discovery (Ritossa 1996, 1962). The core eukaryotic heat shock response (HSR) is regulated by heat shock factor 1 (Hsf1), which induces transcription of a number of heat shock proteins, including the molecular chaperones of the Hsp70 family. Under physiological growth conditions in *S. cerevisiae*, one or more Hsp70 species repressively binds the transcription factor Hsf1 (Zheng et al. 2016; Krakowiak et al. 2018). New and abundant Hsp70 substrates emerging during stress are then thought to titrate Hsp70 away from Hsf1, relieving inhibition and unleashing the HSR. Stress-induced protein misfolding was long thought to generate these substrates, and

significant evidence indicates that misfolded proteins are sufficient to induce Hsf1 at non-shock temperatures (Geiler-Samerotte et al. 2011), yet misfolding of mature endogenous proteins under physiological heat-shock conditions has remained surprisingly difficult to establish. Meanwhile, evidence has accumulated that nascent polypeptides and newly synthesized proteins, whose folding and assembly may be more easily perturbed during stress (Xu et al. 2016), may serve as HSR inducers (Triandafillou et al. 2020). Nevertheless, the HSR can be robustly induced even when translation is inhibited, indicating that nascent/new species cannot be the sole HSR trigger. Moreover, physiological biomolecular condensation in response to thermal stress has repeatedly been shown to be an autonomous property of individual proteins (Riback et al. 2017; Iserman et al. 2020; Kroschwald et al. 2018; Wallace et al. 2015), and such condensates recruit Hsp70 both *in vivo* and *in vitro* (Cherkasov et al. 2013; Yoo et al. 2022), indicating that they may more broadly serve as physiological thermal sensors. Finally, many of the proteins which condense in response to stress are translation initiation and elongation factors, as well as ribosome biogenesis factors, whose condensation—and likely inactivation—accompanies suppression of the associated processes. Together, these observations open the possibility that condensation may serve as a primary sensor, coordinator, and executor of the transcriptional and translational stress responses.

If condensation acts in this central organizing capacity then, as noted above, it should be conserved across related species and coordinated with the other aspects of their responses. For heat shock, the obvious candidate species are those adapted to different thermal niches: thermophiles, mesophiles, and cryophiles. Most tuning of the transcriptional HSR to suit the environmental temperature profile and organism lifestyle is well-established. Interestingly, while there is a theoretical limit to eukaryotic and fungal life (Maheshwari,

Bharadwaj, and Bhat 2000), the absolute temperature is not the cause of the transcriptional response, where instead its activation varies depending on environmental niche (Hoffmann, Sørensen, and Loeschcke 2003; Sørensen, Kristensen, and Loeschcke 2003; Lars Tomanek 2008; L. Tomanek 2010). In other words, the conservation does not exist on a level of temperature itself, but rather conservation is reflected by the same transcriptional changes, just at different temperatures. Therefore, each adaptive response must be tuned and coordinated with the evolutionary history of the organism. What, then, might it mean for the condensation response to be conserved across organisms, given that the same absolute temperatures cause different relative degrees of the response in transcription? Do the same molecules form condensates across species *in vivo* and *in vitro*? Is condensation encoded the same way across the tree of life? Are the organismal phenotypes the same when condensation is perturbed?

Further, how the cell senses the change and coordinates the responses at the appropriate temperature, if at all, remains unclear. Do the growth, transcription, and condensation responses vary in the same way across thermal niche? If so, how is that variation encoded within organisms? Is the activation of the heat-induced transcripts controlled by the biomolecular condensation behavior of proteins, or vice versa?

To answer these questions, we characterized the growth, transcription, and protein condensation of cryophilic, mesophilic, and thermotolerant yeast species across a range of temperatures and molecular scales. Here we show that heat shock responses track each species' temperature tolerance. Further tuning occurs at the protein condensation level, where the behavior of orthologous molecules is conserved but at niche-specific temperatures. We show that condensation is encoded in the primary sequence of stress granule marker Pab1 as

shown by *in vitro* biophysical assays, and disrupting the condensation of Pab1 *in vivo* reduces fitness during temperature stress. Finally, our data suggests a mechanism for both condensation and conservation of Pab1 by comparing structural differences in condensates relative to monomers across species.

2.3 RESULTS

2.3.1 Evolutionary divergence results in distinct growth ranges

For comparison of conservation and divergence after heat shock under controlled conditions, we selected three budding yeast species (Figure 2.1a) known to differ in their thermal profiles yet able to grow robustly on identical media containing D-glucose. Baker's yeast *Saccharomyces cerevisiae*, which grows optimally between 30–34°C, grows naturally on the surface of fruit and on oak bark, but halts its growth above 40°C. Another related yeast, *Saccharomyces kudriavzevii*, also found on oak bark, grows optimally at lower temperatures between 24–28°C, and growth has been shown to cease above 32°C (Sampaio and Gonçalves 2008). We also used a pre-whole-genome duplication relative, *Kluyveromyces marxianus*, a respirative thermotolerant yeast isolated from sugarcane juice in Thailand, which can grow robustly at temperatures as high as 45°C (Limtong, Sringiew, and Yongmanitchai 2007; Sakihama et al. 2019). (We respect the somewhat arbitrary convention that reserves "thermophilic" for fungi which grow more rapidly at 45°C than at 25°C, while labeling others "thermotolerant" (Cooney and Emerson 1964).) Consistent with previous studies, we hypothesized that each species' transcriptional changes would be tuned to the thermal environment to which they have adapted (S. Lindquist 1984; Deegenaars and Watson 1998;

Riehle et al. 2003; Lars Tomanek 2008; Gracey et al. 2008; L. Tomanek 2010).

To characterize growth behavior, we calculated maximum growth rates of log phase cultures at temperatures ranging from 10 to 46°C for at least two biological replicates (Figure 2.1b). *K. marxianus* shows a high maximum growth rate relative to these other species, consistent with other studies on this organism (Banat, Nigam, and Marchant 1992; Limtong, Sringiew, and Yongmanitchai 2007; Nonklang et al. 2008; Salvadó, Arroyo-López, Barrio, et al. 2011) and likely due to its respirative life history (Sakihama et al. 2019; Brion et al. 2016). The estimated growth temperature optimum is different for each species, ranging from 25–38°C. Observations of growth in liquid culture also match longer-term growth on plates (Figure 2.6a). Interestingly, for *S. kudriavzevii*, we do observe growth above 32°C, as high as 38°C, although very slowly and specifically in complete medium liquid culture.

These growth studies yield clear species contrasts: at 37°C, the standard heat-shock temperature commonly used in studies of mesophilic baker's yeast, the thermotolerant species has not yet reached its optimal growth temperature—in this sense, it is truly heat-loving rather than merely heat tolerant—while growth of the cryophilic species has all but ceased.

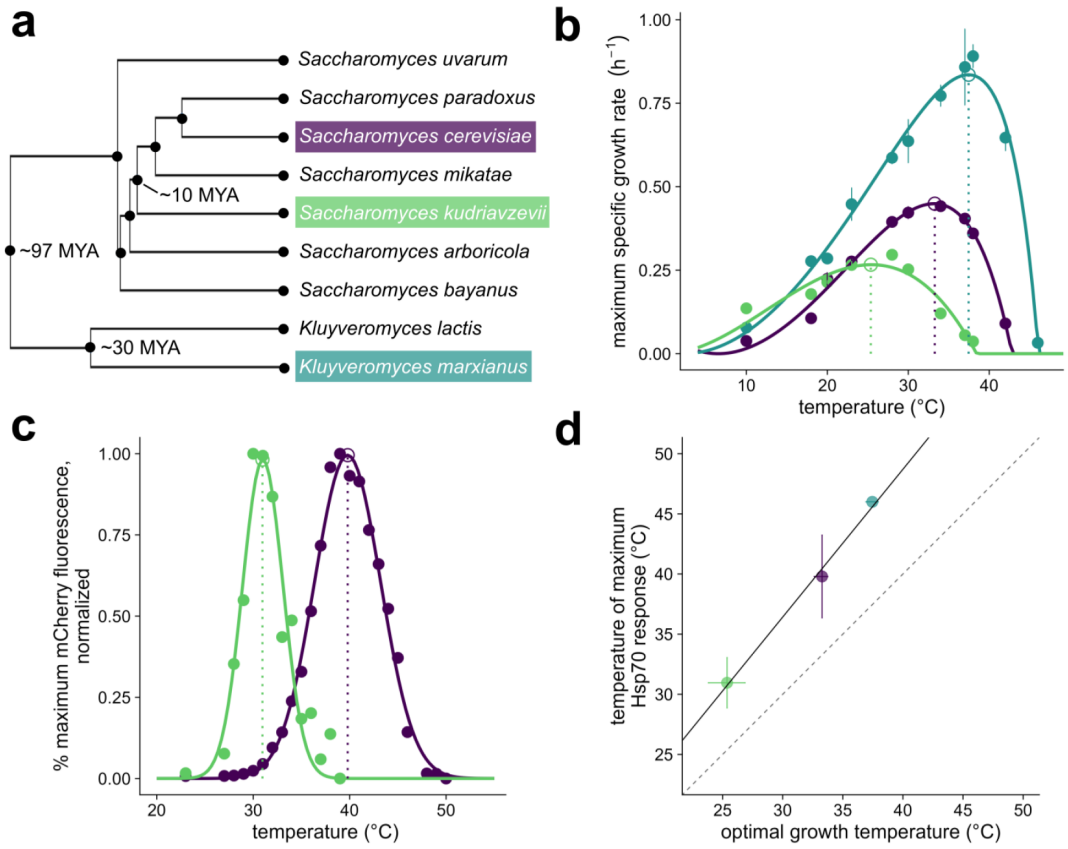

Figure 2.1: Three fungal species are adapted to divergent environments, and transcriptional heat shock responses track their temperature tolerance.
a Phylogenetic tree of the Saccharomycetaceae family. The topology was obtained from Kumar et al. 2022. **b** Fit of the cardinal temperature model with inflection to experimental data obtained for strains *S. cerevisiae* BY4742 (purple), *S. kudriavzevii* FM1389 (green), and *K. marxianus* DMKU3-1042 (blue). Open circles represent the maximum of the fit, and dotted lines show the temperature of the maximum growth rate for each species. **c** SSA4-mCherry fluorescence after 20 minute heat shock at specified temperature with three hours of recovery. Values are plotted as the percent maximum of the response. Each point is the average of at least 5,000 cells, controlled for size and normalized to non-heat shocked cells. Open circles represent the maximum of a gaussian fit, and the dotted lines shows the temperature of the maximum transcriptional response for each species. Error bars represent the standard deviation for the estimated temperature. **d** Correlation of the temperatures at which the three species reach their highest maximum specific growth rate from **b** plotted against the temperature of the maximum normalized SSA4-mCherry fluorescence in **c**. qPCR was used to find the maximum SSA3 response in *K. marxianus*. Line was fit with a linear regression (adjusted R^2 = 0.99, p = 0.05). Dashed line displays y = x.

2.3.2 Heat shock responses track temperature tolerance

How do these species' heat shock responses relate to the temperatures at which they proliferate? To monitor the heat shock response quantitatively, we constructed *S. cerevisiae* and *S. kudriavzevii* strains with heat-induced Hsp70 molecular chaperone *SSA4* tagged with

the red fluorescent protein mCherry (Shaner et al. 2004). We monitored mCherry fluorescence using flow cytometry after a 20-minute temperature treatment followed by a three-hour recovery at room temperature (Figure 2.1c). Each population shows some variance at each temperature, with less variance observed at heat shock temperatures relative to non-heat shock temperatures for both species (Figure 2.7a). As expected, the temperature of maximum response for *S. kudriavzevii* is less than that of *S. cerevisiae*. The maximum response for *K. marxianus* was measured by qPCR of the mRNA encoding its orthologous induced Hsp70 chaperone, Ssa3 (Figure 2.7b).

The data reveal a strong correlation between optimum growth temperature and maximum Hsp70 induction temperature across the three species (Figure 2.1d). The difference between the maximum heat shock response temperature and the optimum growth temperature varies between 6–8°C, where growth rate has begun to decline in each species but has not reached complete growth arrest.

We next wanted to know if the observed Hsp70 response generalizes to the broader HSR, including Hsf1-regulated genes, and to characterize other gene expression changes across species. To measure the global transcriptomic behavior, we performed RNA-seq for each species, comparing transcript levels at the optimum growth temperature to those at the maximum heat shock response temperature. Overall, many of the transcriptomic changes are conserved at each species' respective heat shock temperatures (Figure 2.2a), with genes encoding orthologous ribosomal components, ribosome biogenesis factors, and translation factors downregulated in each species (Methods). Likewise, heat shock factor 1 (Hsf1) controlled orthologs are strongly induced in all three species.

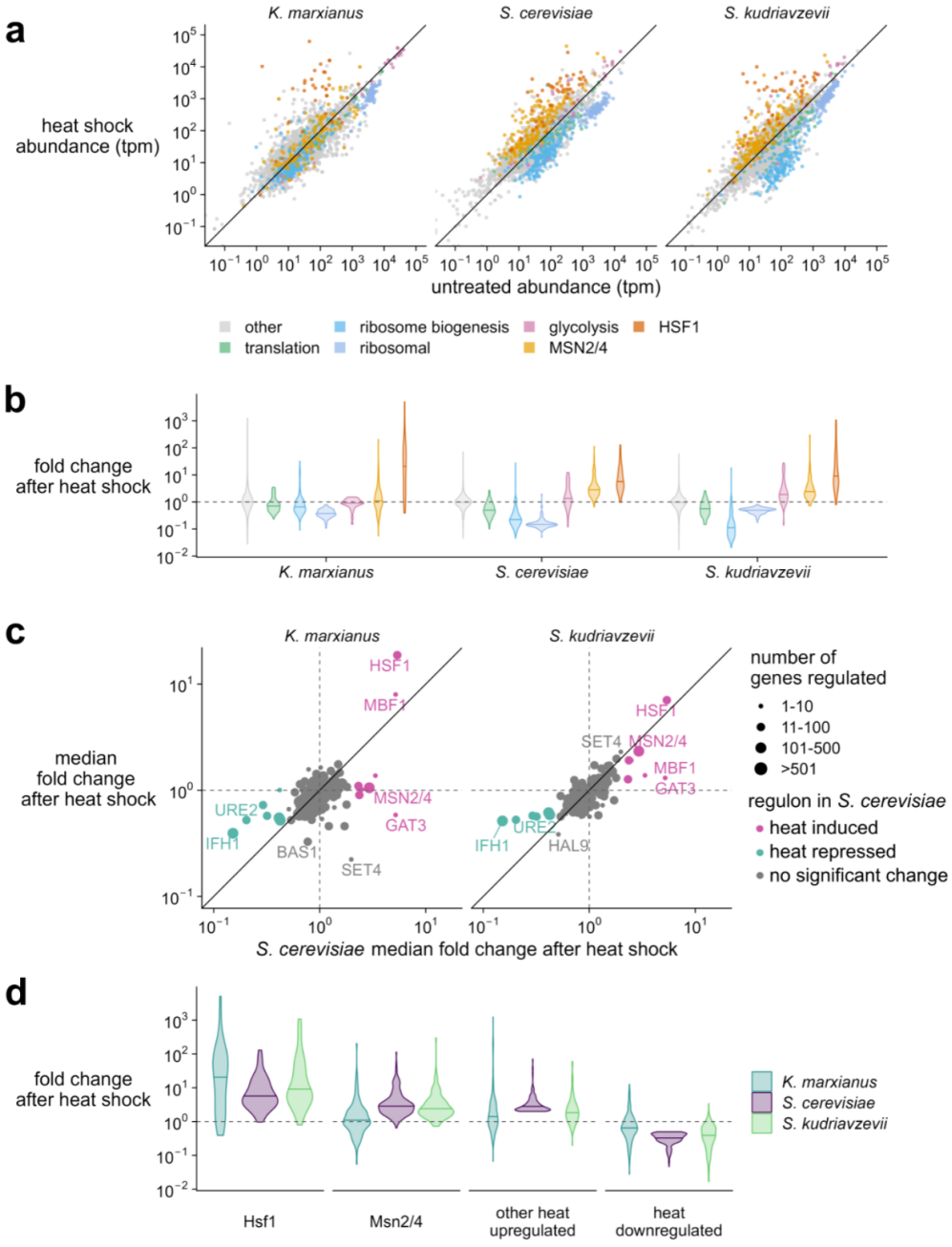

Figure 2.2. Transcriptome changes upon heat shock reflect largely conserved responses to stress, except environmental stress response regulators Msn2/4.
a Transcript abundance (transcripts per million, tpm) in stressed versus unstressed populations of cells. *K. marxianus* was grown at 37°C and stressed at 46°C; *S. cerevisiae* was grown at 33°C and stressed at 40°C; *S. kudriavzevii* was grown at 24°C and stressed at 31°C. Colors correspond to gene type. **b** Fold change distribution for groups of genes (colored by gene type) after stress in each species. **c** Behavior of genes corresponding to orthologous transcription factor regulators in *S. cerevisiae*. Data point size corresponds to number of genes controlled by the regulator, and points are colored according to genes that were observed as two-fold up or down in *S. cerevisiae*. **d** Individual transcript fold change after heat shock, colored by species. Panels correspond to orthologous genes controlled by Hsf1 or Msn2/4 from *S. cerevisiae* (left two panels) or orthologous genes that were observed as two-fold up or down in *S. cerevisiae* (right two panels).

Environmental stress response (ESR) factors Msn2 and Msn4 (Msn2/4) are paralogous transcription factors in fungi which become activated during many stresses, including heat, osmotic, and oxidative stress (Kobayashi and McEntee 1993; Marchler et al. 1993; Martínez-Pastor et al. 1996; Gasch et al. 2000; Elfving et al. 2014). *S. cerevisiae* and *S. kudriavzevii* possess both paralogs, but *K. marxianus* only possesses one version, as it diverged before the fungal whole genome duplication. Msn2/4 bind to stress response element (STRE) promoter sequences and have been shown to regulate more than 200 genes in *S. cerevisiae*, including several that are also induced by Hsf1 (Solís et al. 2016; Pincus et al. 2018). After a 20-minute heat stress, Msn2/4 induces hundreds of genes in *S. cerevisiae* and *S. kudriavzevii* (Figure 2.2b).

Interestingly, full ESR upregulation behavior does not seem to be conserved in *K. marxianus* across the Msn2/4 regulon; instead, many homologs under Msn2/4 control are instead downregulated during heat shock, resulting in a near-zero average response. *K. marxianus* diverged from the *S. cerevisiae* lineage about 100 million years ago, prior to the whole genome duplication. Previous work has described the stress response in *Lachancea kluyveri*, another pre-duplication relative, observing little overlap in the heat-induced ESR response with *S. cerevisiae* (Brion et al. 2016), and proposing that this may be due to differences in life history: respiratory yeast like *K. marxianus* do not require the same ESR responses as fermentative yeast like *S. cerevisiae*. We therefore looked more closely at the subset of Msn2/4 targets showing altered transcriptomic behavior and found consistent results with *K. marxianus*, such that a substantial proportion of downregulated Msn2/4 targets in *K. marxianus* were also downregulated in response to heat shock in *L. kluyveri* (Figure 2.7c, d), consistent with the respiratory hypothesis.

To more broadly identify regulons whose heat-shock behavior might differ between species, we grouped transcripts by their orthologous transcription factors (Methods) from *S. cerevisiae* (Figure 2.2c). Most of these regulons do not respond to temperature in *S. cerevisiae*, but most that do correspond with regulons that change in *S. kudriavzevii* (ρ = 0.72). However, a lower correlation is observed between *K. marxianus* and *S. cerevisiae* (ρ = 0.48), with the median of orthologous Msn2/4 regulated genes showing no net change in the thermotolerant species. With the exception of Msn2/4, orthologous genes that are 2-fold up or downregulated in *S. cerevisiae* seem to be largely conserved across species, including Hsf1 regulated genes (Figure 2.2d), raising the possibility that the upstream sensors of temperature carry much of the niche-specific tuning which is then transmitted to transcription factors.

In the case of Hsf1, these upstream sensors include thermally triggered biomolecular condensates which titrate Hsf1-repressive Hsp70 to activate the Hsf1 portion of the HSR. Moreover, Hsf1 targets include many molecular chaperones, including Hsp70, known to regulate condensation. We therefore sought to measure condensation in these three species across their heat shock temperatures, asking to what extent condensation is conserved and tuned.

2.3.3 Condensation is conserved across species

To survey condensation behavior across species, we performed biochemical fractionation and LC-MS/MS before and after an 8-minute, species-specific temperature treatment much as in our previous study in *S. cerevisiae* (Wallace et al. 2015). We estimate the proportion of a given protein in the supernatant (pSup) using a model which controls for experimental mixing error (Methods). A wide range of purified proteins identified using this method have been shown to

condense *in vitro* when exposed to physiological heat shock—poly(A)-binding protein Pab1 and aminoacyl tRNA synthetase complex components Gus1 and Mes1 (Wallace et al. 2015), RNA helicase Ded1 (Iserman et al. 2020), poly(U)-binding protein Pub1 (Kroschwald et al. 2018)—with no known exceptions to date, motivating our provisional interpretation a change in pSup from high to low during heat shock as reflecting condensation. Nevertheless it remains possible that certain proteins change pSup in this way due to shock-induced binding to membranes or other large structures.

Across the three species, we observe large-scale changes in protein solubility, primarily through increased condensation in heat shock relative to non-heat shock conditions (Figure 2.3a, top). Among orthologous proteins, glycolytic enzymes, ribosomal components, and membrane proteins do not significantly shift their solubility, shown by the pSups falling near the 1:1 line between conditions (Figure 3a, bottom). However, some orthologous proteins appear in the insoluble fraction after temperature stress, including a group of so-called superaggregator proteins identified previously (Wallace et al. 2015) and so named because they lose solubility more rapidly during heat shock than many stress-granule components. Subsequent work has demonstrated that recombinant purified preparations of specific superaggregators, such as Ded1, undergo condensation *in vitro* in response to heat shock. Superaggregator orthologs almost entirely retain this extreme temperature sensitivity, but at temperatures that correspond to each organism's thermal growth range. Superaggregators as a class lose solubility at 37°C in *S. kudriavzevii*, for which this is a heat-shock temperature, yet retain high solubility at the same temperature in *K. marxianus*, for which 37°C is a nearly optimal growth temperature.

To quantify conservation of these responses, we calculated pSup correlations between conditions and among all three species. Under non-heat shock, basal conditions for *S.*

kudriavzevii (23°C) and *K. marxianus* (37°C), we observe that classes of proteins largely display the same behavior (R^2 = 0.93, Figure 2.3b, left). Likewise, after heat shock, the pSups of protein classes are again strongly correlated (R^2 = 0.73, Figure 2.3b, middle). We observe consistently high correlations for all species when comparing within temperature conditions (e.g., heat shock vs. heat shock). Correlations drop significantly when comparing between treatment conditions (heat shock vs. basal), even within species (Figure 3b, right); that is, the condensation status of *S. kudriavzevii* during heat shock is more similar to that of *K. marxianus* during heat shock than it is to that of *S. kudriavzevii* under basal conditions. We conclude that biomolecular condensation is conserved.

Because we performed these experiments under species-specific basal and heat shock temperature conditions, we next aimed to quantify temperature tuning. We focused on glycolytic proteins and superaggregators across three temperatures, because the former shows little temperature sensitivity and the latter the greatest. We observe a striking relationship between temperature and condensation of superaggregators, when as temperature increases, pSup decreases (Figure 2.3c). However, this occurs at different temperatures for each organism, and non-condensing glycolytic enzymes show consistent solubility irrespective of heat shock. Thus, condensation is not only conserved among evolutionarily distinct organisms, but it is tuned to their adapted temperature niche.

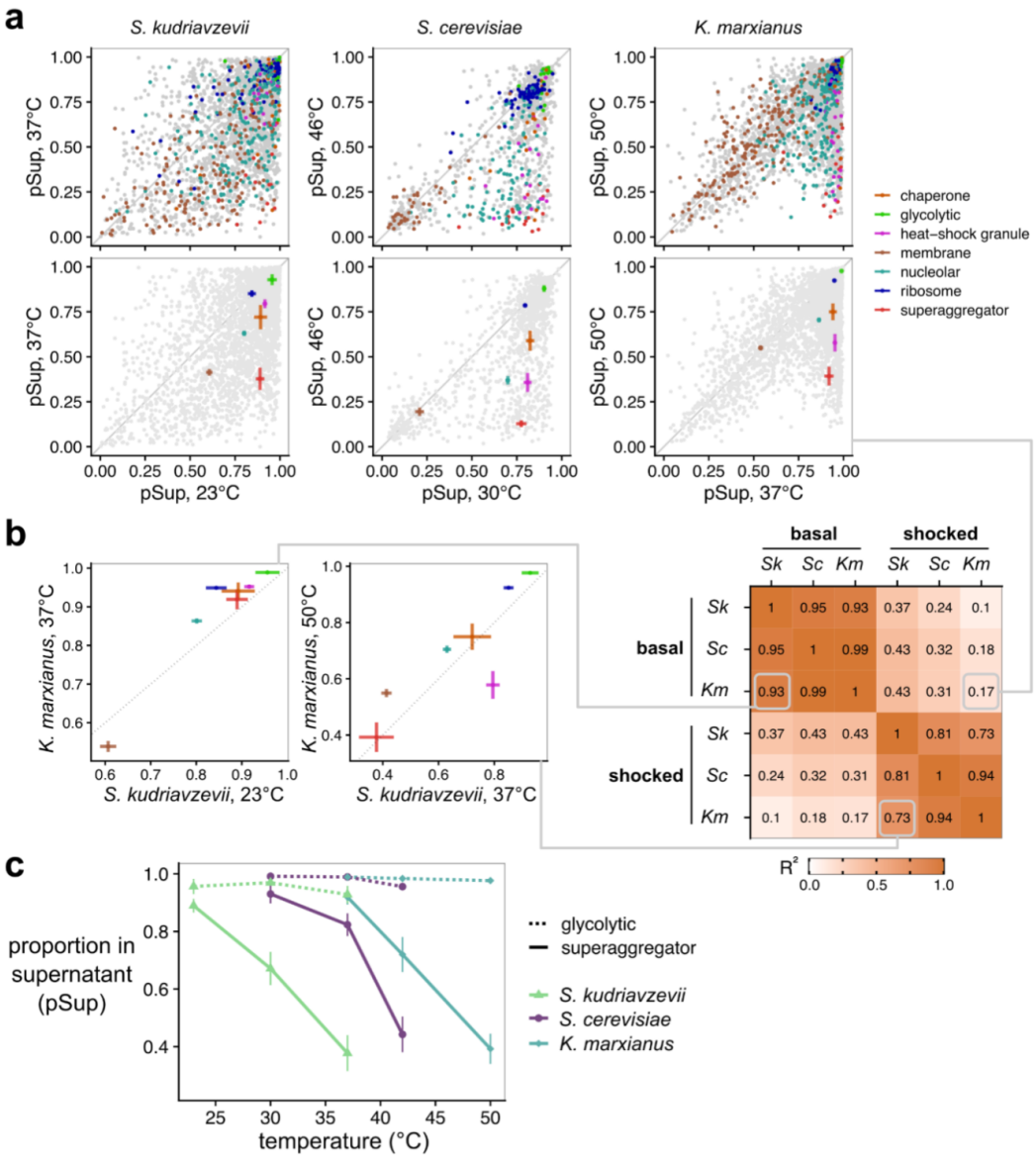

Figure 2.3. Condensation is conserved across species and tuned to their respective thermal niches.

a Proportion in the supernatant (pSup) at basal temperature and after heat shock, at species-specific temperatures, across three fungal species. *S. cerevisiae* data are from Wallace *et al.* 2015. Top, all detected proteins, with important previously identified classes of proteins highlighted, inferred by orthology from *S. cerevisiae*. Bottom, summary statistics (mean plus standard error) for the highlighted classes. **b** Conservation of condensation across classes of proteins is revealed by correlations between their condensation behaviors within and between species. Left, specific comparisons of basal and shocked condensation between *S. kudriavzevii* and *K. marxianus* at their respective optimal growth and shock temperatures; lines connect to their respective entries in the full correlation matrix (showing R^2 values), right. **c** Tuning of condensation is revealed by comparison of non-condensing glycolytic proteins and strongly condensing superaggregators across species.

2.3.4 Condensation of Pab1 is conserved, encoded in sequence, and environmentally tuned

Given previous results that some purified proteins from *S. cerevisiae* are autonomously temperature sensitive, we wondered if this property was tuned in a purified protein from *S. kudriavzevii* and *K. marxianus (Riback et al. 2017; Iserman et al. 2020)*. To test this, we purified poly(A)-binding protein (Pab1) from each species, where sequence identity between *S. cerevisiae* and *S. kudriavzevii* is 98%, and between *S. cerevisiae* and *K. marxianus* is 69%. We used dynamic light scattering (DLS) to monitor the apparent hydration radius (R_h) during a slow temperature ramp, where the apparent R_h of the protein will grow rapidly in a small temperature window when the protein begins to condense. Purified Pab1 from each species condensed at a temperature ($T_{condense}$, see Methods) correlated with both the optimal and maximum growth temperatures (Figure 2.4a,b). We conclude that Pab1's temperature sensitivity and tuning to a thermal niche are both largely encoded directly in its amino-acid sequence, paralleling results from the RNA helicase Ded1 (Iserman et al. 2020).

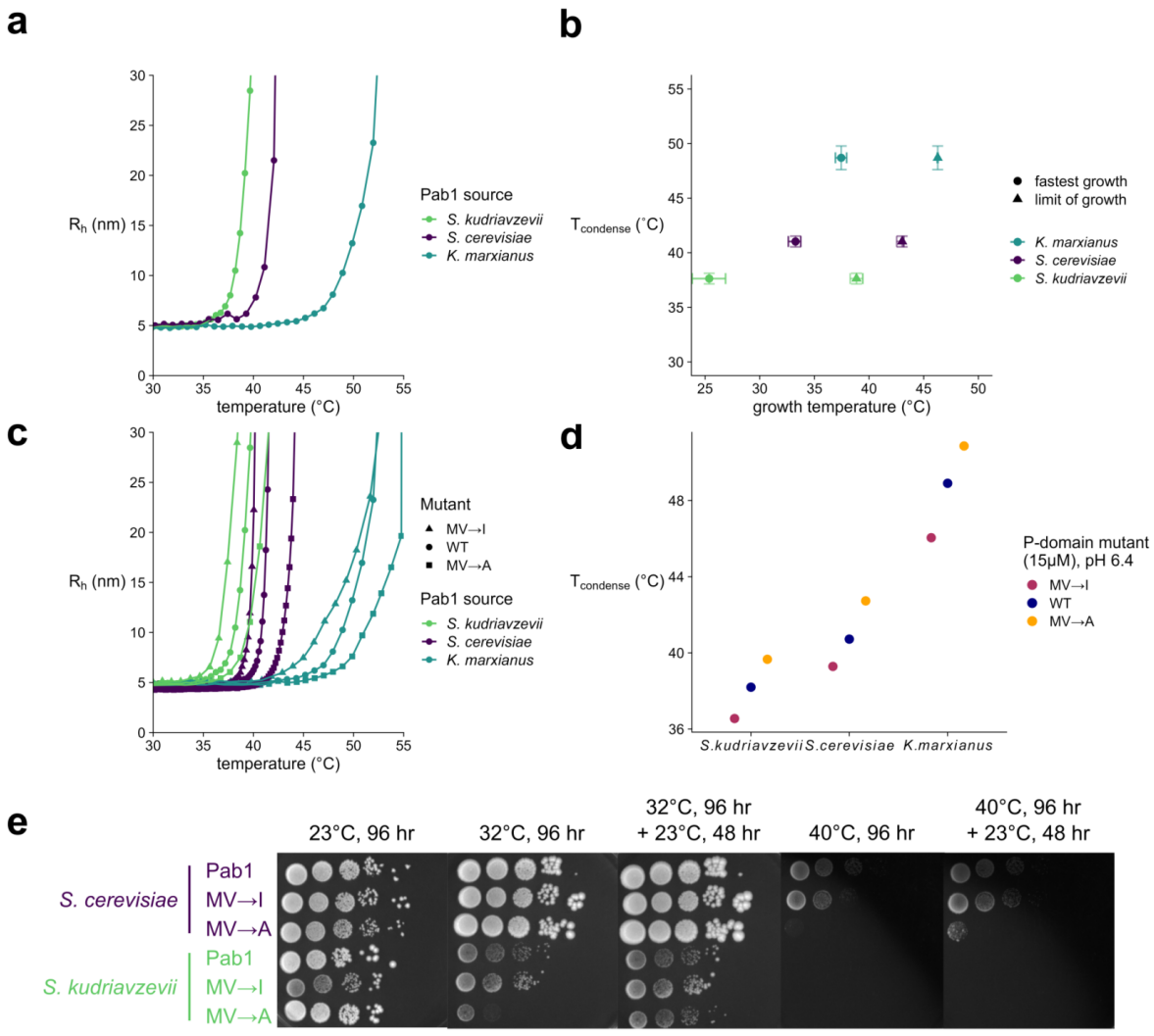

Figure 2.4. Conserved, environmentally tuned condensation response is adaptive across divergent species.

a DLS temperature ramp experiments of 15 μM Pab1 from each species, all at pH 6.4. **b** Correlation of $T_{condense}$ (°C) with optimum growth temperature (circles) or maximum growth temperature (triangles). Error bars for $T_{condense}$ (°C) represent the standard deviation of the mean of at least 3 replicates. Error bars for the optimum and maximum one standard deviation of the parameter estimates from the fit of the the cardinal temperature model with inflection. **c** DLS temperature ramp experiments of 15 μM Pab1 mutants from each species, all at pH 6.4. Curves for *S. cerevisiae* mutants and wildtype are from Riback & Katanski et al. 2017. **d** Comparison of $T_{condense}$ (°C) values calculated for each Pab1 protein. $T_{condense}$ (°C) was calculated *S. cerevisiae* mutants and wildtype from the curves contained in Riback & Katanski et al. 2017. **e** Spot assays of *S. cerevisiae* and *S. kudriavzevii* strains containing mutations in the P domain. Plates were incubated at 23, 32, and 40°C for 4 days, and then shifted to 23°C and grown for 2 days. Columns are 10-fold dilutions.

Previous work has shown that the P domain of Pab1, a poorly conserved low-complexity region enriched for proline, is not required for condensation, but modulates the

temperature at which the *Saccharomyces cerevisiae* protein forms condensates (Riback et al. 2017). We wondered if this modulatory role was also conserved across species.

A simple test for modulation, given our results in *S. cerevisiae*, would be to make the homologous mutations used to establish modulation in the P domains of the other two species. This is straightforward in *S. kudriavzevii*, whose P domain is identical to *S. cerevisiae*, but nontrivial in *K. marxianus*, whose P domain is only 57% identical. We therefore adopted the same strategy as in our previous study: mutating all instances of the weakly hydrophobic residues methionine and valine to isoleucine (MV→I), or to alanine (MV→A), making the domain more or less hydrophobic. We previously observed that condensation propensity positively correlated with the hydrophobicity of each domain, raising the question of whether this specific biophysical change would have similar consequences.

Indeed, the MV→I mutants in both species showed lower-temperature onset of condensation relative to their species' wild type, and the MV→A mutants showed higher-temperature onset, mirroring the *S. cerevisiae* results in both cases. (Figure 2.4c). We conclude that the P domain's modulation of condensation is conserved, and the major biophysical determinant of this modulation is also conserved, across all these species (Figure 2.4d). This is true whether the domain itself is perfectly conserved or sharply divergent in sequence.

2.3.5 Phenotypic consequences of altering condensation is conserved

Previous work has demonstrated that the ability of wild-type Pab1 to form condensates at the appropriate temperature in *S. cerevisiae* is important for fitness of the organism during long-term heat stress (Riback et al. 2017)--in short, Pab1 condensation is adaptive. We

wondered if this adaptive phenotype was conserved among species. To test this hypothesis, we replaced the endogenous version of Pab1 with the P domain mutants (MV→I or MV→A) in both *S. kudriavzevii* and *S. cerevisiae*. Reproducing our earlier results, we observe that *S. cerevisiae* strains grow at the same rates at non-stressful temperatures of 23°C and 32°C, but at a heat shock temperature of 40°C, the MV→A mutant has reduced fitness (Figure 2.4e). When returned to 23°C for 48 hours, the MV→A mutant resumes growth, indicating that the lack of growth was not due to death but rather arrested growth. We observe consistent results in *S. kudriavzevii*, where at 23°C, all strains grow equally, but at 32°C–close to optimal growth for *S. cerevisiae*, but a strong heat shock for *S. kudriavzevii*–the less hydrophobic MV→A Pab1 mutant has reduced fitness, but resumes growth when the stress is relieved after recovery at 23°C for 48 hours. However, growth of *S. kudriavzevii* does not resume after stress at 40°C, presumably due to death (Figure 2.4e). Together, these results suggest that the prevention of condensation *in vivo* decreases the ability of the organism to grow at high temperatures, a phenotype which is consistent across species yet tuned to the evolved environment of the organism.

2.3.6 Pab1 condensate structural dynamics

We have found that the condensation process of different fungi is adapted to their temperature niches related to their optimal growth temperatures. Further, we have found that the set of proteins that condense in response to temperature stress is largely conserved from cryophile to thermophile. In the case of Pab1, we have found that the orthologs' condensation temperature is autonomously encoded in their primary sequences.

Our previous work employing HDX-MS investigating *S. cerevisiae Pab1* condensation observed a mechanism of sequential activation involving the four RNA-recognition motifs

(RRMs) (Chen et al. 2022). Higher temperatures increased the amount of local unfolding in the RRMs, enabling them, and the linkers between them, to form the crosslinks necessary for condensation. Yet, central questions remain: 1) to what degree is the mechanism of condensation conserved, and 2) how does the sequence determine the onset temperature? To answer these questions, we employed HDX-MS to investigate the structural dynamics of both the monomers and condensates of Pab1 from *S. kudriavzevii*, *S. cerevisiae*, and *K. marxianus.*

In contrast to many other structural techniques, HDX-MS is well-suited for the study of insoluble systems such as condensates by providing residue-level insight into the hydrogen bond network in a label-free manner. By measuring the time dependence of uptake of deuterons from solvent, HDX-MS provides a series of snapshots that reveals the changes in structure and dynamics that occur during condensation.

Here, we observe changes in Pab1 percentage of deuterium uptake (%D-uptake) for numerous peptides in each ortholog, where the pattern of %D-uptake is found to be very similar among them (Figure 2.5a). The regions of low uptake in the condensate correspond to the five folded domains, RRM1, RRM2, RRM3, RRM4, and the C-terminal domain (CTD). The regions of high %D-uptake typically correspond to the unstructured regions such as the proline-rich domain (P domain) and inter-domain linkers.

Next, we calculate Δ%D-update, the difference in D-uptake between the condensed and monomeric states (Figure 2.5b). This quantity reflects changes in Pab1 structure and stability upon condensation. Numerous peptides have an increased D-uptake in the condensate, indicating that these regions have either weakened or a reduced number of hydrogen bonds. Strikingly, the pattern of Δ%D-uptake is highly conserved across the Pab1 orthologs. The four RRMs undergo increased exchange relative to the P domain, which may

suggest that this natively unstructured region forms cross-protomer contacts in the condensate. Previously observed putative contacts between Pab1 protomers involving RRM1, the linker connecting RRM3 and RRM4, and the linker carboxy-terminal to RRM4 appear to be conserved in all three species. In sum, the overall structural dynamics of the condensation process are conserved across the Pab1 orthologs, implying a common condensation mechanism.

How, then, is condensation triggered at different temperatures for each ortholog? The sequential activation mechanism proposed in our previous work can rationalize differences in the onset temperature for the three orthologs (Chen et al. 2022). In this model, the onset temperature is reduced by decreasing the stability of an RRM to favor its activation, while stabilizing an RRM should have the opposite effect. To identify factors that may control the onset temperature, we examined the kinetics of %D-uptake in the monomers. The data find that the %D-uptake of RRMs 1 and 3 are similar across the orthologs, implying their stabilities are similar (Figure 2.5c). Compared to *S. cerevisiae*, the *S. kudriavzevii* ortholog possesses an RRM4 with higher %D-uptake, whereas *K. marxianus* Pab1 displays lower uptake, perhaps contributing to varied condensation temperatures. The *K. marxianus* ortholog has the highest $T_{condense}$ temperature, which may be explained by its high relative stability in RRM1, RRM2 and RRM4. RRM3 appears to be the most stable RRM for all orthologs and hence, not a determining factor in the condensation temperature.

Due to the 98% sequence identity between *S. cerevisiae* and *S. kudriavzevii* Pab1 sequences, we can compare the deuteration of identical peptides between these two orthologs (Figure 2.5d, left panel). Regions of the protein with identical sequences (RRM1, RRM2, and P domain) have very similar uptake in both orthologs, which supports the view that exchange for

each domain is independent in the monomer. On the other hand, regions with divergent sequences (RRM3, RRM4, and CTD) can have similar or different deuteration rates. Of note, RRM3, which has 6 amino acid differences, displays similar stability, while RRM4, with only one varied residue (A343T), is less stable in *S. kudriavzevii*. These observations are consistent with onset temperature being linked to RRM stability. Specifically, we hypothesize that *S. kudriavzevii* RRM4 has a lower activation threshold due to its A343T mutation, which is responsible for its lower onset temperature. In contrast, we hypothesize *K. marxianus* RRM2 has a higher activation threshold, which underlies its increased condensation temperature.

We further find that in the condensate, the increased %D-uptake in RRM4 is not as apparent for *S. kudriavzevii* relative to *S. cerevisiae* (Figure 2.5d, right panel). Instead, we observe increased %D-uptake for RRM3 in *S. kudriavzevii*. This indicates there is not an exact correspondence between the monomeric dynamics, which presumably contributes to triggering condensation, and the condensate dynamics, which inform on the structure of the mature condensate.

Overall, we conclude that Pab1 condensate structure and dynamics are similar across three orthologs despite their different onset temperatures, with the stability of their RRMs correlates with onset temperature.

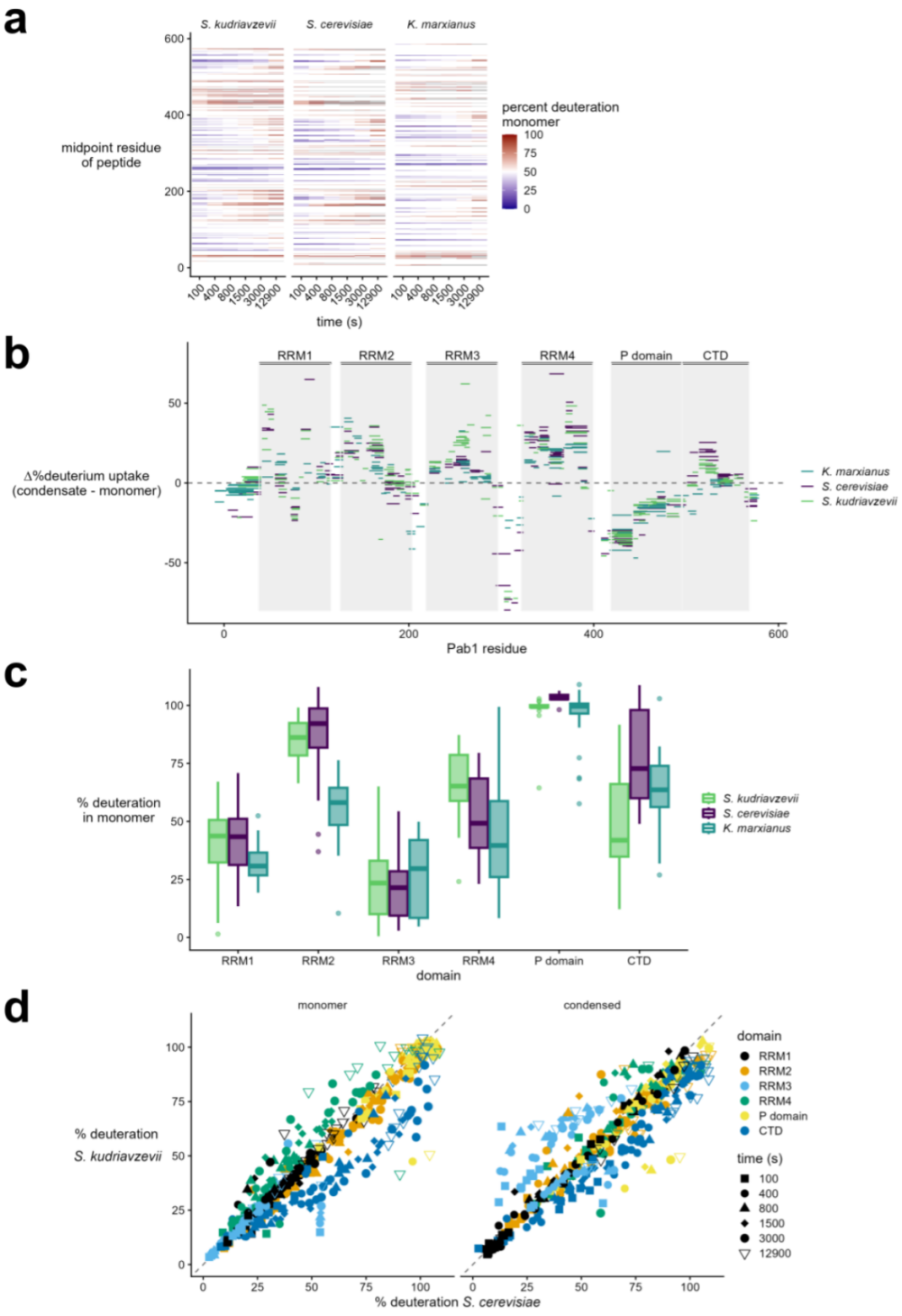

Figure 2.5. HDX-MS investigation of Pab1 ortholog monomers and condensates reveals conservation of condensate structure and mechanism. a Pab1 ortholog peptide percentage deuterium uptake mapped onto primary sequence for each species. **b** Local unfolding of Pab1 RRMs in the condensate is conserved across orthologs, where a positive value indicates higher uptake in the condensate (less stable than monomer) and a negative value indicates lower uptake in the condensate (more stable than monomer). **c** Pab1 monomer deuterium uptake at 3000 s reveals domain stability differences between orthologs. **d** Comparison of peptide deuterium uptake in monomeric (left) and condensed (right) Pab1 of *S. cerevisiae* and *S. kudriavzevii*.

2.4 DISCUSSION

We have measured multiple cellular and molecular responses to temperature in three budding yeast species, diverged by nearly 100 million years, which have adapted to distinct environmental and thermal conditions—the cryophile *S. kudriavzevii*, mesophile *S. cerevisiae*, and thermophile *K. marxianus*. Confirming these designations, cellular growth rate reaches its optimum at different temperatures, and each species' growth ceases at a threshold temperature correlated with this optimum. Upon rapid transfer from optimal growth temperature to near the threshold—heat shock—we observe the classic eukaryotic Hsf1-mediated heat-shock response and sharp downregulation of translation and ribosome biogenesis genes involved in rapid growth in all species. Remarkably, the Msn2/4 regulon, which has long been known to regulate a large fraction of the overall transcriptional response to heat shock and other stresses in *S. cerevisiae*, shows no activation during heat shock in *K. marxianus*.

We carried out what to our knowledge is the first proteome-scale assessment of the conservation of biomolecular condensation across species, examining the condensation response to heat shock which has been previously studied in *S. cerevisiae* (Wallace et al. 2015; Cherkasov et al. 2015; Iserman et al. 2020; Riback et al. 2017). We find that the biomolecular condensation response is also conserved down to individual protein species, yet tuned to each species' thermal niche.

At the molecular level, poly(A)-binding protein (Pab1) isolated from each species condenses at the relevant heat shock temperature, indicating that the tuning of these proteins is encoded in the amino acid sequence itself. The adaptive nature of Pab1 condensation during heat stress, which we discovered in *S. cerevisiae (Riback et al. 2017)*, is conserved in *S. kudriavzevii* at the corresponding temperatures for the cryophile. Finally, by comparing

structural differences in condensates relative to monomers across species, we are able to propose a mechanism by which the proteins' sequence leads to temperature-tuned behavior.

2.4.1 Transcriptomic remodeling

S. cerevisiae and *S. kudriavzevii* show similar transcriptome-level responses as expected from their close evolutionary relationship, with divergence 10 million years ago, long after the whole genome duplication in this clade (Figure 2.1a and (Salvadó, Arroyo-López, Guillamón, et al. 2011; Kumar et al. 2022)). The two genomes are so similar that interspecies hybrids can be constructed which display intermediate growth and heat-induced foci phenotypes (Kempf, Lengeler, and Wendland 2017). *S. cerevisiae* and *K. marxianus,* which diverged ~100 million years ago and before the whole-genome duplication, show more significant divergence in their transcriptional responses. Not only did the ancestor of *K. marxianus* diverge from *S. cerevisiae* ~100 million years ago, but it did so prior to the whole genome duplication in this fungal clade (Kumar et al. 2022). All three species induce the Hsf1-regulated transcriptional response, as well as downregulating genes involved in protein synthesis and ribosome biogenesis, both transcripts encoding ribosomal protein subunits and those encoding auxiliary biogenesis factors. They diverge, however, most notably in the regulation of genes controlled by the transcription factor pair Msn2/4.

The conserved transcriptional responses reflect well-known functional responses to temperature: slowing of growth by suppressing ribosome production and translation factors, as well as massive induction of molecular chaperones in the Hsf1 regulon to respond to temperature-induced protein misfolding and regulate biomolecular condensate formation (Figure 2.2). Despite its name, heat shock factor 1 is activated by a wide range of

environmental stresses (Gasch et al. 2000; Tye and Churchman 2021). Interestingly, in these stresses, biomolecular condensation is also observed (Brengues and Parker 2007; Hoyle et al. 2007; Buchan, Muhlrad, and Parker 2008; Kato, Yamamoto, and Izawa 2011; Buchan, Yoon, and Parker 2011; Cherkasov et al. 2013; Yamamoto and Izawa 2013; Wallace et al. 2015). We hypothesize that Hsf1 is conserved across organisms and across stresses due to its induced proteins and their function: molecular chaperones which aid in the dispersal of condensates. Hsp70 protein, whose transcript can be induced by Hsf1 up to 1,000-fold upon heat shock, has been shown to re-localize to condensates during stress (Cherkasov et al. 2013). Hsp70 also remodels condensates with other Hsf1-induced chaperones like Hsp104 and Sis1 *in vitro* (Yoo et al. 2022). Chaperones induced by Hsf1 are responsible for targeting misfolded protein aggregates generated from nascent polypeptides or newly synthesized proteins for degradation (Trotter et al. 2001; Geiler-Samerotte et al. 2011), but recent work has also shown that proteins in condensates retain structural integrity and are reversible, specific, and active (Wallace et al. 2015; Riback et al. 2017). Given the repressive role of Hsp70 to Hsf1 and its heat-induced recruitment to condensates taken with the near-native structure of proteins in condensates, we propose Hsf1 as a regulon to coordinate the dispersal of biomolecular condensates rather than a heat-specific, degradation-inducing set of genes.

Other regulons across the species, however, do not seem to be completely conserved in their heat regulation (Figure 2.2). One surprisingly divergent regulon is that of Msn2/4, which has long been considered a master regulator of the environmental stress response (Kobayashi and McEntee 1993; Marchler et al. 1993; Martínez-Pastor et al. 1996; Gasch et al. 2000). Msn2/4-controlled genes are induced in many stresses, and help regulate metabolism and glycolysis (Kuang et al. 2017). We confirm this standard role in *S. kudriavzevii*, but observe that

a substantial fraction of the regulon is downregulated in *K. marxianus* despite the robust Hsf1 response, translation repression, and growth-rate reduction that unambiguously mark the onset of the environmental stress response. This result is particularly surprising given that Msn2/4 is the larger of the two regulons. We provide further evidence that organisms with varying life histories utilize distinct transcriptional programs to respond to stress (Brion et al. 2016; Sakihama et al. 2019; Heineike and El-Samad 2021), and the Msn2/4 regulon is not completely conserved in *K. marxianus*, likely due to its non-fermentative energy consumption.

2.4.2 Biomolecular condensation

Biomolecular condensates are ubiquitous in cells under a wide array of conditions. These non-membrane bound assemblies generally contain both protein and RNA and can exist constitutively or form upon stress caused by environmental changes (e.g., temperature increase, nutrient starvation, hypoxia) or exogenous small molecule exposure (e.g., sodium azide, arsenite). However, the physiological function and phenotypic fitness effects of condensation have largely remained elusive due to the various mechanisms of their formation, challenges in physiological biochemical reconstitution, and their diverse molecular composition (Glauninger et al. 2022). Within mammalian cells, the condensing proteome is distinct depending on the stress (Sui et al. 2020). In yeast, stress granules will not form with mild heat or mild ethanol stress alone, but will form stress granules in the presence of both stresses (Yamamoto and Izawa 2013). Interestingly, pre-treatment of either stress affects the components of stress granules upon combined stress (Yamamoto and Izawa 2013). Given the distinct set of proteins observed in condensates upon each stress, it is intriguing that Hsf1 is

also activated, suggesting the Hsf1 regulon is induced not in response to heat, but in fact condensation.

The degree to which condensation is conserved across organisms has not been systematically characterized (Glauninger et al. 2022). Here we have quantified the conservation of condensation using three sister species cultured under identical conditions and exposed to stresses differing only by a temperature shift. Our results provide further evidence that not only is the phenomenon conserved across different niches and over vast timescales, but it is also conserved down to the particular molecular species that are observed in heat-shock-induced condensates (Figure 2.3) and their individual behaviors. For example, Pab1 drastically decreases its solubility in each organism upon heat stress. Importantly, it does so at different temperatures that are tuned to the thermal niche of the organism; a temperature which causes strong condensation of Pab1 from a cryophile, 37°C, is the same temperature which leaves Pab1 from the thermophile fully uncondensed. This phenomenon holds proteome-wide, and is not specific to Pab1: the vast majority of proteins identified as condensing in S. cerevisiae (Wallace et al. 2015) have orthologs in K. marxianus which also condense, albeit at an elevated temperature. We also observe that large classes of proteins which remain uncondensed during stress, such as glycolytic enzymes and ribosomal proteins, are similarly consistently soluble in each species at each species' heat-shock temperature. The conservation of condensation behavior provides strong, additional evidence that stress-induced condensation is functionally important and adaptive, and perhaps even serves as a signaling mechanism for transcriptional reprogramming under stressful conditions.

2.4.3 Sequence-encoded behavior

Many studies have shown that purified components of condensates mirror stress-sensitivity *in vitro* (reviewed in (Villegas, Heidenreich, and Levy 2022)). For example, translation factor Sup35 forms condensates during glucose starvation, when the intracellular pH drops. (Franzmann et al. 2018) showed that Sup35 forms gel-like condensates as pH decreases *in vitro*. Likewise, purified Ded1 from yeast forms heat-induced condensates, and this behavior is conserved and tuned in purified protein from *S. kudriavzevii* as well as thermophile *T. terrestris (Iserman et al. 2020).* Purified Pab1's condensation behavior has been shown to be both pH and temperature dependent (Riback et al. 2017). Taken together, these results indicate that stress sensitivity is genetically encoded. Our results support this model, where Pab1 condensation *in vitro* depends on the organism's thermal niche, and mutating a condensation-modulating domain by making it more or less hydrophobic shifts condensation temperature in the same way across species (Figure 2.4).

When comparing residue accessibility between Pab1 condensates and monomers, we are able to propose a mechanism by which species-specific behavior occurs. Using HDX-MS, we found that Pab1 condensate structure and dynamics are similar across three orthologs despite their different onset temperatures. Importantly, the stability of their RRMs correlates with onset temperature (Figure 2.5). Because Pab1 has been found to condense via a sequential activation mechanism involving local unfolding (Chen et al. 2022), these results provide a parsimonious explanation to how Pab1 condensation can be set to an organism's temperature niche. In sum, our observations argue for the conservation of Pab1 condensation mechanism and structure from cryophile to thermophile. By tuning the stability and the activation threshold of orthologous Pab1 RRMs, nature enables Pab1 condensation to be

triggered in response to each organism's relative stress temperature, but further work using RRM-swapped variants from Pab1 orthologs is still needed. This remarkable conservation of local structural changes and a lack of complete misfolding upon severe heat shock across species further promotes the idea that condensation is advantageous to organisms across the tree of life.

2.4.4 Phenotypic consequences of condensation

The ability to form condensates in *S. cerevisiae* during stress has been shown to be adaptive (Riback et al. 2017; Franzmann et al. 2018; Iserman et al. 2020). Our results demonstrate that endogenous Pab1 mutant replacement in *S. kudriavzevii* mirrors what has been observed in *S. cerevisiae*: the increased condensation temperature of Pab1 reduces the ability of the organism to grow during its commensurate heat stress temperature (Figure 2.4). However, this does not result in death of the organism, shown by resumed growth after recovery at non-stress temperatures. In other words, condensation serves as a mechanism for dealing with increased heat and allowing for continued growth at stress temperatures. Previous work speculated that soluble Pab1 protein represses stress mRNAs, but condensed Pab1 releases the mRNAs which allows for their translation (Riback et al. 2017; Yoo et al. 2022), but the exact function remains unclear. We conclude that the phenotypic consequences of heat-induced condensation are conserved across species.

2.4.5 Evolutionary and molecular insights

From ecological niche, to growth and survival, to gene expression, to purified protein, to individual amino acid residues, we show that condensation is a cellular phenomenon that

organisms must be able to employ to grow and survive at increased temperature. Our systematic characterization of three fungi adapted to different thermal niches demonstrates that cellular responses to temperature are molecularly tuned to the environment to which they are adapted. These data raise questions about other condensation-inducing stresses. Do organisms that metabolize different carbon sources contain condensates of orthologous protein components during nutrient starvation? How does genetic diversity contribute to condensation? For example, do cell lines derived from diverse populations show varied condensation during heat stress? Can we identify how condensation is encoded in the genome, identifying condensation quantitative trait loci (QTLs)? These questions remain open, but our results suggest clear hypotheses. We conclude that condensation is a functional, tuned, and adaptive response to stress.

2.5 METHODS

2.5.1 Experimental model and subject details

Phylogenetic relationships

Evolutionary relationships and divergence times were estimated using timetree.org (Kumar et al. 2022).

Identification of orthologs

Orthologs between *S. cerevisiae* and *S. kudriavzevii* were found using the Yeast Gene Order Browser v8 (http://ygob.ucd.ie/) using Pillars.tab file to confidently assign homology (Byrne and Wolfe 2005). *K. marxianus* orthologs to *S. cerevisiae* were obtained using both the KEGG

BRITE Orthology database (Kanehisa et al. 2023) and the eggNOG v5.0 database (Huerta-Cepas et al. 2019).

Maximum specific growth assays

Three wild-type strains were used to measure growth: *S. cerevisiae* BY4742, *S. kudriavzevii* FM1389, and *K. marxianus* DMKU3-1042. A dense overnight culture was diluted into fresh YPD and allowed to grow to log phase (OD_{600} ~0.1). OD_{600} measurements were taken periodically during log phase growth. At least two biological replicates were performed for each species and time point. Maximum specific growth rates were obtained by estimating the slope of the linear range of growth for each species and time point. Resulting growth curves were fitted using the cardinal temperature model with inflection (Rosso, Lobry, and Flandrois 1993).

Strain construction

Saccharomyces kudriavzevii mutants were obtained using CRISPR-Cas9 genome editing. Briefly, competent FM1389 were prepared (Frozen-EZ Yeast Transformation II Kit™, Zymo Research). Competent cells were transformed according to the protocol except with a 90 min incubation at 23°C. DNA was used at concentrations of at least 200 µg of Cas9/guide RNA-containing plasmid with a *URA3* selectable marker along with >500 µg of linear repair template as previously described (Lee et al. 2015; Akhmetov et al. 2018). Transformation reactions were spread on -Ura plates. Transformants were cured of the Cas9/guide RNA plasmid with patch plating and confirmed by sequencing. Multiple transformants obtained by using distinct guide RNAs were screened to check for morphological and phenotypic homogeneity.

Spot assay

For each strain, a dense overnight culture was diluted into fresh YPD and allowed to grow for at least 6 hours until cells reached OD_{600} of at least 0.1. Each culture was diluted to a matching OD_{600}. Cultures were then serially diluted 10-fold into dH_2O, and 7 µL of each dilution was spotted onto plates. Plates were incubated at the specified temperature for 4 days and then imaged. Plates were then moved to room temperature and incubated for 2 days and imaged again.

Flow cytometry

Cells were grown overnight to OD_{600} ~0.05 in SC-complete medium with 2% dextrose, and heat shocked for 20 minutes at the specified temperature. Cells were allowed to recover for 3 hours with shaking at 23°C. Data were collected on the Attune NxT (Thermo Fisher) using the plate reader functionality at 100 uL/min for 100 uL samples. At least 20,000 events were recorded per 100 uL of cells. Voltage was set as follows: Forward scatter: 1; Side scatter: 200; YL2 (mCherry): 540; BL2 (autofluorescence): 420.

All experiments were performed with the same voltage set, and the fluorescence values reported reflect within-experient forward scatter area and autofluorescence-normalized values. Sub-populations of cells that exhibited high autofluorescence (abnormally high BL2 signal) were filtered out from the analysis. At least 5,000 cells per sample remained for analysis. Fold-change values were calculated from unstressed cells grown, treated, and recovered at 23°C.

qPCR

DMKU-1042 was grown at 23°C until OD_{600} reached between 0.4-0.6, and then 1 mL was aliquoted into 1.5 mL tubes. Samples were then treated at specified temperature for 20 minutes. Cells were centrifuged at 3,000 g for 1 minute at room temperature. The supernatant was removed, and the cell pellet was snap frozen in liquid nitrogen and stored at -80°C.

Total RNA was extracted using Direct-zol RNA Miniprep kit (Zymo cat. no R2052) with Ambion TRI-reagent (Fisher cat. no. AM9738) and Zirconia/Silica 0.5 mm homogenization beads (Biospec cat. no. 11079105Z). Approximately 100 µg of RNA was reverse transcribed (iScript cDNA synthesis kit, cat. no. 1055770) using gene specific priming within the native sequence. All transcript abundances are expressed as a ratio to a control gene (*PGK1*) in the same sample relative to the same value in unstressed cells.

RNA-sequencing

Sample preparation

Each species (strains BY4742, FM1389, DMKU3-1042) was grown at its optimum growth temperature until OD_{600} was between 0.2-0.4. Then, 1.2 mL of cells were transferred to a 1.5 mL tube and treated at either the control temperature or their maximum heat shock temperature for 8 minutes. Cells were then centrifuged at 3,000 g for 1 minute at room temperature, and the supernatant was removed. Cells were flash frozen and stored at -80°C.

Library Generation

Total RNA was extracted using Direct-zol RNA Miniprep kit (Zymo cat. no R2052) with Ambion TRI-reagent (Fisher cat. no. AM9738) and Zirconia/Silica 0.5 mm homogenization beads

(Biospec cat. no. 11079105Z). Samples were treated with Dnase I (NEB M0303S). Two biological replicates were generated for each organism and condition. Sequencing libraries were prepared by Novogene (https://www.novogene.com/us-en/). Messenger RNA was purified from total RNA using poly-T oligo-attached magnetic beads. After fragmentation, the first strand cDNA was synthesized using random hexamer primers followed by the second strand cDNA synthesis, end repair, A-tailing, adapter ligation, size selection, amplification, and purification. Paired-end sequencing of the library was then performed on an Illumina instrument.

Data Processing

RNA sequencing reads were processed using a custom Snakemake pipeline which will be available on Data Dryad (Mölder et al. 2021). Raw reads were first processed using TrimGalore v0.6.10 to remove Illumina sequencing adapters using default settings (doi: 10.5281/zenodo.7598955) (Martin 2011). All genomic DNA sequences and GTF files were downloaded from NCBI using the following versions (*Saccharomyces cerevisiae*: GCF_000146045.2_R64, *Saccharomyces kudriavzevii*: GCA_947243785.1_Skud-ZP591, *Kluyveromyces_marxianus*: GCA_001417885.1_Kmar_1.0). These files were then used by STAR v2.7.10b to generate indices (--sjdbOverhang 99 --sjdbGTFtagExonParentTranscript transcript_id --sjdbGTFfeatureExon CDS --sjdbGTFtagExonParentGene gene_id --genomeSAindexNbases 10)(Dobin et al. 2013). Mapping of the filtered and trimmed fastqs was also done with STAR v2.7.10b (--alignMatesGapMax 20000). The reads mapping to each gene were quantified using HTSeq v2.0.2 (--stranded=no --type=CDS --idattr=gene_id)(Putri et al. 2022).

Data Analysis

Gene lengths were extracted for each gene by first adding exon annotations to the GTF files using a custom script based on gffutils v0.11.1 (https://github.com/daler/gffutils). Gene lengths were then calculated using the GenomicFeatures package in R (Lawrence et al. 2013). These lengths were then used to calculate transcript per million values (TPMs). In addition, fold changes in transcript abundance were calculated using DESeq2 v3.16 (Love, Huber, and Anders 2014). All scripts used for data analysis will be available on Data Dyrad.

Annotation of genes

Protein annotations were derived from the following sources. The targets of HSF1 and Msn2/4 were curated from (Pincus et al. 2018) and (Solís et al. 2016). The genes for core ribosomal proteins, ribosome biogenesis factors, and glycolytic enzymes (superpathway of glucose fermentation) as well as transcription factor regulation assignments were derived from the Saccharomyces Genome Database (Cherry et al. 2012; Engel et al. 2014). Genes for translation factors were derived from the KEGG BRITE database (Kanehisa et al. 2016). Transcription factor regulators were assigned according to (Triandafillou et al. 2020).

In vivo biochemical fractionation and mass spectrometry sample preparation

Yeast cells (BY4743, FM1171, or DMKU3-1042) were grown in SC-complete medium with 2% dextrose (50 mL of medium per treatment) at either 23°C or 30°C with 250 rpm shaking until OD_{600} was between 0.4-0.6. Cells were transferred to a 50 mL conical tube and harvested via centrifugation at 2,500 g for 5 min in a swinging bucket rotor at room temperature. The supernatant was decanted and the conical tubes containing cells were immediately placed in water baths set to the treatment temperature. After the specified time period, cells were

resuspended in 1 mL ice-cold soluble protein buffer (SPB; 20 mM HEPES-KOH pH 7.3, 120 mM KCl, 2 mM EDTA, 0.2 mM DTT, 1 mM PMSF, and 1:1000 protease inhibitors cocktail IV (Millipore Sigma)), transferred to a pre-chilled 1.5 mL tube, and spun for 30 s at 5,000 g at 4°C. The supernatant was discarded, and the cell pellet was resuspended in 200 µL of SPB. Two 100 µL aliquots from the resuspended sample were snap frozen in a safe-lock tube in liquid nitrogen.

Cells were lysed using cryomilling and fractionated with ultracentrifugation as described in (Wallace et al. 2015), with minor modifications. Briefly, cells were lysed with 5x90 s agitations at 30 Hz. After lysis, cellular material was resuspended in 900 µL of SPB and thawed on ice with occasional vortexing. The lysate was clarified to remove very large aggregates and membrane components with a 3,000 g spin for 30 s at 4°C. Then, 650 µL of clarified lysate was moved to a pre-chilled 1.5 mL tube. For a Total sample, 100 µL was mixed with 300 µL total protein buffer (TPB; 20mM HEPES-NaOH pH 7.4, 150mM NaCl, 5mM EDTA, 3% SDS, 1 mM PMSF, 2mM DTT, and 1:1000 protease inhibitors IV) and processed as described in (Wallace et al. 2015). Of the remaining clarified lysate, 500 µL was transferred to a vacuum safe tube spun at 100,000 g for 20 minutes at 4°C (fixed-angle TLA-55 rotor in a Beckman Coulter Optimax tabletop ultracentrifuge). The Supernatant fraction was decanted (as much as 400 µL) and snap frozen in liquid nitrogen. The pellet fraction was isolated as described in (Wallace et al. 2015).

Protein was extracted from each fractionated sample using a chloroform-methanol method adapted from (Wessel and Flügge 1984). To 100 µL of sample, 400 µL of methanol was added and vortexed. Then 100 µL of chloroform was added and vortexed. 300 µL of dH_2O was added and samples were vortexed. Samples were centrifuged for 1 minute at 14,000 g. The top aqueous layer was removed, and 400 µL of methanol was added. Samples were vortexed and

then centrifuged for 5 minutes at 20,000 g. The remaining methanol was removed with a pipette, and the sample was dried at 55°C. The protein flake was submitted for digestion and mass spectrometry at MS Bioworks.

Mass spectrometry

Sample Preparation

Protein flake was solubilized in urea lysis buffer (8M urea, 50mM Tris.HCl pH8, 150mM NaCl, 1X Roche cOmplete protease inhibitor) using a QSonica sonic probe with the following settings: Amplitude 50%, Pulse 10 x 1s. 1 on 1 off. The lysate was incubated at room temperature for 1hr with mixing at 1000 rpm in an Eppendorf ThermoMixer and then centrifuged at 10,000g for 10 minutes at 25°C. Protein quantitation was performed using a Qubit protein assay (Invitrogen), protein yields are provided below. 25µg of each lysate was digested as follows: reduced with 15mM dithiothreitol at 25°C for 30 minutes followed by alkylation with 15mM; iodoacetamide at 25°C for 45 minutes in the dark; digested with 2.5µg sequencing grade trypsin (Promega) at 37°C overnight. The final digest volume was 0.5mL adjusted with 25mM ammonium bicarbonate; cooled to 25°C, acidified with formic acid and desalted using a Waters Oasis HLB solid phase extraction plate; eluted samples were frozen and lyophilized; pooled sample was made by mixing equal amounts of digested material from each sample. This pooled sample was used to generate a gas phase fractionation library.

Mass Spectrometry - DIA Chromatogram Library Generation

1µg of the pooled sample was analyzed by nano LC- MS/MS with a Waters M-class HPLC system interfaced to a ThermoFisher Exploris 480. Peptides were loaded on a trapping column and eluted over a 75µm analytical column at 350nL/min; both columns were packed with

XSelect CSH C18 resin (Waters); the trapping column contained a 5µm particle, the analytical column contained a 2.4µm particle. The column was heated to 55°C using a column heater (Sonation). The sample was analyzed using 6 x 1.5hr gradients. Six gas-phase fractions (GPF) injections were acquired for 6 ranges: 396 to 502, 496 to 602, 596 to 702, 696 to 802, 796 to 902, and 896 to 1002. Sequentially, full scan MS data (60,000 FWHM resolution) was followed by 26 x 4 m/z precursor isolation windows, another full scan and 26 x 4 m/z windows staggered

by 2 m/z; products were acquired at 30,000 FWHM resolution. The automatic gain control (AGC) target was set to 1e6 for both full MS and product ion data. The maximum ion injection time (IIT) was set to 50ms for full MS and dynamic mode for products with 9 data points required across the peak; the NCE was set to 30.

Mass Spectrometry - Sample Analysis

Samples were randomized for acquisition. 1µg per sample was analyzed by nano LC/MS with a Waters M- class HPLC system interfaced to a ThermoFisher Exploris 480. Peptides were loaded on a trapping column and eluted over a 75µm analytical column at 350nL/min; both columns were packed with XSelect CSH C18 resin (Waters); the trapping column contained a 5µm particle, the analytical column contained a 2.4µm particle. The column was heated to 55°C using a column heater (Sonation). Samples were analyzed using 1.5hr gradients. The mass spectrometer was operated in data-independent mode. Sequentially, full scan MS data (60,000 FWHM resolution) from m/z 385-1015 was followed by 61 x 10 m/z precursor isolation windows, another full scan from m/z 385-1015 was followed by 61 x 10 m/z windows staggered by 5 m/z; products were acquired at 15,000 FWHM resolution. The maximum ion

injection time (IIT) was set to 50ms for full MS and dynamic mode for products with 9 data points required across the peak; the NCE was set to 30.

Data Processing

DIA data were analyzed using Scaffold DIA 3.3.1 (Proteome Software) which served several functions: 1) Conversion of RAW files to mzML (ProteoWizard) including deconvolution of staggered windows; 2) Conversion to DIA format; 3) Alignment based on retention times; 4) Searching of data using Prosit library (DLIB) and the chromatogram/reference library to create custom ELIB; 5) Filtering of database search results using Percolator at 1% peptide false discovery rate (FDR); 6) Calculation of peak areas for detected peptides using Encyclopedia (0.9.6). For each peptide the 5 highest quality fragment ions were selected for quantitation.

Data were searched with the following parameters: Enzyme: Trypsin; Database: UniProt *Kluyveromyces marxianus*; Fixed modification: Carbamidomethyl (C); Precursor Mass Tolerance: 10 ppm; Fragment Mass Tolerance: 10 ppm; Library Fragment Tolerance: 10 ppm; Peptide FDR: 0.01; Protein FDR: 0.01; Peptide Length: 6-30AA; Max Missed Cleavages: 1; Min. Peptides: 2; Peptide Charge: 2-3.

The samples table was exported from Scaffold DIA and further analyzed in Perseus (Tyanova et al. “The Perseus computational platform for comprehensive analysis of (prote)omics data” Nature Methods, 2016.)

Calculation of pSup

The statistical model used to estimate the proportion in supernatant (pSup) was based on that used in (Wallace et al. 2015). For each fractionated sample, the relative abundance of proteins within each fraction—total (T), supernatant (S), and pellet (P)—were inferred from mass

spectrometric data (see [MS methods section]). While proteins are expected to obey conservation of mass in the original fractionated lysate ($T_i = S_i + P_i$ for protein species i), this assumption does not hold in the ratios of abundances directly inferred from the data. Instead, for a particular experiment, $T_i = a_S S_i + a_P P_i$ where we refer to the per-experiment constants a_S and a_P as mixing ratios which reflect differential processing and measurement of individual fractions. In order to estimate mixing ratios, and thus recover the original stoichiometry, we assume conservation of mass for each protein in the sample, and then use Markov Chain Monte Carlo sampling to estimate the mixing ratios under this constraint (Robert and Casella n.d.). We also assume negative binomial noise for each measurement. Specifically, we model mRNA abundance as follows:

$$log(T_i) \sim N(log(\alpha_S S_i + \alpha_P P_i), \sigma)$$

where

$T_i =$ measured abundance of protein *i*,

$S_i =$ measured abundance in supernatant of protein *i*,

$P_i =$ measured abundance in pellet of protein *i*,

$\alpha_S =$ mixing ratio of supernatant sample,

$\alpha_P =$ mixing ratio of pellet sample

With the following priors:

$$\alpha_S \sim \Gamma(1, 1)$$

$$\alpha_P \sim \Gamma(1, 1)$$

$$\sigma \sim Cauchy(0, 3)$$

We implemented the model above in R using the probabilistic programming language STAN, accessed using the rstan package (Stan Development Team 2023; R Core Team 2022) and used all proteins with $intensity > 1$ to estimate mixing ratios for each sample. These mixing ratios were then used to calculate the pSup for protein i: $pSup_i = \frac{\alpha_S S_i}{\alpha_S S_i + \alpha_P P_i}$.

Pab1 wild-type and mutant protein purification

Pab1 wild-type and mutant proteins were purified according to (Yoo et al. 2022) with minor modifications. The sizing column used was a Superose 6 Increase 10/300 GL (GE Healthcare), and concentrations were measured using a NanoQuant plate (TECAN).

Dynamic light scattering of purified protein

DLS measurements were performed in a DynaPro NanoStar Plate Reader (Wyatt). Each time point was the average of five 6-second acquisitions. Measurements were performed at a slow ramp (set to 0.25C/min) starting at 25°C and ending at 55°C. All experiments were performed with 30 µL of 15 µM purified Pab1 protein, dialyzed overnight in freshly prepared buffer with 20 mM MES pH 6.4, 150 mM KCl, 2.5 mM $MgCl_2$, and 1 mM DTT. Samples were centrifuged for 20 min at 20,000 g at 20°C before loading in the plate. To prevent evaporation of the sample, 10 µL of light mineral oil was layered on top of the sample. T_{demix} is calculated as previously described (Riback et al. 2017) except that the value of the baseline was calculated as the average R_h values below 35°C. This change was implemented to account for the fewer acquisitions per sample due to use of the plate reader rather than a single cuvette.

Hydrogen-Deuterium Exchange

Condensate preparation for HDX-MS

Condensates were largely prepared as in Chen et al., 2023. A 10 uM Pab1 stock was exposed to the condensing condition at pH 6.5 (ScPab1 at 46°C for 20 min, SkPab1 at 46°C for 20 min, and KmPab1 at 46°C for 20 min, followed by 50°C for 10 min, followed by 55°C for 10 min). After temperature exposure, condensates were collected via a 16kg, 10 min spin. The supernatant was discarded, and the pellets were washed 2x with fresh buffer using the same centrifugation procedure.

HDX labeling

HDX labeling was generally completed as in Chen et al., 2023 with the following exceptions. For both monomer and condensed states for the 3 orthologs, samples at HDX timepoints of 100, 400, 800, 1500, 3000, and 12900 seconds were collected with pDcorr 6. "Saturated" control samples were labeled at pDcorr 6 overnight.

LC-MS and HDX-MS data analysis

LC-MS was completed as in Zmyslowski et al 2022. HDX-MS data analysis was completed as in Chen et al 2023, with the exception that peptides were not filtered by confidence score and downstream analysis was completed using R.

Table 2.1. Yeast strains used in this study.

Organism/strain	Genotype	Source
S. cerevisiae BY4742	MATα ura3Δ0 leu2Δ0 his3Δ1 lys2Δ0	(Brachmann et al. 1998)
S. kudriavzevii FM1389 (original ZP591)	MATα hoΔ::kanMX ura3Δ0 his3Δ0	(Scannell et al. 2011)
K. marxianus DMKU3-1042	MATα	NBRC 104275 (Japan)
S. cerevisiae yCDK061	MATα ura3Δ0 leu2Δ0 his3Δ1 lys2Δ0 PAB1-1255-1506::Pab1*1255-1506, MV→A	(Riback et al. 2017)
S. cerevisiae yCDK066	MATα ura3Δ0 leu2Δ0 his3Δ1 lys2Δ0 PAB1-1255-1506::Pab1*1255-1506, MV→I	(Riback et al. 2017)
S. kudriavzevii ySMK103	MATα hoΔ::kanMX ura3Δ0 his3Δ0 SKDZ_05G2450(PAB1)-1255-1506::SKDZ_05G2450(Pab1)*1255-1506, MV→A	This study
S. kudriavzevii ySMK105	MATα hoΔ::kanMX ura3Δ0 his3Δ0 SKDZ_05G2450(PAB1)-1255-1506::SKDZ_05G2450(Pab1)*1255-1506, MV→I	This study
S. kudriavzevii FM1171	MATa/MATα	(Hittinger et al. 2010)
S. cerevisiae BY4743	MATa/α ura3Δ0/ura3Δ0 leu2Δ0/leu2Δ0 his3Δ0/his3Δ0 MET15/met15Δ0 LYS2/lys2Δ0	(Brachmann et al. 1998)
S. cerevisiae yCGT027	MATα ura3Δ0 leu2Δ0 his3Δ1 lys2Δ0 SSA4::SSA4-mCherry	(Triandafillou et al. 2020)
S. kudriavzevii ySMK009	MATα hoΔ::kanMX ura3Δ0 his3Δ0 SKDZ_05G1830(SSA4)::SKDZ_05G1830(SSA4)-mCherry	This study

Table 2.2. Plasmids used in this study

Plasmid	Details	Source
pSK166	8xHis-(TevC)-SKDZ_05G2450(PAB1) in pET28a backbone	This paper
pSK168	8xHis-(TevC)-SKDZ_05G2450(PAB1) MV→A in pET28a background	This paper
pSK170	8xHis-(TevC)-SKDZ_05G2450(PAB1) MV→I in pET28a background	This paper
pSK172	pV1382 + SKDZ_05G2450(PAB1) P-domain guide CGGCCGCAGCGGTAGCTTGT	(Vyas et al. 2018); this paper
pSK173	pV1382 +SKDZ_05G2450(PAB1) P-domain guide CAACAAATGAACCCAATGGG	(Vyas et al. 2018); this paper
pSK174	pV1382 + SKDZ_05G2450(PAB1) P-domain guide TACGGTGTCCCTCCACAAGG	(Vyas et al. 2018); this paper
pSK180	8xHis-(TevC)-KLMA_30299(PAB1) MV→I in pET28a background	This paper
pSK181	8xHis-(TevC)-KLMA_30299(PAB1) MV→I in pET28a background	This paper
pSK182	8xHis-(TevC)-KLMA_30299(PAB1) MV→I in pET28a background	This paper
pSK022	pCGT07 + SKDZ_05G1830(SSA4)- mCherry repair template carrier	(Triandafillou et al. 2020); this study
pSK025	Cen6-URA + Cas9-PGK1 + SKDZ_05G1830(SSA4) guide CGGAACCGGACCTGCTCCAG	(Lee et al. 2015); this paper
pSK026	Cen6-URA + Cas9-PGK1 + SKDZ_05G1830(SSA4) guide GGTGCTGGAGCAGGCCCAAG	(Lee et al. 2015); this paper
pJAR006	8xHis-(TevC)-Pab1 in pET28a backbone	(Riback et al. 2017)
pJAR033	8xHis-(TevC)-Pab1 MV→A in pET28a background	(Riback et al. 2017)
pJAR035	8xHis-(TevC)-Pab1 MV→I in pET28a background	(Riback et al. 2017)

2.5.2 Data Code and Availability

Code and data analysis

All data analysis was performed with R (R Development Core Team, 2017) using packages from the tidyverse (Wickham et al. 2019). Plots were made with ggplot2 (Wickham n.d.). Custom packages can be found on GitHub (Triandafillou, 2020a; https://github.com/ctriandafillou/flownalysis; copy archived at https://github.com/elifesciences-publications/flownalysis; Triandafillou, 2020b; https://github.com/ctriandafillou/cat.extras; copy archived at https://github.com/elifesciences-publications/cat.extras). Raw data and scripts that produce plots that appear in this work will be available on Data Dryad.

Statistical Tests

All correlations were calculated with Pearson's correlation coefficient and executed in R.

Data Availability

Data used in this study are from publicly available datasets: yeast proteome available from Saccharomyces Genome Database http://sgd-archive.yeastgenome.org/sequence/S288C_reference/orf_protein/,

2.6 SUPPORTING INFORMATION

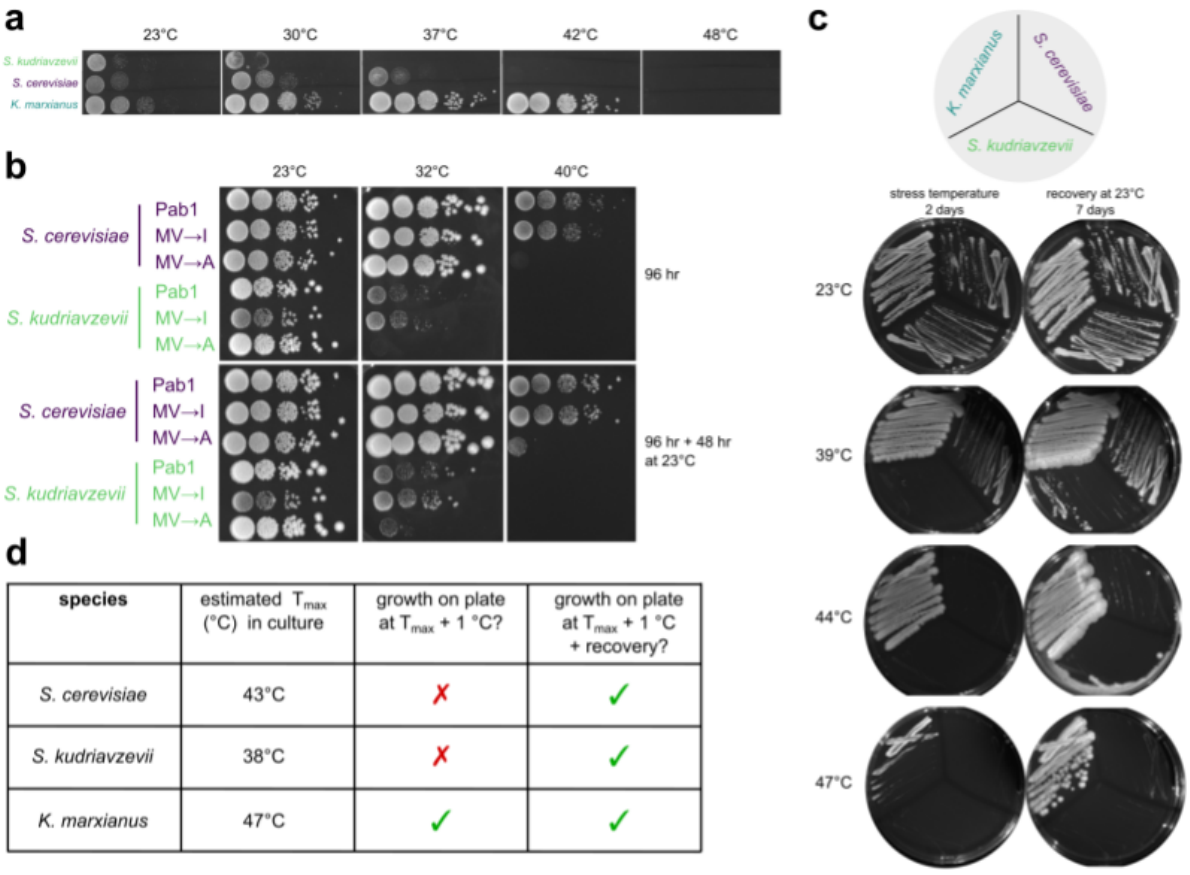

d

species	estimated T_{max} (°C) in culture	growth on plate at T_{max} + 1 °C?	growth on plate at T_{max} + 1 °C + recovery?
S. cerevisiae	43°C	✗	✓
S. kudriavzevii	38°C	✗	✓
K. marxianus	47°C	✓	✓

Figure 2.6. Growth, recovery, and death phenotypes of each three species. a Spot assays of S. cerevisiae, S. kudriavzevii, and K. marxianus strains. Plates were incubated at 23, 30, 37, 42, or 48°C for 2 days and then imaged. Columns are 10-fold dilutions. **b** Biological replicate of Figure 4e. **c** Growth on plates of each wild-type yeast species after a single-colony streak on a YPD plate. Each plate was incubated at either control or each species' T_{max} +1°C (calculated from culture) for two days, imaged, then shifted to room temperature, grown for 7 days, and imaged again. **d** Summary table of panel c.

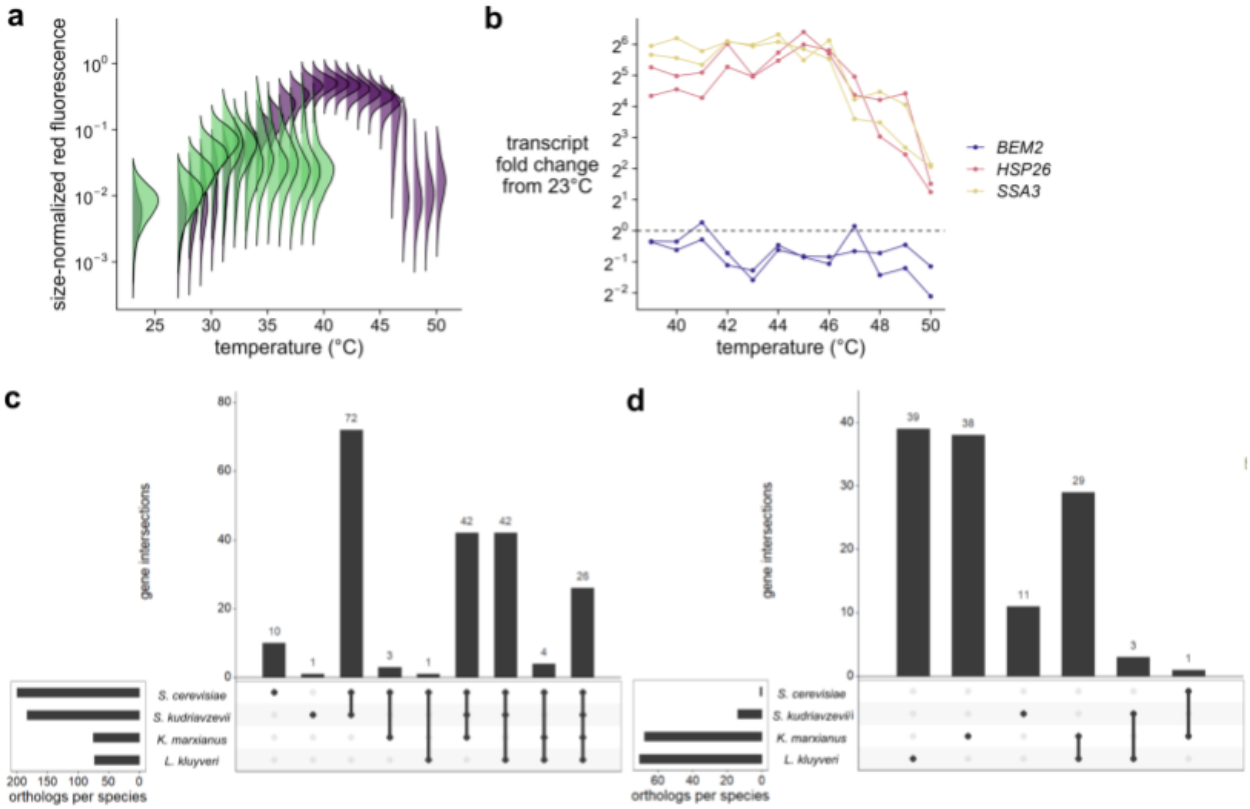

Figure 2.7. Expression dynamics across temperatures.
a Density distributions of red fluorescence normalized by forward scatter for each species and temperature. *S. cerevisiae* distributions are shown in purple, and *S. kudriavzevii* are shown in green. **b** qPCR data from *K. marxianus*, after growth at 23°C and 20-minute heat shock at indicated temperature. Fold change values were calculated from abundance at 23°C after normalization to control gene, *PGK1*. **c**, **d** comparison of Msn2/4 up (**c**) and downregulated (**d**) genes from our study and *L. kluyveri* from Brion et al., 2016. There is strong overlap in upregulated genes and lack of overlap in downregulated genes between pre- and post-duplication relatives, consistent with the hypothesis that the post-duplication orthologs should be substantially similar if there are some ancestral genes which were only recruited into the Msn2/4 post-whole-genome duplication.

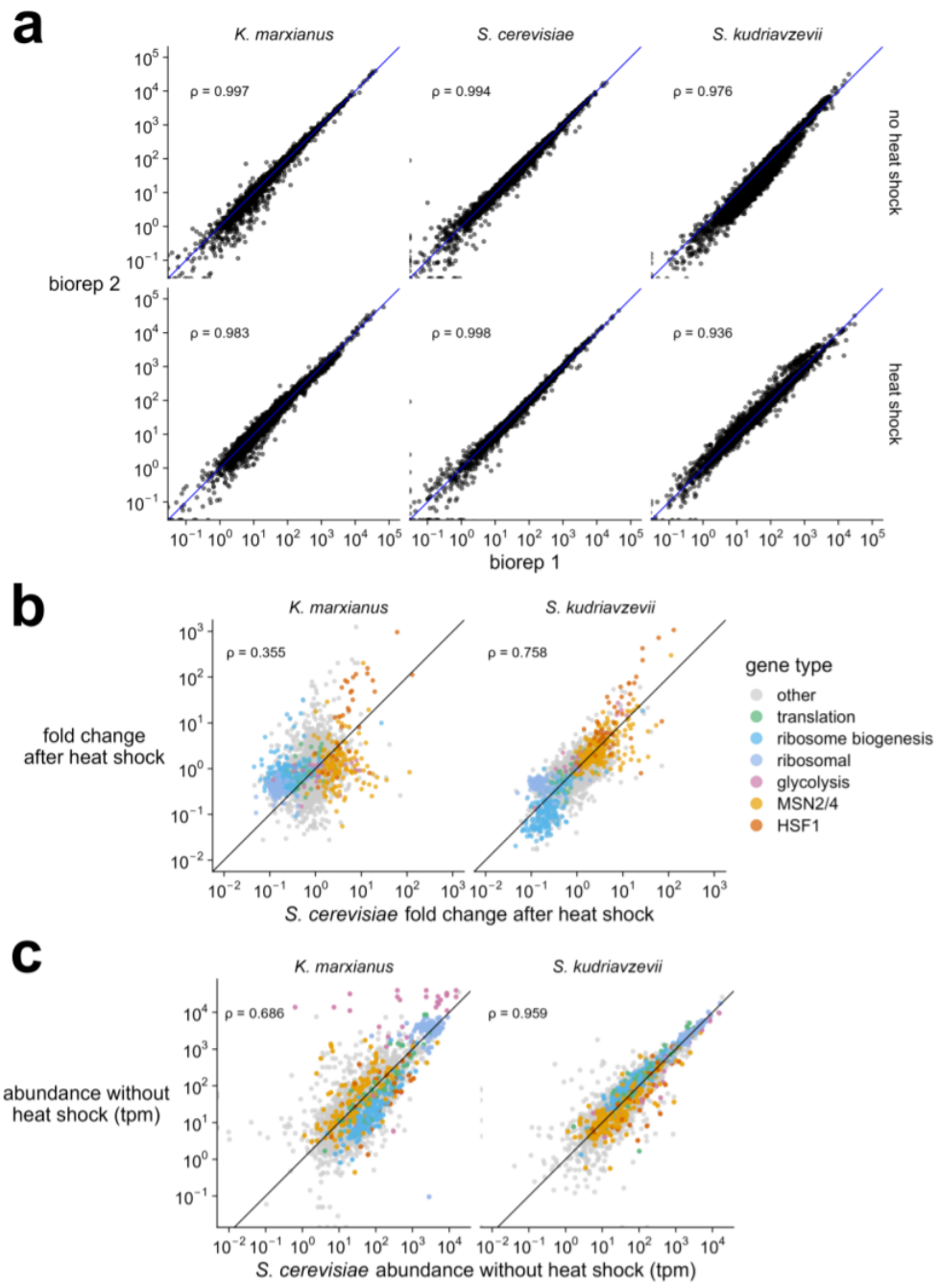

Figure 2.8. Strong correlations in biological replicates and within treatment condition comparisons.
a Transcript abundance (transcripts per million, tpm) between biological replicates in each species. Correlations are represented by Pearson's rho (ρ) calculated between replicates. **b** Fold change distribution for groups of genes (colored by gene type) after stress in each species. Correlations are represented by Pearson's rho (ρ) calculated between species. **c** Transcript abundance (transcripts per million, tpm) in each species without a heat shock. Correlations are represented by Pearson's rho (ρ) calculated between species.

Well	Protein	baseline_radius	baseline_radius_sd	sd_check
F2	SkPab1WT	4.907570444444445	0.10385392527609397	TRUE
H3	KmPab1MV.I	5.020872173913044	0.0895518637924171	TRUE
K4	KmPab1WT	4.873762608695652	0.14987312516735884	TRUE
K5	KmPab1MV.A	4.745623125	0.0936844469282388	TRUE
K9	SkPab1MV.A	4.7453607692307695	0.09255458339646018	TRUE
L12	SkPab1MV.I	5.165217826086956	0.232538851357174	TRUE
NA	J-ScPab1MV.A	4.314985806451613	0.07610316652445605	TRUE
NA	J-ScPab1MV.I	4.351886913580247	0.05017632628147393	TRUE
NA	J-ScPab1WT	4.392046875	0.08042537087253118	TRUE

Table 2.3. Pab1 baseline size estimations. Well indicates DLS experimental well; Protein indicates species abbreviation + Pab1 + mutant version; baseline_radius shows value of the mean radius of data below 35°C; baseline_radius_sd indicates the standard deviation of baseline_radius under 35°C; sd_check: TRUE if baseline_radius_sd is less than 5% of baseline_radius.

Well	Protein	Tdemix	Radius	Rep	Species	Mutant
F2	SkPab1WT	38.1963	10.4914	rep_1	Skud	WT
H3	KmPab1MV.I	46.0497	9.03576	rep_1	Kmarx	MV.I
K4	KmPab1WT	48.9093	10.2584	rep_4	Kmarx	WT
K5	KmPab1MV.A	50.8701	9.70903	rep_2	Kmarx	MV.A
K9	SkPab1MV.A	39.6627	11.0515	rep_2	Skud	MV.A
L12	SkPab1MV.I	36.5503	9.43427	rep_4	Skud	MV.I
NA	J-ScPab1MV.A	40.7226	9.13283	rep_1	Scere	WT
NA	J-ScPab1MV.I	39.2875	8.23502	rep_1	Scere	MV.I
NA	J-ScPab1WT	42.7316	8.99349	rep_1	Scere	MV.A

Table 2.4. Pab1 $T_{condense}$ and estimations and size measurements. Well indicates DLS experimental well; Protein indicates species abbreviation + Pab1 + mutant version; Tdemix represents the temperature where the radius is as close to double the average baseline value below 35°C; Radius is the measured diameter of the radius and Tdemix temperature; rep indicates which replicate is used for the calculation; Species shows an abbreviation of species used; Mutant indicates the version of Pab1 mutant used.

2.7 COMPETING INTERESTS

The authors declare no competing interests.

2.8 AUTHOR CONTRIBUTIONS

Conceptualization, D.A.D.; methodology S.K.K., D.C., C.W.H., H.G., J.A.M.B., M.F., T.R.S., and D.A.D.; investigation, S.K.K., D.C., C.W.H, and H.G.; formal analysis, S.K.K., D.C., C.W.H., H.G., J.A.M.B., and D.A.D.; visualization, S.K.K. and D.A.D.; writing - original draft, S.K.K. and H.G.;

writing - review & editing, S.K.K., D.C., C.W.H., H.G., J.A.M.B., M.F., T.R.S., and D.A.D.; funding acquisition, S.K.K. and D.A.D.; resources, T.R.S. and D.A.D.; supervision, T.R.S. and D.A.D.

2.9 ACKNOWLEDGEMENTS

We thank Dr. Kevin Byrne, Macías LG, Peris D, Martos AAR, Toft C, Hittinger CT, Barrio E, Wolfe KH for graciously sharing *S. kudriavzevii* annotations. We thank Dr. Ian Wheeldon and Sangcheon Lee from the University of California-Riverside for sharing knowledge and plasmids for *K. marxianus*. We thank Dr. David Pincus and Dr. Asif Ali for helpful comments and collaborations with previous iterations of this project. Thank you to D. Edward J. Wallace and Xuejia Ke for assistance with modeling and coding. We thank Dr. Hisashi Hoshida from Yamaguchi University for sharing auxotrophic *K. marxianus* strains. We thank the Biophysics Facility and the Sequencing Core Facility at the University of Chicago. D.A.D. acknowledges support from the NIH (award numbers GM144278 and GM127406). S.K.K. acknowledges support from the NIGMS (award number T32 GM007197-43) and the NIEHS (award number F31 ES032337-01). The content is solely the responsibility of the authors and does not necessarily represent the official views of the NIH.

CHAPTER 3

CHARACTERIZATION OF HEAT SENSITIVE PROTEIN NUG1

This chapter was written and executed by Sammy Keyport Kik and under the guidance of D. Allan Drummond, with the exception of Figure 3.5d, where the qPCR experiment was performed by Catherine G. Triandafillou. Detailed author contributions are listed in section 3.5.

3.1 INTRODUCTION

From microbes to multicellular organisms, all forms of life must respond to changes in their environment. Upon a sub-lethal increase in temperature, for instance, cells carry out a series of adaptive changes. These include inducing massive transcriptional upregulation of a specific set of stress-response genes, many of which encode molecular chaperones (Susan Lindquist 1986; Solís et al. 2016; Pincus et al. 2018); shifting translational activity toward these induced messages (Cherkasov et al. 2013); and downregulating growth and ribosome production (Verghese et al. 2012). Intracellular protein aggregates also form under these conditions as well as under a variety of stresses, including hypoxia, nutrient starvation, and osmotic stress (Grousl et al. 2009; Cherkasov et al. 2013; Wallace et al. 2015; Cherkasov et al. 2015; Fuller et al. 2020; Brengues and Parker 2007; Hoyle et al. 2007; Buchan, Muhlrad, and Parker 2008; Shah et al. 2016). While aggregation has long been viewed as a toxic consequence of stress, recent work suggests that condensation of endogenous proteins reflects an adaptive biomolecular

condensation process and may be an essential step in executing the adaptive changes (Wallace et al. 2015; Riback et al. 2017). The large-scale changes which occur in the cell begin to take place almost instantaneously after receiving the signal of heat, yet surprisingly, the endogenous sensing mechanism for heat shock remains elusive.

As stated, transcriptional upregulation of heat-shock specific genes is a defining feature of the cellular response to heat shock. The core eukaryotic heat shock response (HSR) is regulated by heat shock factor 1 (Hsf1), which induces the transcription of a number of heat shock proteins, including the molecular chaperone Hsp70, which then help refold proteins that have lost their native conformation and aid in dispersing stress-induced condensates (Figure 3.1a). Under physiological growth conditions in *S. cerevisiae*, molecular chaperone Hsp70 repressively binds the transcription factor Hsf1 (Zheng et al. 2016; Krakowiak et al. 2018). The standard model of HSR induction states that increases in temperature cause misfolding of proteins, primarily of newly synthesized polypeptides, which recruits Hsp70 and thus de-represses Hsf1. In this way, protein misfolding serves as the primary sensor of temperature (Morano, Grant, and Moye-Rowley 2012; Kmiecik, Le Breton, and Mayer, n.d.; Vabulas et al. 2010; Sottile and Nadin 2018).

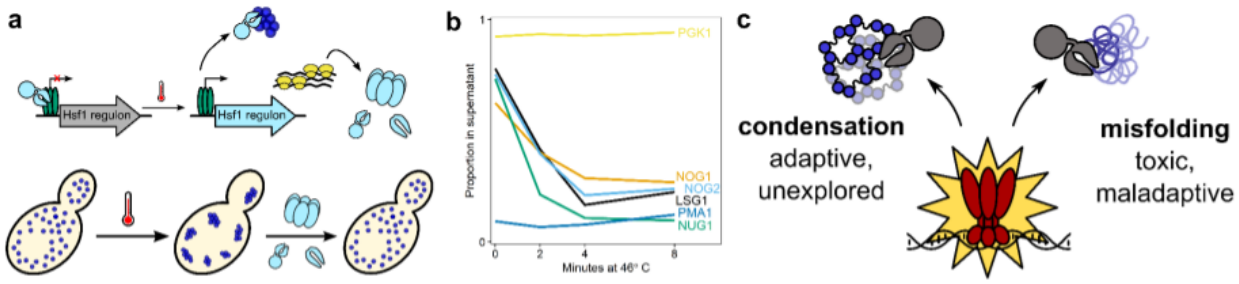

Figure 3.1. The transcriptional heat shock response and biomolecular condensation are induced by temperature. **a** Cells upregulate the production of molecular chaperones (e.g., Hsp70) to disperse biomolecular condensates. **b** Potential candidates, including Nug1, which are predicted to bind Hsp70 are also very sensitive to temperature. **c** During stress, non-random, adaptive condensates form. Most proteins which enter condensates are resolubilized instead of degraded, an observation which is inconsistent with a large-scale protein misfolding model where many misfolded proteins would be degraded. Further, condensation is well-positioned to serve as an adaptive sensing mechanism and has not been fully explored.

Consistent with this model, inducing protein misfolding by introducing an analog of proline or the expression of exogenous unstable proteins have been shown to induce the expression of components of the Hsf1-mediated stress response, indicating that the presence of misfolded proteins is sufficient to activate the response (Trotter et al. 2001; Geiler-Samerotte et al. 2011). However, no endogenous protein has yet been identified which misfolds or exposes an Hsp70 binding site upon heat shock. Additionally, recent evidence shows that although dozens of endogenous proteins aggregate during stress, most are rapidly returned to solubility after stress without degradation via the action of molecular chaperones like Hsp70, in contrast to unstable reporter proteins (Wallace et al. 2015; Yoo et al. 2022). In isolation, several endogenous proteins have been shown to form condensates in response to physiological heat shock *in vitro*, while retaining structure and/or function (Riback et al. 2017; Franzmann et al. 2018; Iserman et al. 2020). In specific cases, interfering with endogenous protein condensation compromises cell fitness during stress (Riback et al. 2017). These observations raise the possibility that condensation is adaptive, and that the formation of stress-triggered assemblies is the primary sensing act which then initiates downstream responses. However, the specific proteins involved in sensing temperature changes in yeast have yet to be identified.

Sensing mechanisms for temperature are diverse in nature yet remain incompletely characterized (Sengupta and Garrity 2013). Small temperature changes, on the order of a few degrees, induce the large-scale cellular reprogramming observed among all organisms during heat stress, so cellular sensors which can detect these changes must exist to facilitate this response. Biomolecular condensation serves as a good fit for temperature sensing because the process is cooperative, reversible, and fast (Yoo, Triandafillou, and Drummond 2019). Additionally, proteins whose temperature and pH phase boundaries exist near physiological

conditions may be hypersensitive to small changes in the environment. Several recent studies have identified sensory function of the condensation process (Franzmann et al. 2018; Riback et al. 2017; Iserman et al. 2020). Proteins which are very sensitive to heat shock serve as candidates for stress sensing (Figure 3.1b).

One class of temperature sensors for the HSR would combine two key features: temperature-dependent condensation and exposure of a region capable of recruiting Hsp70. We therefore selected rapidly condensing proteins (Wallace et al. 2015) to search computationally for preferred binding sites of Hsp70 within the yeast proteome by using experimental binding data generated from its bacterial homolog, DnaK (Rüdiger et al. 1997; Van Durme et al. 2009). Among condensing proteins, candidate Nug1 contains a high-scoring Hsp70 binding motif. The crystal structure of a bacterial homolog of Nug1, YlqF (PDB, 1puj), indicates that the predicted Hsp70 binding site is buried in its native structure. It is possible that such a sensor protein changes its conformation and exposes its Hsp70 binding site only during heat shock conditions, thus titrating Hsp70 away from Hsf1. This model differs from the classical misfolding model in several important ways: condensation is predicted to be nontoxic, linked to adaptive functions, reversible, and tuned to the heat shock temperature of the host organism (Figure 3.1c).

Candidate sensor Nug1 belongs to a family of related and functionally similar proteins, many of which are also predicted to bind Hsp70. Intriguingly, each protein is also extraordinarily sensitive to temperature *in vivo* (Figure 3.1b). Candidates Nug1, Nog1, Nog2, and Lsg1 each are well conserved, essential GTPases which rapidly condense upon heat shock in cells (Kallstrom, Hedges, and Johnson 2003; Bassler, Kallas, and Hurt 2006; Matsuo et al. 2014; Wallace et al. 2015). These proteins are thus excellent candidates for endogenous

temperature sensors with the potential to recruit Hsp70 (and thus activate Hsf1) in a heat-shock-dependent manner.

Even more enticing is that all of these GTPases share connections with another central change which occurs upon heat shock: downregulation of ribosome production. Upon heat shock, wild-type proliferating cells cease budding and halt growth in the G1 stage of the cell cycle by initiating the silencing of several growth genes (Rowley et al. 1993). The major factor limiting cellular growth is the production of ribosomes (Neidhardt and Magasanik 1960; Koch 1988), indicating that this mechanism may be accompanied by, or even partially caused by, cessation of ribosome production. Certain stresses in yeast have been shown to lead to the downregulation of ribosome production (Guerra-Moreno et al. 2015), and similar halts in ribosome synthesis have been shown for other organisms under heat stress (Pelham, Mosier, and Hurley 2018; Bell, Neilson, and Pellegrini 1988; Ghoshal and Jacob 1996; Zhao et al. 2016). Restoration of cellular growth is linked to the clearance of stress-associated condensates of endogenous proteins; cell cycle resumption correlates with condensate dissolution but not with the disaggregation of exogenous misfolding-prone proteins, suggesting that endogenous condensates are functional (Kroschwald et al. 2015). Nug1, Nog1, Nog2, and Lsg1 are all non-ribosomal trans-acting factors which are associated with the ribosome at various stages within ribosome biogenesis, with Nug1, Nog1, and Nog2 involved in nuclear maturation and Lsg1 involved in cytoplasmic maturation. It is known that both growth and ribosome biogenesis are attenuated during stress, but the sensing mechanism which initiates these responses remains poorly defined. I hypothesize that the stress-triggered condensation of these factors render them unavailable for function during heat shock and ultimately lead to reduced ribosome production and growth. While the biological function of these proteins

elevates their potential significance, we were not able to experimentally explore this line of inquiry.

Taken together, not only are the candidates very sensitive to heat, but they share connections with two major heat-induced cellular changes within the cell, Hsf1-mediated HSR and ribosome biogenesis shut off. I hypothesize that biomolecular condensation serves as a major mechanism for heat shock sensing and downstream responses, and that these four stress-sensitive candidates are connected to the activation of the HSR and ribosome biogenesis shutoff. To do this, I aimed to characterize the molecular determinants of their condensation, focusing initially on candidate Nug1.

This new view of biomolecular condensation as an adaptive response to deal with environmental stress directly relates to how we view protein aggregation-associated diseases such as ALS and dementia (Mackenzie et al. 2011; Patel et al. 2015; An et al. 2019). The hallmarks of these diseases, aberrant protein accumulation, may be the result of dysregulation of a normally adaptive condensation process, with direct implications for how we view pathology and potential treatment. Untangling the connection between environmental stress-induced biomolecular condensates and the cellular response to them promises to reveal important insights into the nature of adaptive condensation processes, setting the stage for understanding how such processes may be dysregulated in disease.

3.2 RESULTS

3.2.1 Identification of sensor candidates

We sought to find potential candidates by searching the yeast proteome for potential Hsp70 binding sites. The preferred binding sites for bacterial homolog of Hsp70, DnaK, has been

described as hydrophobic residues flanked on either side by basic residues. Using this position specific scoring matrix generated for DnaK (Rüdiger et al. 1997), we performed a sliding window analysis among all *S. cerevisiae* proteins, but focusing on those which condense under heat stress because those are the most likely to engage with Hsp70. We define the condensing proteome as those 177 proteins identified in (Wallace et al. 2015).

It is known that Hsf1 is repressively bound by Hsp70 under non-stressful conditions (Zheng et al. 2016; Krakowiak et al. 2018). Indeed, using our method to search for binding sites in Hsf1 identified a sequence overlapping the known binding site of Hsp70 (Krakowiak et al. 2018). This serves as a positive control for our method (Figure 3.2a).

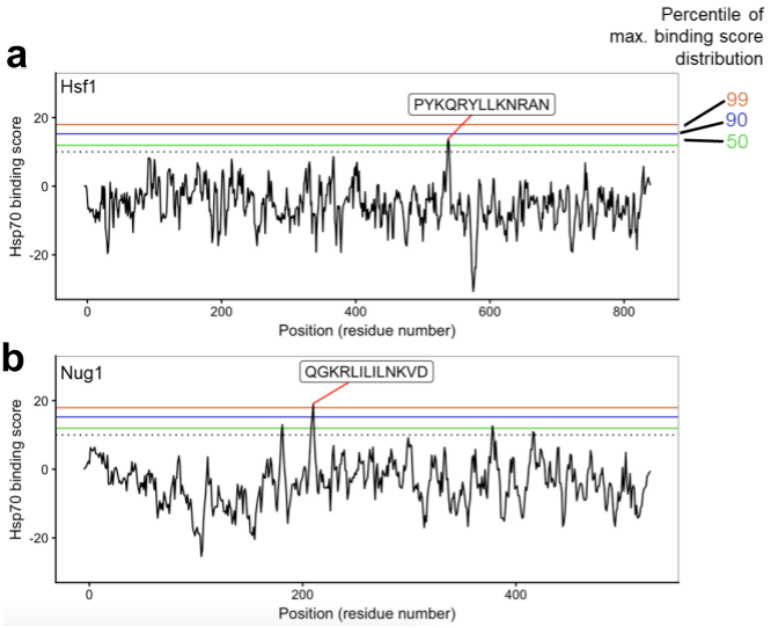

Figure 3.2. Identifying potential Hsp70 binding sites using a sliding window analysis of the condensing proteome. a Scans of 13-residue long peptides within Hsf1 identify the known Hsp70 binding site in Hsf1, scoring above the 50th percentile of predicted binding sites in the condensing yeast proteome. **b** Same as **a**, except analyzing Nug1 sequence, within which we observe the top-scoring peptide identified in the condensing yeast proteome.

From this analysis, we found that the condensing protein which contained the peptide with the best predicted Hsp70 binding site was nuclear GTPase 1, or Nug1 (Figure 3.2b), a

GTPase involved in nucleolar 60S ribosome maturation (Bassler, Kallas, and Hurt 2006). The predicted binding site overlaps within the GTPase domain of Nug1, over a sequence motif which is responsible for guanine base-binding specificity. Intriguingly, this peptide is buried in the native structure of Nug1, suggesting that it is not able to bind Hsp70 under non-stress conditions, but perhaps becomes exposed during stress conditions when it is condensed. Further, several GTPases which also condense (Nog1, Nog2, and Lsg1, data not shown) have predicted Hsp70 binding overlapping this exact region. All GTPases contain this sequence motif, but not all GTPases condense or are predicted to bind Hsp70. Because of these features, I decided to characterize Nug1's *in vitro* and *in vivo* behavior to better understand its stress sensitivity.

3.2.2 Description of Nug1 behavior *in vitro*

Using purified protein (see Methods), we wanted to test Nug1's solubility after exposure to various conditions. To do this, we used a biochemical fractionation technique termed TSP – Total, Supernatant, Pellet. In brief, we expose purified protein to various conditions, often including temperature treatment. We take a total sample, then spin the protein in a centrifuge, where large condensates will move to the bottom of the tube. We then take a sample of the supernatant fraction, which should contain any soluble, non-condensed protein. After a wash step, we isolate the pellet fraction, which contains condensed protein. We then run each fraction on a SDS-PAGE gel to look for shifts in solubility depending on the condition.

It is known that salt concentration can affect protein solubility as well as propensity to form condensates (Riback et al. 2017; Jung et al. 2020; Iserman et al. 2020; Bianchi et al. 2020). We therefore tested whether there were any changes in solubility as a result of heat

stress while varying the salt concentration (Figure 3.3a). We find that salt consistently inhibits the condensation of Nug1 around its physiological concentration (4-5 μM), even after a 20-minute incubation at heat shock temperatures. Further, the purified protein is relatively insoluble even at 4°C at lower salt concentrations, suggesting that it may be somewhat unstable in solution. From these data we can also conclude that Nug1 solubility is dependent on temperature, where less protein is observed in the supernatant fraction at 42°C relative to

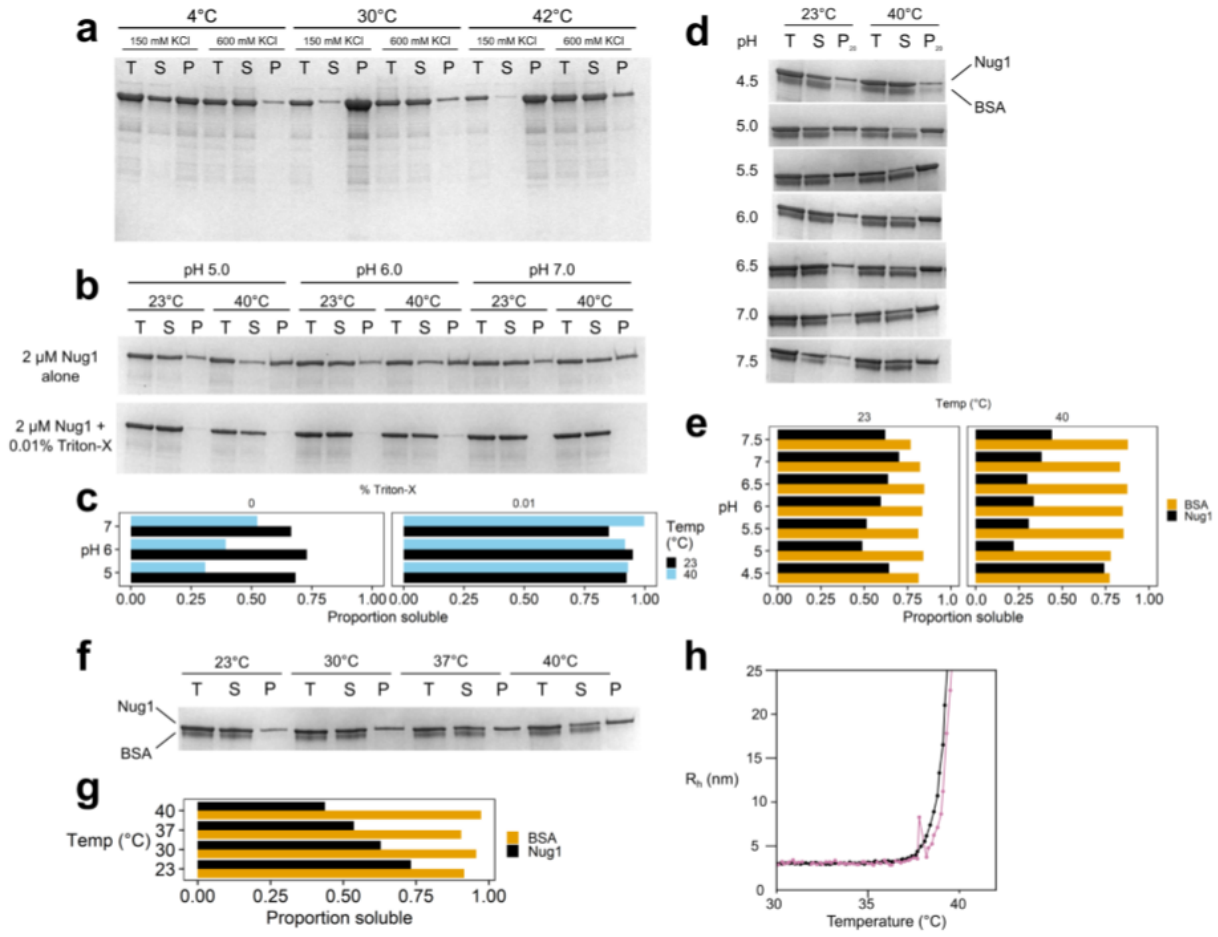

Figure 3.3. Purified Nug1's condensation is sensitive to salt, detergent, pH, and temperature. a Purified Nug1 (5 μM) fractions after TSP assay under different salt and temperature conditions. Nug1 was treated at indicated temperature for 20 minutes, and then fractionated at 20,000 g. **b** Purified Nug1 (2 μM) TSP gel with or without 0.01% Triton-X added in the buffer. Reactions were performed at indicated pH and temperature treated, then spun at 20,000 g. **c** Quantification of **b**, where each fraction is estimated by intensity of the signal in supernatant fraction divided by the sum of the supernatant and pellet fraction. **d** Purified Nug1 (4 μM) and BSA (0.1 mg/mL) after a 20-minute exposure to 23 and 40°C in various pH-buffered media. **e** Quantification of **d**, where reported values were calculated as in **c**. **f** Purified Nug1 (4 μM) and BSA (0.1 mg/mL) after a 20-minute treatment at indicated temperatures, and then fractionated at 20,000 g. **g** Quantification of **f**, calculated as in **c**. **h** DLS temperature ramp of two replicates of Nug1 at 4 μM.

30°C, and similarly less in 30°C than 4°C. Our results are consistent with previous work with other proteins that finds high salt conditions inhibit condensation.

Many condensates can also be solubilized by detergents, but it has been shown that some disease-associated aggregates are detergent-insoluble (Basso et al. 2009). We therefore wondered if detergent would alter Nug1 condensates after exposure to various temperature and pH conditions (Figure 3.3b and 3.3c). We found that inclusion of a low concentration (0.01%) of mild detergent Triton-X completely prevented condensation regardless of pH or temperature. On the other hand, in the absence of detergent, we did observe a mild effect of pH: lower pH leads to more condensation at heat shock temperatures (40°C), but not at control temperatures. However, quantification of condensation is difficult without a proper loading control on the gel. To further investigate the pH effects, we performed a more comprehensive pH scan that included BSA as a loading control.

Because of pipetting error, different amounts of protein could theoretically be loaded on the gel, leading to biased comparisons across fractions. As such, we supplemented the reaction mixture with a low concentration of BSA, a non-condensing protein, as a loading control in the subsequent experiments. To do this, we mixed Nug1 and BSA prior to temperature treatment. Since BSA does not form condensates in response to temperature, it should remain completely soluble after heat shock or pH manipulation. We performed the final wash step in pH-buffered solution in the absence of BSA. If all soluble proteins were removed in the wash, then no BSA should appear in the pellet fraction. We are then able to compare Nug1 pellet fractions with the supernatant fractions with more confidence.

In this assay, our quantification of the gels suggest that there is indeed an effect of pH on condensation (Figure 3.3d and 3.3e). Interestingly, we see a decrease in Nug1 solubility at

both the control and heat shock temperature (with the exception of pH 4.5). The solubility decreases even more, however, with the combination of temperature and pH. Consistent with other studies, low pH leads to increased condensation (Riback et al. 2017). However, pH 4.5 appears to be a strong outlier in both control and treatment conditions, with relatively high solubility in both. This could be due to experimental error or some other physical property of Nug1 at very low pH.

After observing this graded response to pH, we wanted to further investigate the temperature-dependent condensation of Nug1 in the presence of the BSA loading control. We again find a strong relationship between temperature and amount of protein in the pellet fraction at a non-stress pH of 7.25 (Figure 3.3f and 3.3g). As expected, BSA's solubility does not appear to be affected by temperature.

To obtain more sensitive measurements, we used Dynamic Light Scattering (DLS) to measure the apparent hydration radius (R_h) of Nug1 at physiological concentrations (Figure 3.3h). We used a slow temperature ramp (0.25°C/min) and monitored the maximum size of particles in solution. As the temperature reaches a critical point, the maximum size of the hydration radius of the protein will grow rapidly. We use this as a proxy for the onset of condensation as described in (Riback et al. 2017). It is important to note that due to Nug1's instability in solution, reliable and consistent results were difficult to obtain. Nonetheless, we were able to measure purified Nug1's condensation temperature (T_{demix}) as 38°C with two replicates, which is lower than what has been observed in other purified proteins from *S. cerevisiae*. We confirm with DLS what we have observed in the TSP gels – Nug1 shows extreme temperature sensitivity *in vitro*.

3.2.3 Evolutionary structural analysis of Nug1

The *in vitro* work on purified Nug1 demonstrates that the protein autonomously condenses as a result of temperature changes. I wanted to investigate how Nug1's propensity to heat sensitivity is coded in its protein sequence. In fact, Nug1 only has one predicted protein domain aside from its NLS according to several domain predictors: a GTPase domain (Marchler-Bauer et al. 2017; Mistry et al. 2021; Paysan-Lafosse et al. 2023). This domain makes up less than half of the protein sequence, meaning the majority of the protein does not contain known functional, folded domains. Since intrinsically disordered regions have been shown in some cases to modulate or even promote condensate formation (Riback et al. 2017; Schmidt et al. 2021; Shin et al. 2017), we wondered if the regions outside of this predicted domain have structure or are disordered.

However, it is first important to note a unique property of Nug1. Aside from containing a potential Hsp70 binding site, the GTPase domain is circularly permuted, meaning it has a shift in the N to C order of its canonical GTPase motifs (Marchler-Bauer et al. 2017; Mistry et al. 2021; Paysan-Lafosse et al. 2023). While this type of GTPase is unique from most others, it is highly conserved and a bacterial homolog from *B. subtilis* has a described structure (Wittinghofer and Vetter 2011). As we proceed with structure prediction for Nug1, this known structure can be used as a benchmark for the accuracy of prediction algorithms.

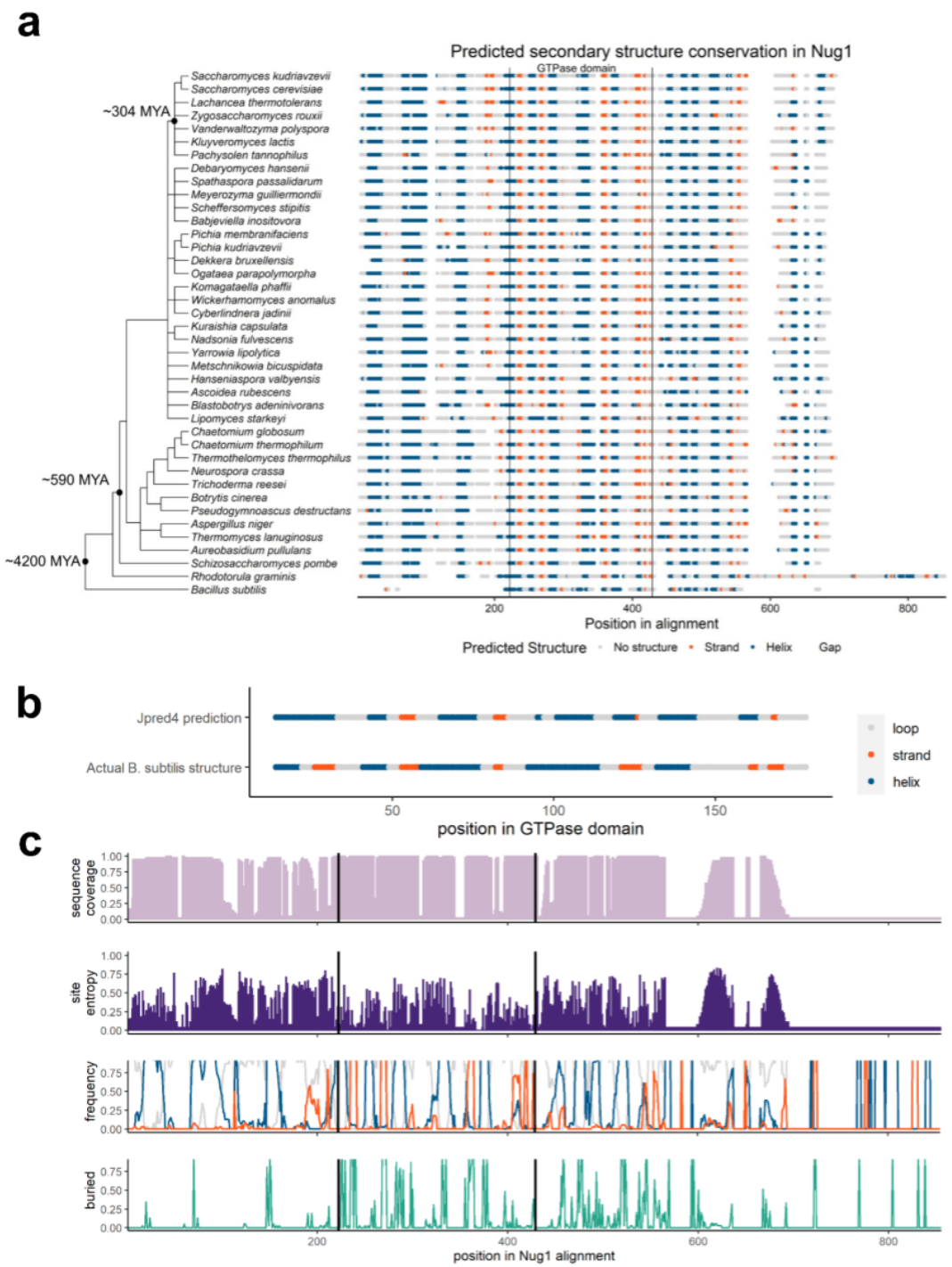

Figure 3.4. Predicted structural properties of Nug1 are largely conserved among fungi. a Using AYbRAH database of sequences combined with MUSCLE, we generated alignments of Nug1 sequences spanning over 4,000 million years, and subsequently plotted Jpred4 structural predictions across the alignment. The GTPase domain is annotated between two vertical black lines. Helices are colored in blue, strands in orange, loops/unstructured in gray, and alignment gaps in white. **b** Prediction accuracy of the *B. subtilis* GTPase domain compared to known structure is 69.1% ($p < 0.01$ compared to random shuffle of sequence). **c** Summary data for Nug1 sequences across the alignment. Sequence coverage, site entropy, predicted structure, and predicted solvent accessibility are plotted. The GTPase domain is annotated between two vertical black lines.

To compare predicted structure across evolutionary time, we gathered sequences of Nug1 orthologs from AYbRAH ortholog database (Correia, Yu, and Mahadevan 2019). I supplemented the sequences with *B. subtilis* as a bacterial outgroup. Then I aligned all of the sequences with MUSCLE using default parameters (Madeira et al. 2022). The alignments were then input into Jpred4 (Drozdetskiy et al. 2015) to estimate the secondary structure for each sequence. The resulting output allows us to compare predictions across evolutionary time. Using fungal species spanning 600 million years, we observe predicted helices and strands both inside and outside of the GTPase domain, which is annotated between the black lines (Figure 3.4a). There appear to be conserved helical structures N-terminal to the GTPase domain, and a mixture of strands and helices C-terminal to the GTPase domain. Since the predictions are based largely on previously described sequence-structure relationships, we therefore wondered about the accuracy of the predictions.

The ortholog of Nug1 in bacteria *B. subtilis* has been crystallized. We extracted the structural state (helix, strand, or loop) of the GTPase domain in the crystal structure and compared it to the prediction generated by Jpred4 (Figure 3.4b). We found that the structure prediction accuracy to be nearly 70%, and compared to shuffled structure the accuracy was only 36% ($p < 0.01$). We are looking for potential structure outside of the domain, so we proceed with the caveat that the following analysis contains at least the same amount of error.

We next wondered about other properties of the Nug1 alignment and structure prediction. The coverage of the alignment varies throughout the sequence, with the C-terminal domain lacking the most coverage due to an extended sequence in *R. graminis* (Figure 3.4c, top panel). Most other regions of the alignment are well-represented. However, the site entropy, or residue diversity at each site in the alignment, demonstrates that the sequence identity itself

is not well conserved (Figure 3.4c, second panel from top). Strikingly, however, the secondary structure is still predicted to be consistent across the sequence despite the lack of sequence identity (Figure 3.4c, third panel from the top). This result suggests that the structure of not only the GTPase domain but also the regions outside of it appear to be conserved, implying functional importance for structure in these regions. Consistent with this, the solvent accessibility calculated by Jpred4, or the two-state prediction (exposed or buried) that the residue is exposed to solvent in native structure (Cuff and Barton 2000; Cole, Barber, and Barton 2008; Drozdetskiy et al. 2015), corresponds to several structured regions in the sequence (Figure 3.4c, bottom panel). Some potential buried regions also have predicted structure, which indicate that these regions reside inside the folded, soluble protein. Despite the lack of sequence homogeneity, we still see predicted conservation of secondary structure and accessibility.

Overall, our results strongly suggest that even though there is only one classifiable fully structured domain, Nug1 protein across the tree of life does not appear to be natively disordered outside of the domain. From these results, we conclude that there appears to be structure outside of the GTPase domain, which opens the possibility of conserved functional importance that is not due to disordered sequence.

3.2.4 Cryophilic replacement of Nug1

We hypothesized that Nug1 condenses upon heat shock and recruits Hsp70, thus activating the Hsf1 transcriptional heat shock response. Yeast cold-adapted relatives display dramatically decreased fitness at temperatures where *S. cerevisiae* thrives (Salvadó, Arroyo-López, Guillamón, et al. 2011; Tronchoni et al. 2014). We reasoned that sensor proteins in

cold-adapted relatives must be more sensitive at lower temperatures than the homologous sensors in *S. cerevisiae* and thus are sufficient to induce the heat shock response in *S. cerevisiae* at temperatures where it would otherwise grow normally. To test this, we designed a set of experiments to replace Nug1 in *S. cerevisiae* with an orthologous sequence from cryophilic *S. kudriavzevii* and subsequently monitor Hsf1-regulated gene induction.

I used flow cytometry of *S. cerevisiae* and cold-adapted relative *S. kudriavzevii* expressing fluorescently-tagged endogenous SSA4, a strongly heat-inducible Hsp70, to test the assumption that the cryophilic relative executes its transcriptional HSR at lower temperatures. Indeed, mCherry-tagged heat-induced protein Ssa4 is induced at lower temperatures in the cryophile *S. kudriavzevii* relative to mesophile *S. cerevisiae* after a 20-minute temperature treatment followed by 120 minutes of recovery at room temperature (Figure 3.5a). Using CRISPR-Cas9, I replaced the endogenous copy of Nug1 in *S. cerevisiae* with its ortholog from *S. kudriavzevii* in an Ssa4-mCherry background (Figure 3.5b). To test the sufficiency of a sensor candidate in *S. cerevisiae*, I again monitored heat shock response induction via flow cytometry. In the strain with the Nug1 replacement, induction is observed at the same temperatures where *S. cerevisiae* is executing its HSR but with an enhanced response (Figure 3.5c). While we expected lower-temperature induction rather than increased induction, this result may be consistent with the idea that a cryophilic sensor is condensing more at mesophilic temperatures, perhaps titrating Hsp70 away from Hsf1.

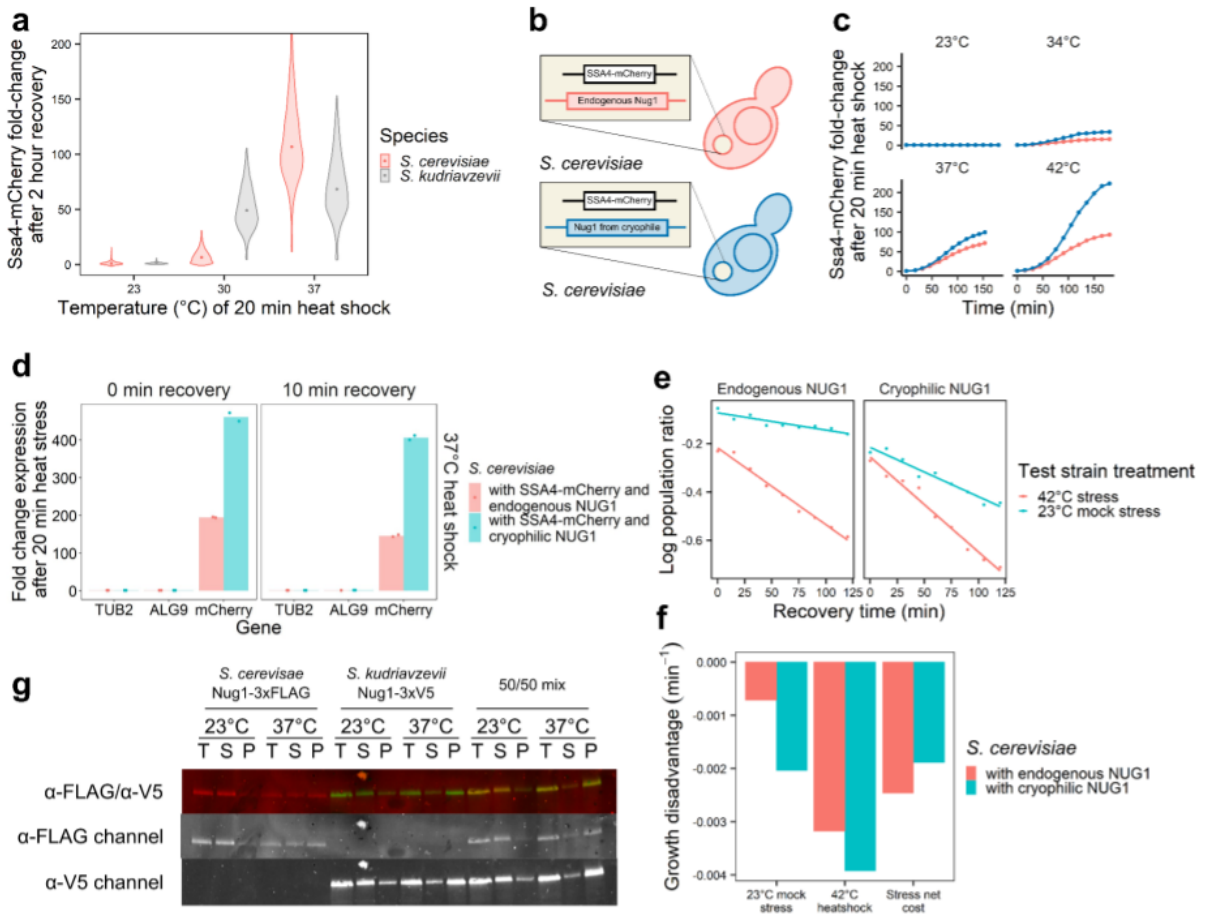

Figure 3.5. Using a cryophilic replacement allele to search for transcriptional and condensation phenotype.
a Monitoring the induction of mCherry-tagged Ssa4, a reporter for the Hsf1-mediated heat shock response, in both *S. cerevisiae* and *S. kudriavzevii* after a 20-minute temperature treatment and 2 hours of recovery at 23°C. Points in the center of the violins represent the median. **b** Cartoon of the genetic manipulation to replace NUG1 in *S. cerevisiae* with that of *S. kudriavzevii* at its endogenous locus in the background of mCherry-tagged SSA4 in its endogenous locus. **c** Monitoring the strains in **b** over time after a 20-minute temperature treatment and recovery at 23°C. Points represent the median fold change of fluorescence at each time point. **d** Fold change from 23°C of the relative abundance of each transcript to control gene TUB2 with 0 or 10 minute recovery after a 10-minute heat shock at 37°C. Bars represent the mean of two technical replicates (points). **e** Relative change in population ratio between strain of interest and GFP-labeled wild-type cells during recovery after a 20-minute temperature treatment. The slope of the line represents the relative growth rate. **f** Quantification of the growth rate (estimated slope from **e**) cost relative to wild-type cells of mock-treated and heat shocked cells. Stress net cost is the difference between the growth disadvantage for each strain between 42°C and 23°C treatment. **g** Tagged Nug1 western blot (3xFLAG for endogenous, 3xV5 for cryophilic) after 20-minute temperature treatment. Lysates were fractionated yielding total (T), supernatant (S), and pellet (P) fractions. 50/50 mix contained equal proportions of each tagged strain to control for experimental variation.

We next wanted to test whether the increased signal of Hsf1 induction is indeed due to production of the SSA4 gene rather than downstream SSA4 protein regulation that may be

affected by our genetic manipulation. We used qPCR in both strains to test the expression of SSA4-mCherry and two control genes that should not be affected by heat shock. We observed that there are more SSA4 transcripts produced in the strain harboring the cryophilic Nug1 immediately and 10 minutes after a 20 minute heat shock (Figure 3.5d). This result suggests that the *SSA4* transcript is being transcribed to a different extent in both species, rather than some sort of preferential translation mechanism in the cryophilic strain.

Due to the differential transcriptional response, I wondered if producing more Hsf1 target genes had an effect on fitness of the organism. To test this, I quantified growth rate at different temperatures using a competition assay. Growth rate is a useful measure of fitness for single-cell organisms such as yeast. Comparing the growth rate of our strains of interest to a wild-type strain can allow us to make indirect but robust fitness measurements between the strains of interest, as was performed in (Triandafillou et al. 2020). This experiment relies on the quantification of population fitness relative to a control strain to make these comparisons.

After a 20-minute temperature treatment, we mixed known proportions of *S. cerevisiae* containing endogenous NUG1 with exponentially growing, GFP-labeled wild-type cells as a competitive reference. We also made mixtures of *S. cerevisiae* containing S. *kuriavzevii*'s NUG1 with GTP-labeled wild-type cells. We then monitored the relative proportions in the two population mixtures over time (Figure 3.5e). We found that *S. cerevisiae* with the cryophilic version of NUG1 is at a slight growth disadvantage to the strain with its endogenous copy of NUG1 (Figure 3.5f). This is true at both control (23°C) and heat shock (42°C) temperatures. However, when comparing the net disadvantage due to stress, we observe that *S. cerevisiae* with its endogenous copy of NUG1 has a greater cost. The difference is small but notable when compared to the net cost of stress relative to the strain possessing cryophilic NUG1. With the

previous result that more *SSA4* transcript is produced in the strain with *S. kudriavzevii*'s Nug1, perhaps having an enhanced response is overall protective against any detrimental heat shock fitness effects.

Given the phenotypes that the transcriptional response is greater and the net fitness cost is lower in the cryophilic swap strain, we wondered if it was due to the Nug1 in those cells forming more condensates at the same temperatures. To test this, we used biochemical fractionation of yeast lysate, which allows us to separate the large condensates from soluble, non-condensing protein. We tagged WT Nug1 with a C-terminal 3xFLAG tag, and in another strain of *S. cerevisiae*, we tagged the cryophilic Nug1 with a C-terminal 3xV5 tag. This genetic manipulation allowed us to blot for the tags to quantify shifts in solubility of Nug1 due to heat shock. Because we used different tags, we were able to mix the cultures pre-fractionation, which reduces variation and provides an internal loading control.

Prior to lysis and fractionation, we exposed the cells to non-heat shock conditions (23°C) as well as a mild temperature stress (37°C). After fractionation, we blotted against FLAG and V5, and we observed shifts in Nug1 solubility in both versions of Nug1. At 23°C in both strains, most Nug1 remained soluble (Figure 3.5g). At 37°C in both strains, there was a shift in solubility where Nug1 appears with higher intensity in the pellet and less in the supernatant. Quantification of the blot (data not shown) shows small differences in solubility, with cryophilic Nug1 appearing at a slightly higher ratio in the pellet. The observation was consistent when comparing the individual and mixed fractions. We conclude that indeed the cryophilic Nug1 is condensing more after a 37°C heat shock, which may be leading to the increased activation of the Hsf1-mediated heat shock response.

Considering the Hsf1 response again, we wondered if we could isolate the amino acid substitutions that lead to increased heat sensitivity in our swap mutant. *S. cerevisiae*'s endogenous Nug1 is 92% identical to Nug1 from *S. kudriavzevii*, so we decided to create chimeras of the two proteins to home in on the sensitivity-determining amino acids. We again used CRISPR-Cas9 to generate the chimeric proteins. Surprisingly, we isolated multiple transformants which displayed divergent behavior: from what should be the same mutation, we observed some transformants that produced the enhanced HSR response, but some that behaved like wild type. Concerned about our original genetic manipulation in the initial swap strain, I redid the CRISPR using new guide RNAs. Unfortunately, all of the transformants behaved like wild type. We concluded that the phenotype was due to some off-target effect of the CRISPR guide RNAs used throughout the project to create the edits, which has been observed before (Zhang et al. 2015). Given the lack of phenotype, we decided to move on from Nug1 as a potential candidate.

3.3 CONCLUSIONS AND FUTURE DIRECTIONS

Here we have shown a promising approach for identifying potential activators of the Hsf1 response during heat shock. We used a prediction algorithm based on the preferred binding sites bacterial homolog of Hsp70 to analyze the heat-sensitive yeast proteome in order to identify potential proteins that could titrate Hsp70 away from Hsf1. Many promising candidates were identified, and we further characterized one strong candidate, Nug1, *in vitro*, *in silico*, and *in vivo*. Using purified Nug1, we showed that the protein is very sensitive to temperature and pH, but condensation is prevented under high salt or detergent-containing conditions. To better

understand the structure of the protein, we performed evolutionary analysis and secondary structure prediction to predict structure outside of the GTPase domain. We found that secondary structure appears to be conserved even though sequence diversity is high within the fungal clade. In *S. cerevisiae*, we swapped the cryophilic ortholog of Nug1 into the endogenous locus and tested if the protein is sufficient to induce the heat shock response and if the protein forms condensates at lower temperatures. While the induction phenotype appears to be a CRISPR artifact, *in vivo* biochemical fractionation suggests that cryophilic Nug1 forms quantitatively more condensates in *S. cerevisiae*. Taken together, we describe the biochemical properties of an essential, autonomously heat sensitive protein which served as a strong potential candidate for Hsf1 regulation.

Ultimately, the enhanced induction phenotype was determined to not be due to the cryophilic Nug1 swap but instead due to a mutation of unknown origin. Reconstructing the strain with new guide RNAs led to loss of the observed phenotype, indicating that the original guides must have caused an off-target mutation. As a result, we eliminated Nug1 as the primary sensor of the Hsf1-mediated transcriptional response. However, this unintended phenotype as a result of the CRISPR methodology serves as a cautionary tale for future work: each transformation reaction should be executed with multiple guide RNAs, and resulting transformants should be screened to make sure they are morphologically consistent and present the same phenotypes of interest. I have written a protocol for screening transformants that can help prevent the selection of mutants with unintended background mutations (see Methods - Screening CRISPR Genetic Manipulations).

While our findings largely exclude Nug1 as being the primary sensor of heat shock leading to the activation of the Hsf1 response, we believe that this project as a whole remains

completely open. The methodology to identify potential candidates has highlighted other intriguing proteins, including the Nog1, Nog2, and Lsg1 (the other GTPases not fully explored in this project), among others that have not been characterized at all. Besides Nug1, the condensing proteins containing the highest scoring peptides include Cdc39, Sec14, Msh6, Drs1, Urb1, Ccr4, Utp8, Rsp5, and Blm10. In my view, these proteins warrant further characterization.

Nug1 was a particularly strong candidate because of its natively buried Hsp70-binding peptide. Our hypothesis relies on the idea that the peptide must not be exposed during non-stressful conditions. This may manifest as a buried region, or a protein-protein or protein-RNA interaction. A systematic review of the other top-scoring candidates, including the relative heat sensitivity and location of the top-scoring peptide in the native structure (including predicted interaction interfaces), would be the next logical step in the search for heat shock sensors.

Following the identification of potential Hsp70 binding sites, I believe that the *in vivo* approaches to isolate a transcriptional phenotype will be instrumental in isolating any temperature sensors. The original phenotype that we observed was promising but somewhat problematic: the response in the swap mutant was enhanced at mesophilic heat shock temperatures, but not observed to occur at lower, cryophilic heat shock temperatures. Going forward, when using a cryophilic mutant, we would expect the response to occur at lower relative temperatures rather than be higher at *S. cerevisiae* heat shock temperatures. With that said, *S. kudriavzevii* ortholog replacement continues to be a robust and promising approach to look for non-canonical induction of the Hsf1-regulated response. *S. kudriavzevii* shares a close evolutionary relationship with *S. cerevisiae*, which makes genetic manipulations feasible.

However, due to their overlapping growth ranges, it may be useful to search for another closely related cryophilic yeast to increase the dynamic range in which a non-wild-type transcriptional response could be observed.

The transcriptional response occurs within minutes after heat stress, which is why we searched the condensing proteome for potential sensors. Nug1 was again a particularly strong candidate because it is considered a “superaggregator,” meaning it significantly decreased its solubility after only a two-minute heat shock (Wallace et al. 2015). Other good candidates should also display significant sensitivity.

It is possible, if not likely, that organisms have evolved multiple mechanisms for sensing temperature that are encoded in protein sequence. In other words, there may be many proteins that may be sufficient to activate the response, but not necessary. For example, a cryophilic swap prematurely induces the response, but replacing that candidate with a thermophilic ortholog does change the response. A single sensor would be both sufficient and necessary, but if there were multiple sensors, they need only be sufficient, and perhaps only in combination.

As such, the next experiment I propose would be to generate cryophilic swap mutants for each superaggregating protein, giving priority to those which have strong predicted Hsp70 binding sites. There are only 17 annotated superaggregating proteins, making this approach feasible to generate genetic modifications with CRISPR and use high-throughput flow cytometry screening in the background of a Hsf1 reporter. I believe isolating a phenotype before proceeding with *in vitro* characterization is essential.

With that said, *in vitro* experiments are still vital to classify a protein as a sensor. To sense temperature means to change in some qualitative way and transduce the signal to the

next component in the system. In a simple case, the sensor changes in response to temperature and as a result directly recruits Hsp70, which activates Hsf1 and leads to the transcriptional heat shock response. In a more complicated case, there are signal transducers between the temperature sensor and the clients of Hsp70. However, those intermediate transducers would not be the sensors, but merely components in the pathway to the Hsf1 response, because they themselves do not directly change in response to temperature, but instead respond to the temperature sensor. In either case, a temperature sensor's transformation into an identifiable signal that can be detected must be autonomous. It must shift from "off" to "on" in direct response to temperature.

Our original hypothesis states that condensation of heat sensitive proteins leads to Hsf1 response because it is fast, reversible, and specific. Because of this, we reasoned that our primary list of candidates should all form condensates *in vivo*. However, as stated, sensors must respond directly to heat, and in this case, the change from "off" to "on" is a condensation mechanism. In other words, the sensor must autonomously sense heat, with the switch from "off" to "on" being the transformation from soluble to condensed. A reliable read out of autonomous condensation is our *in vitro* TSP assay where shifts in solubility can be observed on an SDS-PAGE gel after exposure to conditions of interest, such as heat shock-relevant pH and temperature treatments.

The hypothesis that condensation leads to the activation of the Hsf-1 mediated heat shock response remains strong. While my project was not fruitful in the case of Nug1, I believe the approaches we have undertaken will be instrumental for future iterations of this project. Importantly, the approach should initially focus on the isolation of a phenotype in living cells, with careful selection of genetic mutants. Afterwards, biochemical reconstitution of candidates

and characterization of their biophysical properties is essential to test for temperature sensitivity and autonomous behavior. Cells may utilize multiple temperature sensors or nontrivial pathways to activate the transcriptional response, but the pathway to their identification is clear and feasible.

3.4 METHODS

3.4.1 Data and Code Availability

Experimental data and code for analysis

All data analysis and visualization were performed with R (version 4.2.2) in RStudio (RStudio Team 2020) or Fiji (Schindelin et al. 2012). The raw and processed data, and the custom scripts for data process, data analysis, and figure generation will be available on Data Dryad.

3.4.2 Experimental model and subject details

Identification of Hsf1 binding sites in the yeast proteome

Using the previously defined position specific scoring matrix for DnaK, the bacterial homolog of Hsp70, we scanned each yeast protein for 13-residue long sequences which produced a score for each peptide spanning the length of each protein. The score is based on a sum of the PSSM from DnaK for the given sequence. The condensing proteome was defined by the 177 proteins identified in (Wallace et al. 2015). Scripts and data for this analysis can be found at https://github.com/dad/hsp70-binding.

Protein purification

N-terminally 6xHis-MBP-SUMO-tagged Nug1 containing plasmid was transformed into an *E. coli* strain BL21 (Rosetta 2) and grown overnight at 37°C. The overnight culture was used to inoculate 2 L of Terrific Broth (RPI). Cells were grown until OD_{600} between 0.4 and 0.6 and then the flask was moved into a 16°C incubator and 500 µM of IPTG was added. The cells were then grown overnight. The following day, cells were harvested and resuspended in His binding buffer (25 mM HEPES pH 7.1, 600 mM KCl, 5 mM $MgCl_2$, 30 mM imidazole, 5 % glycerol) supplemented with 1x homemade protease inhibitors AEBSF/E-64/Leupeptin, 1x Aprotinin, 1x Pepstatin, 62.5 µg/mL lysozyme, 1 µL of Pierce Universal Nuclease for Cell Lysis (#88702) per 50 mL, and NP-40 detergent to a final concentration of 0.2%. Cells were placed into the -80°C freezer to aid in lysis.

When ready to purify, cells were thawed and lysed by sonication in the presence of 2 mM BME and 0.2% Tween-20. Cleared lysate was loaded onto a 5 mL HisTrap FF column equilibrated with His binding buffer on an AKTA FPLC system. After loading, the column was washed with more His binding buffer until the UV reading returned to baseline level. The protein was eluted with a 20 mL gradient from 0 to 100 % His elution buffer (25 mM HEPES pH 7.1, 600 mM KCl, 5 mM $MgCl_2$, 400 mM imidazole, 5 % glycerol, 2 mM BME). The fractions of interest were pooled and loaded onto a 5 mL MBPTrap HP column, and the column was washed with His binding buffer. The protein was then eluted with a 20 mL gradient from 0 to 100 % with MBP elution buffer (25 mM HEPES pH 7.1, 600 mM KCl, 5 mM $MgCl_2$, 30 mM imidazole, 5 % glycerol, 10 mM maltose, 2 mM BME). The fractions containing the protein were pooled and dialyzed against 500 mL His binding buffer containing homemade Ulp1 protease in a 4°C cold room with light stirring overnight. The next day, the cleaved protein was recovered

by running the dialyzed solution through the His column and collecting the flow through. Flow-through fractions containing tag-free Nug1 proteins were combined and concentrated to <500 µL. The sample was filtered with a 0.45 µM filter (Whatman) to remove any large aggregates. The protein was then run on the Superdex 200 10/300 GL (GE Healthcare) with SEC buffer (25 mM HEPES pH 7.1, 600 mM KCl, 10 mM $MgCl_2$, 5 % glycerol, 0.5 mM TCEP). Fractions containing Nug1 were pooled and further concentrated if needed. Protein concentration was measured using Bradford assay. Protein aliquots were snap-frozen in liquid nitrogen and stored at -80°C.

In vitro TSP

The following protocol was used for Nug1 purified protein. Gel quantification was performed by calculating the band intensity of S/(S+P) in ImageLab software.

Dialyze samples using 3 MWCO dialysis cups (Fisher #69550) in appropriate buffers (see Experimental buffers for *in vitro* TSP below). Dilute samples to desired concentration (using a buffer supplemented with 0.01 mg/mL BSA if using). Aliquot 15 µL into each treatment tube. Treat samples at desired temperature for 8 min. Take 4 µL of sample for “total” sample, and add to 10 uL SDS buffer. Spin treatment tubes at 20,000 g for 20 minutes at 4°C. Take 4 µL sample for “supernatant” sample and add to 10 µL SDS buffer. Remove the remaining sample from the treatment tube, careful not to disturb any pellet at the bottom of the tube. Add 40 µL of appropriate experimental buffer to each treatment tube (without BSA, if using). Spin again at 20,000 g for 20 minutes at 4°C. Remove all of the supernatant. Add 10 µL SDS buffer to the remaining sample and resuspend the “pellet” sample. Run on a gel.

Experimental buffers for *in vitro* TSP

For Figure 3.3a (salt and temperature): 5 µM Nug1 final concentration using buffer with 25 mM HEPES pH 7.1, 10 mM $MgCl_2$, 5% glycerol, 0.5 mM TCEP, and either 150 or 600 mM KCl.

For Figure 3.3b/c (detergent, temperature, and pH): 2 µM Nug1 final concentration using buffer with 50 mM ammonium acetate, 50 mM MES, 20 mM HEPES, 300 mM KCl, 2.5 mM $MgCl_2$, 1 mM DTT, and +/- 0.01% Triton-X.

For Figure 3.3d/e (pH and temperature): 2 µM Nug1 final concentration with 50 mM ammonium acetate, 50 mM MES, 20 mM HEPES, 300 mM KCl, 2.5 mM $MgCl_2$, 1 mM DTT, and +/- 0.1 mg/mL BSA .

For Figure 3.3 f/g (temperature alone): 2 µM Nug1 final concentration with 20 mM HEPES, pH 7.25, 300 mM KCl, 2.5 mM $MgCl_2$, 1 mM DTT, and +/- 0.1 mg/mL BSA.

Dynamic light scattering

Results were acquired and analyzed according to (Riback et al. 2017).

Evolutionary analysis

Sequences of Nug1 (HOG02920) were obtained from AYbRAH (https://lmse.github.io/aybrah/, (Correia, Yu, and Mahadevan 2019)) and NCBI for *B. subtilis* (Gene ID: 940134). Sequences were aligned using MUSCLE with default parameters (Madeira et al. 2022). The multiple sequence alignment was then input into Jpred4 (Drozdetskiy et al. 2015) to estimate the secondary structure for each alignment. Jpred4 takes a sequence input, searches the PDB for sequence-structure matches, removes redundancies with UniRef90, blasts the sequence to generate an alignment, and generates a hidden markov model and a position-specific scoring matrix which are then used in the Jnet algorithm. All analyses were done in R (R Development

Core Team, 2017) using packages from the tidyverse (Wickham et al. 2019). Plots were made with ggplot2 (Wickham n.d.).

Strain construction

Saccharomyces kudriavzevii and *Saccharomyces cerevisiae* mutants were obtained using CRISPR-Cas9 genome editing. Briefly, competent cells were prepared (Frozen-EZ Yeast Transformation II Kit™, Zymo Research) and transformed according to the protocol except with a 90-minute incubation at 23°C for *S. kudriavzevii* (30°C for *S. cerevisiae*). DNA was used at concentrations of at least 200 µg of Cas9/guide RNA-containing plasmid with a *URA3* selectable marker along with >500 µg of linear repair template as previously described (Lee et al. 2015; Akhmetov et al. 2018). Transformation reactions were spread on SC-Ura plates. Transformants were cured of the Cas9/guide RNA plasmid with patch plating and confirmed by sequencing. Multiple transformants obtained by using distinct guide RNAs were screened to check for morphological and phenotypic homogeneity.

Screening CRISPR genetic manipulations

The following protocol should be followed after transformation of the CRISPR guide-containing plasmid and linear repair DNA. If you used multiple different guides, proceed with the following protocol for each guide used.

On your original CRISPR transformation plate, pick at least 3 colonies that contain your edit of interest (check by cPCR and sequencing using primers outside of the homology arms). Streak on YPD to get single colonies. After a few days of growth, patch at least 6 single colonies onto a new CRISPR selection plate (e.g., SC-Ura) and a YPD plate. In other words, use the same colony and toothpick to streak onto both plates. Make sure to label your colonies

on each plate so the corresponding colony is apparent on both plates. After a few days of growth, pick colonies that grew on YPD but not SC-Ura to select for the loss of the CRISPR guide plasmid. Streak these colonies on a new YPD plate to get single colonies. Repeat cPCR on the final streaks (using single colonies) to verify presence of the edit of interest. Sequence the entire length of your amplicon, using multiple primers if necessary. At this point, you should have multiple transformants (at least 3) that contain your insert and have lost the CRISPR guide plasmid. For your measurement of interest (e.g., flow cytometry, fitness assay, auxin depletion), test that your three transformants phenocopy each other. If so, choose one to save at random. If not, you must select more colonies to screen to avoid any unintended genetic manipulations caused by the methodology.

In vivo TSP and western blot analysis

Yeast cells (ySMK011 or ySMK039) were grown in SC-complete medium with 2% dextrose (50 mL of medium per treatment) at 23°C with 250 rpm shaking until OD_{600} was between 0.4-0.6. Cells were transferred to a 50 mL conical tube and harvested via centrifugation at 2,500 g for 5 min in a swinging bucket rotor at room temperature. The supernatant was decanted and the conical tubes containing cells were immediately placed in water baths set to the treatment temperature (room temperature or 37°C). After the specified time period, cells were resuspended in 1 mL ice-cold soluble protein buffer (SPB; 20 mM HEPES-KOH pH 7.3, 120 mM KCl, 2 mM EDTA, 0.2 mM DTT, 1 mM PMSF, and 1:1000 protease inhibitors cocktail IV (Millipore Sigma)), transferred to a pre-chilled 1.5 mL tube, and spun for 30 s at 5,000 g at 4°C. The supernatant was discarded, and the cell pellet was resuspended in 200 µL of SPB. Two 100 µL aliquots from the resuspended sample were snap frozen in a safe-lock tube in liquid nitrogen.

Cells were lysed using cryomilling and fractionated with ultracentrifugation as described in (Wallace et al. 2015), with minor modifications. Briefly, cells were lysed with 5 x 90 s agitations at 30 Hz. After lysis, cellular material was resuspended in 900 µL of SPB and thawed on ice with occasional vortexing. The lysate was clarified to remove very large aggregates and membrane components with a 3,000 g spin for 30 s at 4°C. Then, 650 µL of clarified lysate was moved to a pre-chilled 1.5 mL tube. For a Total sample, 100 µL was mixed with 300 µL total protein buffer (TPB; 20mM HEPES-NaOH pH 7.4, 150mM NaCl, 5mM EDTA, 3% SDS, 1 mM PMSF, 2mM DTT, and 1:1000 protease inhibitors IV) and processed as described in (Wallace et al. 2015). Of the remaining clarified lysate, 500 µL was transferred to a vacuum safe tube spun at 100,000 g for 20 minutes at 4°C (fixed-angle TLA-55 rotor in a Beckman Coulter Optimax tabletop ultracentrifuge). The Supernatant fraction was decanted (as much as 400 µL) and snap frozen in liquid nitrogen. The pellet fraction was isolated as described in (Wallace et al. 2015).

SDS-PAGE gels were run with 1:1:2 ratio of T:S:P samples. Proteins were transferred to 0.2 µm nitrocellulose membranes (Bio-Rad #9004-70-0) in 20% methanol and 1x Tris-Glycine buffer using the Criterion blotter system (Bio-Rad). The membrane was blocked with 5% milk solution. The membrane was treated with 1x TBS + 1% Tween-20, a 1:6,000 dilution of anti-FLAG antibody (mouse; Sigma M2 #087K6011), and a 1:3,000 dilution of anti-V5 antibody (rabbit; Rockland #29087). Protein was detected with IRDye 680RD (donkey anti-mouse; LiCor #D00226-01) and IRDye 800CW (donkey anti-rabbit; LiCor #D20503-11), and imaged on a Odyssey DLx (LiCor). Quantification was done in ImageLab (Bio-Rad) and Fiji (Schindelin et al. 2012).

Flow cytometry

The Ssa4-mCherry monitoring assay was performed by growing cells (ySMK009, ySMK006, or yCGT027) overnight to OD_{600} ~0.05 in SC-complete medium with 2% dextrose, and heat shocked for 20 minutes at the specified temperature, the recovered at 23°C with 250 rpm shaking. Fluorescence was measured every 20 minutes, or as an end point measurement after 120 minutes of recovery at 23°C with shaking at 250 rpm.

The competition assay was performed as in (Triandafillou et al. 2020) with minor modifications: strains used were ySMK006, yCGT027, and yCGT006 (GFP-labeled, wild type) cells. Cells were grown overnight to OD_{600} ~0.05 in SC-complete medium with 2% dextrose and then heat shocked for 20 minutes at the specified temperature. Cells were mixed at known proportions with wild type as described.

All data were collected on the Attune NxT (Thermo Fisher) using the plate reader functionality at 100 uL/min for 100 uL samples. At least 20,000 events were recorded per 100 uL of cells. Voltage was set as follows: Forward scatter: 1; Side scatter: 200; YL2 (mCherry): 540; BL2 (autofluorescence): 420.

Each experiment was performed with the same voltage set, and the fluorescence values reported reflect within-experient forward scatter area and autofluorescence-normalized values. Sub-populations of cells that exhibited high autofluorescence (abnormally high BL2 signal) were filtered out from the analysis. At least 5,000 cells per sample remained for analysis.

Plasmids used in this study

All plasmids and yeast strains used in this study can be found https://docs.google.com/spreadsheets/d/1PTszRmmkMAvTRz-KyBR7rwSMbTfme6KLrPhs1yC6pQA/edit?usp=sharing.

3.5 AUTHOR CONTRIBUTIONS

Conceptualization, D.A.D.; methodology S.K.K. and D.A.D.; investigation, S.K.K. and Catherine G. Triandafillou (qPCR in Figure 3.5d); formal analysis, S.K.K. and D.A.D.; visualization, S.K.K. and D.A.D.; writing - original draft, S.K.K.; writing - review & editing, S.K.K. and D.A.D.; funding acquisition, S.K.K. and D.A.D.; resources, D.A.D.; supervision, D.A.D.

CHAPTER 4

CONCLUSIONS AND FUTURE DIRECTIONS

This thesis began with the posing of a major open question of biology: how do cells sense temperature? I presented emergent evidence which supports my hypothesis that temperature is interpreted by a specific set of proteins which have evolved to form biomolecular condensates in response to temperature changes imposed by the environment. My findings – that condensation is a conserved, tuned, and adaptive process – provide new evidence for this hypothesis. Conservation is often used in biology as a test for function: highly conserved genes, pathways, and overall cellular responses are likely to serve an essential purpose for life. My results further demonstrate an adaptive role via species-tuned fitness defects when condensation is prevented. The exact function, however, remains unclear, but the answers are within reach. In this final chapter, I summarize some potential approaches to address these major open questions in our field.

4.1 Biomolecular condensation as a sensing mechanism

Perhaps the most important finding of my thesis work is that fitness is negatively affected during heat shock when condensation temperatures of a single protein are shifted higher using genetic mutations. The reason for this fitness defect is unclear, but it demonstrates that the formation of condensates at the proper temperature is adaptive. In the beginning of this thesis,

I proposed that condensates as temperature sensors are recruiting Hsp70 away from Hsf1 and leading to the activation of the response. Indeed, when Hsf1 activation is prevented during heat stress, severe fitness defects are also observed (Tye et al. 2019). Notably, this phenotype is not apparent at non-stress temperatures, where stress-induced condensates also do not form. These two results – that preventing condensation at heat shock temperatures reduces fitness, and that arrested Hsf1 activation at heat shock temperatures leads to halted growth – warrant further investigation. I propose that the Hsf1 induction response should be analyzed at heat shock temperatures in the background of the condensation-preventing mutants using RNA-seq. This would be even further bolstered by the identification of other sensitive and autonomous condensate-forming proteins, which could then be knocked out or genetically modified to prevent their condensation. This approach would screen specifically for Hsf1 induction and holds promise to identify sensors for Hsf1. One may consider the use of the Yeast Deletion Collection to select mutants for known condensing proteins, and prioritize those mutants for RNA-seq or Hsf1-targeted qPCR (Giaever and Nislow 2014).

As Hsf1 induction is considered a proxy of cellular proteostasis (Solís et al. 2016; Zheng et al. 2016; Pincus et al. 2018; Albert et al. 2019; Masser et al. 2019; Peffer, Gonçalves, and Morano 2019), perhaps condensates can also fit within this definition. The state of the proteins is indeed changing, with re-localization to condensates and perhaps small, local conformation changes among individual proteins (Riback et al. 2017; Chen et al. 2022). One of my hypotheses posits that condensing proteins expose Hsp70 binding sites, which leads to Hsf1-target gene induction. Small local changes of proteins within condensates, to which Hsp70 is recruited, is consistent with existing evidence as well as a translation-independent model of Hsf1 sensing of cellular proteostasis. In Chapter 2, I proposed that condensates

themselves may serve as the activators of Hsf1, as one sign of overall cellular proteostasis, as we know condensates form under a wide array of stresses in which Hsf1 is also activated. As discussed in Chapter 3, this hypothesis remains unproven yet feasible with the proposed approaches.

4.2 The function(s) of biomolecular condensation

A central theme of this thesis has been the identification of function for biomolecular condensates. However, condensation is unlike other cellular processes, where, for example, knocking out a protein of interest is sufficient to survey for a phenotypic effect. The condensing proteome in yeast that our lab has identified contains 177 proteins whose functions are largely known and distinct from the observation that they form condensates during stress. How can one identify an adaptive condensation-related function without affecting the other function of the protein, with or without stress? I believe that using orthologous protein swaps of cyrophilic and thermophilic yeast relatives of *S. cerevisiae* remains a straightforward approach, with careful monitoring of non-stress phenotypic or fitness changes.

Isolating effects on fitness itself is challenging in the condensation field, and much work has focused on biochemical or microscopy-based methods to establish phenotypic changes (Glauninger et al. 2022). While these methods have been informative for a mechanistic understanding of condensation, they lack consideration of the physiological effects on organismal fitness. Without this, the definitive functions of condensation remain largely uncharacterized. Future research should focus on isolating growth and survival phenotypes coupled with careful perturbations on condensation.

4.3 Hot topic

The field is at an exciting juncture, where the open questions are basic and fundamental, and the approaches to address them are expanding among scientific disciplines. A lot of condensate-related research has focused on the characterization of protein aggregates associated with disease (Mackenzie et al. 2011; Patel et al. 2015; An et al. 2019). Indeed, this is a worthy motivation. However, as this thesis has highlighted, we still do not have the full mechanistic picture of the formation, detection, disaggregation, or functional output of protein condensates, even in one of the most basic eukaryotic systems. Understanding these details can help us understand what is going wrong in protein aggregation diseases like ALS and FTLD. After all, our conserved systems of sensing and responding to temperature have been fine-tuned by evolution for millions of years.

REFERENCES

Akhmetov, Azat, Jon M. Laurent, Jimmy Gollihar, Elizabeth C. Gardner, Riddhiman K. Garge, Andrew D. Ellington, Aashiq H. Kachroo, and Edward M. Marcotte. 2018. "Single-Step Precision Genome Editing in Yeast Using CRISPR-Cas9." *Bio-Protocol* 8 (6). https://doi.org/10.21769/BioProtoc.2765.

Albert, Benjamin, Isabelle C. Kos-Braun, Anthony K. Henras, Christophe Dez, Maria Paula Rueda, Xu Zhang, Olivier Gadal, Martin Kos, and David Shore. 2019. "A Ribosome Assembly Stress Response Regulates Transcription to Maintain Proteome Homeostasis." *eLife* 8 (May): e45002.

Amici, C., L. Sistonen, M. G. Santoro, and R. I. Morimoto. 1992. "Antiproliferative Prostaglandins Activate Heat Shock Transcription Factor." *Proceedings of the National Academy of Sciences of the United States of America* 89 (14): 6227–31.

An, Haiyan, Lucy Skelt, Antonietta Notaro, J. Robin Highley, Archa H. Fox, Vincenzo La Bella, Vladimir L. Buchman, and Tatyana A. Shelkovnikova. 2019. "ALS-Linked FUS Mutations Confer Loss and Gain of Function in the Nucleus by Promoting Excessive Formation of Dysfunctional Paraspeckles." *Acta Neuropathologica Communications* 7 (1): 7.

Baler, R., W. J. Welch, and R. Voellmy. 1992. "Heat Shock Gene Regulation by Nascent Polypeptides and Denatured Proteins: hsp70 as a Potential Autoregulatory Factor." *The Journal of Cell Biology* 117 (6): 1151–59.

Banat, I. M., P. Nigam, and R. Marchant. 1992. "Isolation of Thermotolerant, Fermentative Yeasts Growing at 52°C and Producing Ethanol at 45°C and 50°C." *World Journal of Microbiology & Biotechnology* 8 (3): 259–63.

Bassler, Jochen, Martina Kallas, and Ed Hurt. 2006. "The NUG1 GTPase Reveals and N-Terminal RNA-Binding Domain That Is Essential for Association with 60 S Pre-Ribosomal Particles." *The Journal of Biological Chemistry* 281 (34): 24737–44.

Basso, Manuela, Giuseppina Samengo, Giovanni Nardo, Tania Massignan, Giuseppina D'Alessandro, Silvia Tartari, Lavinia Cantoni, et al. 2009. "Characterization of Detergent-Insoluble Proteins in ALS Indicates a Causal Link between Nitrative Stress and Aggregation in Pathogenesis." *PloS One* 4 (12): e8130.

Bell, J., L. Neilson, and M. Pellegrini. 1988. "Effect of Heat Shock on Ribosome Synthesis in Drosophila Melanogaster." *Molecular and Cellular Biology* 8 (1): 91–95.

Bianchi, Greta, Sonia Longhi, Rita Grandori, and Stefania Brocca. 2020. "Relevance of Electrostatic Charges in Compactness, Aggregation, and Phase Separation of Intrinsically Disordered Proteins." *International Journal of Molecular Sciences* 21 (17). https://doi.org/10.3390/ijms21176208.

Brachmann, C. B., A. Davies, G. J. Cost, E. Caputo, J. Li, P. Hieter, and J. D. Boeke. 1998.

"Designer Deletion Strains Derived from Saccharomyces Cerevisiae S288C: A Useful Set of Strains and Plasmids for PCR-Mediated Gene Disruption and Other Applications." *Yeast* 14 (2): 115–32.

Brengues, Muriel, and Roy Parker. 2007. "Accumulation of Polyadenylated mRNA, Pab1p, eIF4E, and eIF4G with P-Bodies in Saccharomyces Cerevisiae." *Molecular Biology of the Cell* 18 (7): 2592–2602.

Brion, Christian, David Pflieger, Sirine Souali-Crespo, Anne Friedrich, and Joseph Schacherer. 2016. "Differences in Environmental Stress Response among Yeasts Is Consistent with Species-Specific Lifestyles." *Molecular Biology of the Cell* 27 (10): 1694–1705.

Buchan, J. Ross, Denise Muhlrad, and Roy Parker. 2008. "P Bodies Promote Stress Granule Assembly in Saccharomyces Cerevisiae." *The Journal of Cell Biology* 183 (3): 441–55.

Buchan, J. Ross, Je-Hyun Yoon, and Roy Parker. 2011. "Stress-Specific Composition, Assembly and Kinetics of Stress Granules in Saccharomyces Cerevisiae." *Journal of Cell Science* 124 (Pt 2): 228–39.

Byrne, Kevin P., and Kenneth H. Wolfe. 2005. "The Yeast Gene Order Browser: Combining Curated Homology and Syntenic Context Reveals Gene Fate in Polyploid Species." *Genome Research* 15 (10): 1456–61.

Chen, Ruofan, Darren Kahan, Julia Shangguan, Joseph R. Sachleben, Joshua A. Riback, D. Allan Drummond, and Tobin R. Sosnick. 2022. "Sequential Activation and Local Unfolding Control Poly(A)-Binding Protein Condensation." *bioRxiv*. https://doi.org/10.1101/2022.09.21.508844.

Cherkasov, Valeria, Tomas Grousl, Patrick Theer, Yevhen Vainshtein, Christine Gläßer, Cyril Mongis, Günter Kramer, et al. 2015. "Systemic Control of Protein Synthesis through Sequestration of Translation and Ribosome Biogenesis Factors during Severe Heat Stress." *FEBS Letters*, October. https://doi.org/10.1016/j.febslet.2015.10.010.

Cherkasov, Valeria, Sarah Hofmann, Silke Druffel-Augustin, Axel Mogk, Jens Tyedmers, Georg Stoecklin, and Bernd Bukau. 2013. "Coordination of Translational Control and Protein Homeostasis during Severe Heat Stress." *Current Biology: CB* 23 (24): 2452–62.

Cherry, J. Michael, Eurie L. Hong, Craig Amundsen, Rama Balakrishnan, Gail Binkley, Esther T. Chan, Karen R. Christie, et al. 2012. "Saccharomyces Genome Database: The Genomics Resource of Budding Yeast." *Nucleic Acids Research* 40 (Database issue): D700–705.

Cole, Christian, Jonathan D. Barber, and Geoffrey J. Barton. 2008. "The Jpred 3 Secondary Structure Prediction Server." *Nucleic Acids Research* 36 (Web Server issue): W197–201.

Cooney, Donald G., and Ralph Emerson. 1964. *Thermophilic Fungi. An Account of Their Biology, Activities, and Classification*. San Francisco & London, WH Freeman & Co.

Correia, Kevin, Shi M. Yu, and Radhakrishnan Mahadevan. 2019. "AYbRAH: A Curated Ortholog Database for Yeasts and Fungi Spanning 600 Million Years of Evolution." *Database: The Journal of Biological Databases and Curation* 2019 (January).

https://doi.org/10.1093/database/baz022.

Cuff, J. A., and G. J. Barton. 2000. “Application of Multiple Sequence Alignment Profiles to Improve Protein Secondary Structure Prediction.” *Proteins* 40 (3): 502–11.

Deegenaars, M. L., and K. Watson. 1998. “Heat Shock Response in Psychrophilic and Psychrotrophic Yeast from Antarctica.” *Extremophiles: Life under Extreme Conditions* 2 (1): 41–49.

Dobin, Alexander, Carrie A. Davis, Felix Schlesinger, Jorg Drenkow, Chris Zaleski, Sonali Jha, Philippe Batut, Mark Chaisson, and Thomas R. Gingeras. 2013. “STAR: Ultrafast Universal RNA-Seq Aligner.” *Bioinformatics* 29 (1): 15–21.

Drozdetskiy, Alexey, Christian Cole, James Procter, and Geoffrey J. Barton. 2015. “JPred4: A Protein Secondary Structure Prediction Server.” *Nucleic Acids Research* 43 (W1): W389–94.

Elfving, Nils, Răzvan V. Chereji, Vasudha Bharatula, Stefan Björklund, Alexandre V. Morozov, and James R. Broach. 2014. “A Dynamic Interplay of Nucleosome and Msn2 Binding Regulates Kinetics of Gene Activation and Repression Following Stress.” *Nucleic Acids Research* 42 (9): 5468–82.

Engel, Stacia R., Fred S. Dietrich, Dianna G. Fisk, Gail Binkley, Rama Balakrishnan, Maria C. Costanzo, Selina S. Dwight, et al. 2014. “The Reference Genome Sequence of Saccharomyces Cerevisiae: Then and Now.” *G3* 4 (3): 389–98.

Franzmann, Titus M., Marcus Jahnel, Andrei Pozniakovsky, Julia Mahamid, Alex S. Holehouse, Elisabeth Nüske, Doris Richter, et al. 2018. “Phase Separation of a Yeast Prion Protein Promotes Cellular Fitness.” *Science* 359 (6371). https://doi.org/10.1126/science.aao5654.

Fuller, Gregory G., Ting Han, Mallory A. Freeberg, James J. Moresco, Amirhossein Ghanbari Niaki, Nathan P. Roach, John R. Yates 3rd, Sua Myong, and John K. Kim. 2020. “RNA Promotes Phase Separation of Glycolysis Enzymes into Yeast G Bodies in Hypoxia.” *eLife* 9 (April). https://doi.org/10.7554/eLife.48480.

Gasch, A. P., P. T. Spellman, C. M. Kao, O. Carmel-Harel, M. B. Eisen, G. Storz, D. Botstein, and P. O. Brown. 2000. “Genomic Expression Programs in the Response of Yeast Cells to Environmental Changes.” *Molecular Biology of the Cell* 11 (12): 4241–57.

Geiler-Samerotte, Kerry A., Michael F. Dion, Bogdan A. Budnik, Stephanie M. Wang, Daniel L. Hartl, and D. Allan Drummond. 2011. “Misfolded Proteins Impose a Dosage-Dependent Fitness Cost and Trigger a Cytosolic Unfolded Protein Response in Yeast.” *Proceedings of the National Academy of Sciences of the United States of America* 108 (2): 680–85.

Ghoshal, K., and S. T. Jacob. 1996. “Heat Shock Selectively Inhibits Ribosomal RNA Gene Transcription and down-Regulates E1BF/Ku in Mouse Lymphosarcoma Cells.” *Biochemical Journal* 317 (Pt 3) (August): 689–95.

Giaever, Guri, and Corey Nislow. 2014. “The Yeast Deletion Collection: A Decade of Functional Genomics.” *Genetics* 197 (2): 451–65.

Glauninger, Hendrik, Caitlin J. Wong Hickernell, Jared A. M. Bard, and D. Allan Drummond. 2022. “Stressful Steps: Progress and Challenges in Understanding Stress-Induced mRNA Condensation and Accumulation in Stress Granules.” *Molecular Cell* 82 (14): 2544–56.

Gracey, Andrew Y., Maxine L. Chaney, Judson P. Boomhower, William R. Tyburczy, Kwasi Connor, and George N. Somero. 2008. “Rhythms of Gene Expression in a Fluctuating Intertidal Environment.” *Current Biology: CB* 18 (19): 1501–7.

Grousl, Tomás, Pavel Ivanov, Ivana Frýdlová, Pavla Vasicová, Filip Janda, Jana Vojtová, Katerina Malínská, et al. 2009. “Robust Heat Shock Induces eIF2alpha-Phosphorylation-Independent Assembly of Stress Granules Containing eIF3 and 40S Ribosomal Subunits in Budding Yeast, Saccharomyces Cerevisiae.” *Journal of Cell Science* 122 (Pt 12): 2078–88.

Guerra-Moreno, Angel, Marta Isasa, Meera K. Bhanu, David P. Waterman, Vinay V. Eapen, Steven P. Gygi, and John Hanna. 2015. “Proteomic Analysis Identifies Ribosome Reduction as an Effective Proteotoxic Stress Response.” *The Journal of Biological Chemistry* 290 (50): 29695–706.

Heineike, Benjamin M., and Hana El-Samad. 2021. “Paralogs in the PKA Regulon Traveled Different Evolutionary Routes to Divergent Expression in Budding Yeast.” *Frontiers in Fungal Biology* 2. https://doi.org/10.3389/ffunb.2021.642336.

Hittinger, Chris Todd, Paula Gonçalves, José Paulo Sampaio, Jim Dover, Mark Johnston, and Antonis Rokas. 2010. “Remarkably Ancient Balanced Polymorphisms in a Multi-Locus Gene Network.” *Nature* 464 (7285): 54–58.

Hoffmann, Ary A., Jesper G. Sørensen, and Volker Loeschcke. 2003. “Adaptation of Drosophila to Temperature Extremes: Bringing Together Quantitative and Molecular Approaches.” *Journal of Thermal Biology* 28 (3): 175–216.

Hoyle, Nathaniel P., Lydia M. Castelli, Susan G. Campbell, Leah E. A. Holmes, and Mark P. Ashe. 2007. “Stress-Dependent Relocalization of Translationally Primed mRNPs to Cytoplasmic Granules That Are Kinetically and Spatially Distinct from P-Bodies.” *The Journal of Cell Biology* 179 (1): 65–74.

Huerta-Cepas, Jaime, Damian Szklarczyk, Davide Heller, Ana Hernández-Plaza, Sofia K. Forslund, Helen Cook, Daniel R. Mende, et al. 2019. “eggNOG 5.0: A Hierarchical, Functionally and Phylogenetically Annotated Orthology Resource Based on 5090 Organisms and 2502 Viruses.” *Nucleic Acids Research* 47 (D1): D309–14.

Iserman, Christiane, Christine Desroches Altamirano, Ceciel Jegers, Ulrike Friedrich, Taraneh Zarin, Anatol W. Fritsch, Matthäus Mittasch, et al. 2020. “Condensation of Ded1p Promotes a Translational Switch from Housekeeping to Stress Protein Production.” *Cell* 0 (0). https://doi.org/10.1016/j.cell.2020.04.009.

Jung, Jae-Hoon, Antonio D. Barbosa, Stephanie Hutin, Janet R. Kumita, Mingjun Gao, Dorothee Derwort, Catarina S. Silva, et al. 2020. “A Prion-like Domain in ELF3 Functions as a Thermosensor in Arabidopsis.” *Nature* 585 (7824): 256–60.

Kallstrom, George, John Hedges, and Arlen Johnson. 2003. “The Putative GTPases Nog1p and Lsg1p Are Required for 60S Ribosomal Subunit Biogenesis and Are Localized to the Nucleus and Cytoplasm, Respectively.” *Molecular and Cellular Biology* 23 (12): 4344–55.

Kanehisa, Minoru, Miho Furumichi, Yoko Sato, Masayuki Kawashima, and Mari Ishiguro-Watanabe. 2023. “KEGG for Taxonomy-Based Analysis of Pathways and Genomes.” *Nucleic Acids Research* 51 (D1): D587–92.

Kanehisa, Minoru, Yoko Sato, Masayuki Kawashima, Miho Furumichi, and Mao Tanabe. 2016. “KEGG as a Reference Resource for Gene and Protein Annotation.” *Nucleic Acids Research* 44 (D1): D457–62.

Kato, Kenta, Yosuke Yamamoto, and Shingo Izawa. 2011. “Severe Ethanol Stress Induces Assembly of Stress Granules in Saccharomyces Cerevisiae.” *Yeast* 28 (5): 339–47.

Kempf, Claudia, Klaus Lengeler, and Jürgen Wendland. 2017. “Differential Stress Response of Saccharomyces Hybrids Revealed by Monitoring Hsp104 Aggregation and Disaggregation.” *Microbiological Research* 200 (July): 53–63.

Kmiecik, Szymon W., Laura Le Breton, and Matthias P. Mayer. n.d. “Molecular Mechanism of Attenuation of Heat Shock Transcription Factor 1 Activity.” https://doi.org/10.1101/803361.

Kobayashi, N., and K. McEntee. 1993. “Identification of Cis and Trans Components of a Novel Heat Shock Stress Regulatory Pathway in Saccharomyces Cerevisiae.” *Molecular and Cellular Biology* 13 (1): 248–56.

Koch, A. L. 1988. “Why Can’t a Cell Grow Infinitely Fast?” *Canadian Journal of Microbiology* 34 (4): 421–26.

Krakowiak, Joanna, Xu Zheng, Nikit Patel, Zoë A. Feder, Jayamani Anandhakumar, Kendra Valerius, David S. Gross, Ahmad S. Khalil, and David Pincus. 2018. “Hsf1 and Hsp70 Constitute a Two-Component Feedback Loop That Regulates the Yeast Heat Shock Response.” *eLife* 7 (February). https://doi.org/10.7554/eLife.31668.

Kroschwald, Sonja, Shovamayee Maharana, Daniel Mateju, Liliana Malinovska, Elisabeth Nüske, Ina Poser, Doris Richter, and Simon Alberti. 2015. “Promiscuous Interactions and Protein Disaggregases Determine the Material State of Stress-Inducible RNP Granules.” *eLife* 4 (August): e06807.

Kroschwald, Sonja, Matthias C. Munder, Shovamayee Maharana, Titus M. Franzmann, Doris Richter, Martine Ruer, Anthony A. Hyman, and Simon Alberti. 2018. “Different Material States of Pub1 Condensates Define Distinct Modes of Stress Adaptation and Recovery.” *Cell Reports* 23 (11): 3327–39.

Kuang, Zheng, Sudarshan Pinglay, Hongkai Ji, and Jef D. Boeke. 2017. “Msn2/4 Regulate Expression of Glycolytic Enzymes and Control Transition from Quiescence to Growth.” *eLife* 6 (September). https://doi.org/10.7554/eLife.29938.

Kumar, Sudhir, Michael Suleski, Jack M. Craig, Adrienne E. Kasprowicz, Maxwell Sanderford, Michael Li, Glen Stecher, and S. Blair Hedges. 2022. “TimeTree 5: An Expanded Resource

for Species Divergence Times." *Molecular Biology and Evolution* 39 (8). https://doi.org/10.1093/molbev/msac174.

Lawrence, Michael, Wolfgang Huber, Hervé Pagès, Patrick Aboyoun, Marc Carlson, Robert Gentleman, Martin T. Morgan, and Vincent J. Carey. 2013. "Software for Computing and Annotating Genomic Ranges." *PLoS Computational Biology* 9 (8): e1003118.

Le Breton, Laura, and Matthias P. Mayer. 2016. "A Model for Handling Cell Stress." *eLife*. https://doi.org/10.7554/eLife.22850.

Lee, Michael E., William C. DeLoache, Bernardo Cervantes, and John E. Dueber. 2015. "A Highly Characterized Yeast Toolkit for Modular, Multipart Assembly." *ACS Synthetic Biology* 4 (9): 975–86.

Limtong, Savitree, Chutima Sringiew, and Wichien Yongmanitchai. 2007. "Production of Fuel Ethanol at High Temperature from Sugar Cane Juice by a Newly Isolated Kluyveromyces Marxianus." *Bioresource Technology* 98 (17): 3367–74.

Lindquist, S. 1984. "Heat Shock--a Comparison of Drosophila and Yeast." *Journal of Embryology and Experimental Morphology* 83 Suppl (November): 147–61.

Lindquist, Susan. 1986. "The Heat-Shock Response." *Annual Review of Biochemistry* 55: 1151–91.

Liu, H., R. Lightfoot, and J. L. Stevens. 1996. "Activation of Heat Shock Factor by Alkylating Agents Is Triggered by Glutathione Depletion and Oxidation of Protein Thiols." *The Journal of Biological Chemistry* 271 (9): 4805–12.

Love, Michael I., Wolfgang Huber, and Simon Anders. 2014. "Moderated Estimation of Fold Change and Dispersion for RNA-Seq Data with DESeq2." *Genome Biology* 15 (12): 550.

Mackenzie, Ian R. A., David G. Munoz, Hirofumi Kusaka, Osamu Yokota, Kenji Ishihara, Sigrun Roeber, Hans A. Kretzschmar, Nigel J. Cairns, and Manuela Neumann. 2011. "Distinct Pathological Subtypes of FTLD-FUS." *Acta Neuropathologica* 121 (2): 207–18.

Madeira, Fábio, Matt Pearce, Adrian R. N. Tivey, Prasad Basutkar, Joon Lee, Ossama Edbali, Nandana Madhusoodanan, Anton Kolesnikov, and Rodrigo Lopez. 2022. "Search and Sequence Analysis Tools Services from EMBL-EBI in 2022." *Nucleic Acids Research* 50 (W1): W276–79.

Maheshwari, R., G. Bharadwaj, and M. K. Bhat. 2000. "Thermophilic Fungi: Their Physiology and Enzymes." *Microbiology and Molecular Biology Reviews: MMBR* 64 (3): 461–88.

Marchler-Bauer, Aron, Yu Bo, Lianyi Han, Jane He, Christopher J. Lanczycki, Shennan Lu, Farideh Chitsaz, et al. 2017. "CDD/SPARCLE: Functional Classification of Proteins via Subfamily Domain Architectures." *Nucleic Acids Research* 45 (D1): D200–203.

Marchler, G., C. Schüller, G. Adam, and H. Ruis. 1993. "A Saccharomyces Cerevisiae UAS Element Controlled by Protein Kinase A Activates Transcription in Response to a Variety of Stress Conditions." *The EMBO Journal* 12 (5): 1997–2003.

Martínez-Pastor, M. T., G. Marchler, C. Schüller, A. Marchler-Bauer, H. Ruis, and F. Estruch. 1996. “The Saccharomyces Cerevisiae Zinc Finger Proteins Msn2p and Msn4p Are Required for Transcriptional Induction through the Stress Response Element (STRE).” *The EMBO Journal* 15 (9): 2227–35.

Martin, Marcel. 2011. “Cutadapt Removes Adapter Sequences from High-Throughput Sequencing Reads.” *EMBnet.journal* 17 (1): 10–12.

Masser, Anna E., Wenjing Kang, Joydeep Roy, Jayasankar Mohanakrishnan Kaimal, Jany Quintana-Cordero, Marc R. Friedländer, and Claes Andréasson. 2019. “Cytoplasmic Protein Misfolding Titrates Hsp70 to Activate Nuclear Hsf1.” *eLife* 8 (September). https://doi.org/10.7554/eLife.47791.

Matsuo, Yoshitaka, Sander Granneman, Matthias Thoms, Rizos-Georgios Manikas, David Tollervey, and Ed Hurt. 2014. “Coupled GTPase and Remodelling ATPase Activities Form a Checkpoint for Ribosome Export.” *Nature* 505 (7481): 112–16.

Mistry, Jaina, Sara Chuguransky, Lowri Williams, Matloob Qureshi, Gustavo A. Salazar, Erik L. L. Sonnhammer, Silvio C. E. Tosatto, et al. 2021. “Pfam: The Protein Families Database in 2021.” *Nucleic Acids Research* 49 (D1): D412–19.

Mölder, Felix, Kim Philipp Jablonski, Brice Letcher, Michael B. Hall, Christopher H. Tomkins-Tinch, Vanessa Sochat, Jan Forster, et al. 2021. “Sustainable Data Analysis with Snakemake.” *F1000Research* 10 (January): 33.

Morano, Kevin A., Chris M. Grant, and W. Scott Moye-Rowley. 2012. “The Response to Heat Shock and Oxidative Stress in Saccharomyces Cerevisiae.” *Genetics* 190 (4): 1157–95.

Mosser, D. D., N. G. Theodorakis, and R. I. Morimoto. 1988. “Coordinate Changes in Heat Shock Element-Binding Activity and HSP70 Gene Transcription Rates in Human Cells.” *Molecular and Cellular Biology* 8 (11): 4736–44.

Munder, Matthias Christoph, Daniel Midtvedt, Titus Franzmann, Elisabeth Nüske, Oliver Otto, Maik Herbig, Elke Ulbricht, et al. 2016. “A pH-Driven Transition of the Cytoplasm from a Fluid- to a Solid-like State Promotes Entry into Dormancy.” *eLife* 5 (March). https://doi.org/10.7554/eLife.09347.

Neidhardt, F. C., and B. Magasanik. 1960. “Studies on the Role of Ribonucleic Acid in the Growth of Bacteria.” *Biochimica et Biophysica Acta* 42 (July): 99–116.

Nonklang, Sanom, Babiker M. A. Abdel-Banat, Kamonchai Cha-aim, Nareerat Moonjai, Hisashi Hoshida, Savitree Limtong, Mamoru Yamada, and Rinji Akada. 2008. “High-Temperature Ethanol Fermentation and Transformation with Linear DNA in the Thermotolerant Yeast Kluyveromyces Marxianus DMKU3-1042.” *Applied and Environmental Microbiology* 74 (24): 7514–21.

Patel, Avinash, Hyun O. Lee, Louise Jawerth, Shovamayee Maharana, Marcus Jahnel, Marco Y. Hein, Stoyno Stoynov, et al. 2015. “A Liquid-to-Solid Phase Transition of the ALS Protein FUS Accelerated by Disease Mutation.” *Cell* 162 (5): 1066–77.

Pattanayak, Gopal K., Yi Liao, Edward W. J. Wallace, Bogdan Budnik, D. Allan Drummond, and Michael J. Rust. 2020. “Daily Cycles of Reversible Protein Condensation in Cyanobacteria.” *Cell Reports* 32 (7): 108032.

Paysan-Lafosse, Typhaine, Matthias Blum, Sara Chuguransky, Tiago Grego, Beatriz Lázaro Pinto, Gustavo A. Salazar, Maxwell L. Bileschi, et al. 2023. “InterPro in 2022.” *Nucleic Acids Research* 51 (D1): D418–27.

Peffer, Sara, Davi Gonçalves, and Kevin A. Morano. 2019. “Regulation of the Hsf1-Dependent Transcriptome via Conserved Bipartite Contacts with Hsp70 Promotes Survival in Yeast.” *The Journal of Biological Chemistry* 294 (32): 12191–202.

Pelham, Jacqueline F., Alexander E. Mosier, and Jennifer M. Hurley. 2018. “Chapter Sixteen - Characterizing Time-of-Day Conformational Changes in the Intrinsically Disordered Proteins of the Circadian Clock.” In *Methods in Enzymology*, edited by Elizabeth Rhoades, 611:503–29. Academic Press.

Pincus, David, Jayamani Anandhakumar, Prathapan Thiru, Michael J. Guertin, Alexander M. Erkine, and David S. Gross. 2018. “Genetic and Epigenetic Determinants Establish a Continuum of Hsf1 Occupancy and Activity across the Yeast Genome.” *Molecular Biology of the Cell* 29 (26): 3168–82.

Protter, David S. W., and Roy Parker. 2016. “Principles and Properties of Stress Granules.” *Trends in Cell Biology* 26 (9): 668–79.

Putri, Givanna H., Simon Anders, Paul Theodor Pyl, John E. Pimanda, and Fabio Zanini. 2022. “Analysing High-Throughput Sequencing Data in Python with HTSeq 2.0.” *Bioinformatics* 38 (10): 2943–45.

R Core Team. 2022. “R: A Language and Environment for Statistical Computing.” Vienna, Austria: R Foundation for Statistical Computing. https://www.R-project.org/.

Riback, Joshua A., Christopher D. Katanski, Jamie L. Kear-Scott, Evgeny V. Pilipenko, Alexandra E. Rojek, Tobin R. Sosnick, and D. Allan Drummond. 2017. “Stress-Triggered Phase Separation Is an Adaptive, Evolutionarily Tuned Response.” *Cell* 168 (6): 1028–40.e19.

Riehle, Michelle M., Albert F. Bennett, Richard E. Lenski, and Anthony D. Long. 2003. “Evolutionary Changes in Heat-Inducible Gene Expression in Lines of Escherichia Coli Adapted to High Temperature.” *Physiological Genomics* 14 (1): 47–58.

Ritossa, F. 1962. “A New Puffing Pattern Induced by Temperature Shock and DNP in Drosophila.” *Experientia* 18 (12): 571–73.

Ritossa, F. 1996. “Discovery of the Heat Shock Response.” *Cell Stress & Chaperones* 1 (2): 97–98.

Robert, Christian P., and George Casella. n.d. *Monte Carlo Statistical Methods*. Springer New York. Accessed May 9, 2023.

Rosso, L., J. R. Lobry, and J. P. Flandrois. 1993. “An Unexpected Correlation between Cardinal Temperatures of Microbial Growth Highlighted by a New Model.” *Journal of Theoretical Biology* 162 (4): 447–63.

Rowley, Adele, 1. Gerald C. Johnston, Braeden Butler, 2. Margaret Werner-Washburne, and Richard A. Singer3’. 1993. “Expression in the Yeast Saccharomyces Cerevisiae.” *Molecular and Cellular Biology* 13 (2): 1034–41.

RStudio Team. 2020. “RStudio: Integrated Development Environment for R.” Boston, MA: RStudio, PBC. http://www.rstudio.com/.

Rüdiger, S., L. Germeroth, J. Schneider-Mergener, and B. Bukau. 1997. “Substrate Specificity of the DnaK Chaperone Determined by Screening Cellulose-Bound Peptide Libraries.” *The EMBO Journal* 16 (7): 1501–7.

Sakihama, Yuri, Ryota Hidese, Tomohisa Hasunuma, and Akihiko Kondo. 2019. “Increased Flux in Acetyl-CoA Synthetic Pathway and TCA Cycle of Kluyveromyces Marxianus under Respiratory Conditions.” *Scientific Reports* 9 (1): 5319.

Salvadó, Z., F. N. Arroyo-López, E. Barrio, A. Querol, and J. M. Guillamón. 2011. “Quantifying the Individual Effects of Ethanol and Temperature on the Fitness Advantage of Saccharomyces Cerevisiae.” *Food Microbiology* 28 (6): 1155–61.

Salvadó, Z., F. N. Arroyo-López, J. M. Guillamón, G. Salazar, A. Querol, and E. Barrio. 2011. “Temperature Adaptation Markedly Determines Evolution within the Genus Saccharomyces.” *Applied and Environmental Microbiology* 77 (7): 2292–2302.

Sampaio, José Paulo, and Paula Gonçalves. 2008. “Natural Populations of Saccharomyces Kudriavzevii in Portugal Are Associated with Oak Bark and Are Sympatric with S. Cerevisiae and S. Paradoxus.” *Applied and Environmental Microbiology* 74 (7): 2144–52.

Scannell, Devin R., Oliver A. Zill, Antonis Rokas, Celia Payen, Maitreya J. Dunham, Michael B. Eisen, Jasper Rine, Mark Johnston, and Chris Todd Hittinger. 2011. “The Awesome Power of Yeast Evolutionary Genetics: New Genome Sequences and Strain Resources for the Saccharomyces Sensu Stricto Genus.” *G3* 1 (1): 11–25.

Schindelin, Johannes, Ignacio Arganda-Carreras, Erwin Frise, Verena Kaynig, Mark Longair, Tobias Pietzsch, Stephan Preibisch, et al. 2012. “Fiji: An Open-Source Platform for Biological-Image Analysis.” *Nature Methods* 9 (7): 676–82.

Schmidt, Helen, Andrea Putnam, Dominique Rasoloson, and Geraldine Seydoux. 2021. “Protein-Based Condensation Mechanisms Drive the Assembly of RNA-Rich P Granules.” *eLife* 10 (June). https://doi.org/10.7554/eLife.63698.

Sengupta, Piali, and Paul Garrity. 2013. “Sensing Temperature.” *Current Biology: CB* 23 (8): R304–7.

Shah, Khyati H., Sapna N. Varia, Laura A. Cook, and Paul K. Herman. 2016. “A Hybrid-Body Containing Constituents of Both P-Bodies and Stress Granules Forms in Response to Hypoosmotic Stress in Saccharomyces Cerevisiae.” *PloS One* 11 (6): e0158776.

Shaner, Nathan C., Robert E. Campbell, Paul A. Steinbach, Ben N. G. Giepmans, Amy E. Palmer, and Roger Y. Tsien. 2004. “Improved Monomeric Red, Orange and Yellow Fluorescent Proteins Derived from Discosoma Sp. Red Fluorescent Protein.” *Nature Biotechnology* 22 (12): 1567–72.

Shin, Yongdae, Joel Berry, Nicole Pannucci, Mikko P. Haataja, Jared E. Toettcher, and Clifford P. Brangwynne. 2017. “Spatiotemporal Control of Intracellular Phase Transitions Using Light-Activated optoDroplets.” *Cell*.

Shi, Y., D. D. Mosser, and R. I. Morimoto. 1998. “Molecular Chaperones as HSF1-Specific Transcriptional Repressors.” *Genes & Development* 12 (5): 654–66.

Solís, Eric J., Jai P. Pandey, Xu Zheng, Dexter X. Jin, Piyush B. Gupta, Edoardo M. Airoldi, David Pincus, and Vladimir Denic. 2016. “Defining the Essential Function of Yeast Hsf1 Reveals a Compact Transcriptional Program for Maintaining Eukaryotic Proteostasis.” *Molecular Cell* 63 (1): 60–71.

Sørensen, Jesper Givskov, Torsten Nygaard Kristensen, and Volker Loeschcke. 2003. “The Evolutionary and Ecological Role of Heat Shock Proteins.” *Ecology Letters* 6 (11): 1025–37.

Sottile, Mayra L., and Silvina B. Nadin. 2018. “Heat Shock Proteins and DNA Repair Mechanisms: An Updated Overview.” *Cell Stress & Chaperones* 23 (3): 303–15.

Stan Development Team. 2023. “RStan: The R Interface to Stan.” https://mc-stan.org/.

Sui, Xiaojing, Douglas E. V. Pires, Angelique R. Ormsby, Dezerae Cox, Shuai Nie, Giulia Vecchi, Michele Vendruscolo, David B. Ascher, Gavin E. Reid, and Danny M. Hatters. 2020. “Widespread Remodeling of Proteome Solubility in Response to Different Protein Homeostasis Stresses.” *Proceedings of the National Academy of Sciences of the United States of America*, January. https://doi.org/10.1073/pnas.1912897117.

Tanabe, M., A. Nakai, Y. Kawazoe, and K. Nagata. 1997. “Different Thresholds in the Responses of Two Heat Shock Transcription Factors, HSF1 and HSF3.” *The Journal of Biological Chemistry* 272 (24): 15389–95.

Tissières, A., H. K. Mitchell, and U. M. Tracy. 1974. “Protein Synthesis in Salivary Glands of Drosophila Melanogaster: Relation to Chromosome Puffs.” *Journal of Molecular Biology* 84 (3): 389–98.

Tomanek, L. 2010. “Variation in the Heat Shock Response and Its Implication for Predicting the Effect of Global Climate Change on Species’ Biogeographical Distribution Ranges and Metabolic Costs.” *The Journal of Experimental Biology* 213 (6): 971–79.

Tomanek, Lars. 2008. “The Importance of Physiological Limits in Determining Biogeographical Range Shifts due to Global Climate Change: The Heat-Shock Response.” *Physiological and Biochemical Zoology: PBZ* 81 (6): 709–17.

Triandafillou, Catherine G., Christopher D. Katanski, Aaron R. Dinner, and D. Allan Drummond. 2020. “Transient Intracellular Acidification Regulates the Core Transcriptional Heat Shock Response.” *eLife* 9 (August). https://doi.org/10.7554/eLife.54880.

Tronchoni, Jordi, Victor Medina, Jose Manuel Guillamón, Amparo Querol, and Roberto Pérez-Torrado. 2014. “Transcriptomics of Cryophilic Saccharomyces Kudriavzevii Reveals the Key Role of Gene Translation Efficiency in Cold Stress Adaptations.” *BMC Genomics* 15 (June): 432.

Trotter, E. W., L. Berenfeld, S. A. Krause, G. A. Petsko, and J. V. Gray. 2001. “Protein Misfolding and Temperature up-Shift Cause G1 Arrest via a Common Mechanism Dependent on Heat Shock Factor in Saccharomyces cerevisiae.” *Proceedings of the National Academy of Sciences of the United States of America* 98 (13): 7313–18.

Tye, Blake W., and L. Stirling Churchman. 2021. “Hsf1 Activation by Proteotoxic Stress Requires Concurrent Protein Synthesis.” *Molecular Biology of the Cell* 32 (19): 1800–1806.

Tye, Blake W., Nicoletta Commins, Lillia V. Ryazanova, Martin Wühr, Michael Springer, David Pincus, and L. Stirling Churchman. 2019. “Proteotoxicity from Aberrant Ribosome Biogenesis Compromises Cell Fitness.” *eLife* 8 (March). https://doi.org/10.7554/eLife.43002.

Vabulas, R. Martin, Swasti Raychaudhuri, Manajit Hayer-Hartl, and F. Ulrich Hartl. 2010. “Protein Folding in the Cytoplasm and the Heat Shock Response.” *Cold Spring Harbor Perspectives in Biology* 2 (12): a004390.

Van Durme, Joost, Sebastian Maurer-Stroh, Rodrigo Gallardo, Hannah Wilkinson, Frederic Rousseau, and Joost Schymkowitz. 2009. “Accurate Prediction of DnaK-Peptide Binding via Homology Modelling and Experimental Data.” *PLoS Computational Biology* 5 (8): e1000475.

Verghese, Jacob, Jennifer Abrams, Yanyu Wang, and Kevin A. Morano. 2012. “Biology of the Heat Shock Response and Protein Chaperones: Budding Yeast (Saccharomyces Cerevisiae) as a Model System.” *Microbiology and Molecular Biology Reviews: MMBR* 76 (2): 115–58.

Villegas, José A., Meta Heidenreich, and Emmanuel D. Levy. 2022. “Molecular and Environmental Determinants of Biomolecular Condensate Formation.” *Nature Chemical Biology* 18 (12): 1319–29.

Vyas, Valmik K., G. Guy Bushkin, Douglas A. Bernstein, Matthew A. Getz, Magdalena Sewastianik, M. Inmaculada Barrasa, David P. Bartel, and Gerald R. Fink. 2018. “New CRISPR Mutagenesis Strategies Reveal Variation in Repair Mechanisms among Fungi.” *mSphere* 3 (2). https://doi.org/10.1128/mSphere.00154-18.

Wallace, Edward W. J., Jamie L. Kear-Scott, Evgeny V. Pilipenko, Michael H. Schwartz, Pawel R. Laskowski, Alexandra E. Rojek, Christopher D. Katanski, et al. 2015. “Reversible, Specific, Active Aggregates of Endogenous Proteins Assemble upon Heat Stress.” *Cell* 162 (6): 1286–98.

Wessel, D., and U. I. Flügge. 1984. “A Method for the Quantitative Recovery of Protein in Dilute Solution in the Presence of Detergents and Lipids.” *Analytical Biochemistry* 138 (1): 141–43.

Wickham, Hadley. n.d. *ggplot2*. Springer New York. Accessed March 28, 2023.

Wickham, Hadley, Mara Averick, Jennifer Bryan, Winston Chang, Lucy McGowan, Romain François, Garrett Grolemund, et al. 2019. “Welcome to the Tidyverse.” *Journal of Open Source Software* 4 (43): 1686.

Wittinghofer, Alfred, and Ingrid R. Vetter. 2011. “Structure-Function Relationships of the G Domain, a Canonical Switch Motif.” https://doi.org/10.1146/annurev-biochem-062708-134043.

Xu, Guilian, Amrutha Pattamatta, Ryan Hildago, Michael C. Pace, Hilda Brown, and David R. Borchelt. 2016. “Vulnerability of Newly Synthesized Proteins to Proteostasis Stress.” *Journal of Cell Science* 129 (9): 1892–1901.

Yamamoto, Yosuke, and Shingo Izawa. 2013. “Adaptive Response in Stress Granule Formation and Bulk Translational Repression upon a Combined Stress of Mild Heat Shock and Mild Ethanol Stress in Yeast.” *Genes to Cells: Devoted to Molecular & Cellular Mechanisms* 18 (11): 974–84.

Yoo, Haneul, Jared A. M. Bard, Evgeny V. Pilipenko, and D. Allan Drummond. 2022. “Chaperones Directly and Efficiently Disperse Stress-Triggered Biomolecular Condensates.” *Molecular Cell* 82 (4): 741–55.e11.

Yoo, Haneul, Catherine Triandafillou, and D. Allan Drummond. 2019. “Cellular Sensing by Phase Separation: Using the Process, Not Just the Products.” *The Journal of Biological Chemistry* 294 (18): 7151–59.

Zhang, Xiao-Hui, Louis Y. Tee, Xiao-Gang Wang, Qun-Shan Huang, and Shi-Hua Yang. 2015. “Off-Target Effects in CRISPR/Cas9-Mediated Genome Engineering.” *Molecular Therapy. Nucleic Acids* 4 (November): e264.

Zhao, Zhongliang, Marcel A. Dammert, Sven Hoppe, Holger Bierhoff, and Ingrid Grummt. 2016. “Heat Shock Represses rRNA Synthesis by Inactivation of TIF-IA and lncRNA-Dependent Changes in Nucleosome Positioning.” *Nucleic Acids Research* 44 (17): 8144–52.

Zheng, Xu, Joanna Krakowiak, Nikit Patel, Ali Beyzavi, Jideofor Ezike, Ahmad S. Khalil, and David Pincus. 2016. “Dynamic Control of Hsf1 during Heat Shock by a Chaperone Switch and Phosphorylation.” *eLife* 5 (November). https://doi.org/10.7554/eLife.18638.